U.S.NRC
United States Nuclear Regulatory Commission
*Protecting People and the Environment*

NUREG/CR-7132

# Application of Radar-Rainfall Estimates to Probable Maximum Precipitation in the Carolinas

Office of Nuclear Regulatory Research

# AVAILABILITY OF REFERENCE MATERIALS IN NRC PUBLICATIONS

## NRC Reference Material

As of November 1999, you may electronically access NUREG-series publications and other NRC records at the NRC's Library at www.nrc.gov/reading-rm.html. Publicly released records include, to name a few, NUREG-series publications; *Federal Register* notices; applicant, licensee, and vendor documents and correspondence; NRC correspondence and internal memoranda; bulletins and information notices; inspection and investigative reports; licensee event reports; and Commission papers and their attachments.

NRC publications in the NUREG series, NRC regulations, and Title 10, "Energy," in the *Code of Federal Regulations* may also be purchased from one of these two sources:

1. **The Superintendent of Documents**
   U.S. Government Publishing Office
   Washington, DC 20402-0001
   Internet: www.bookstore.gpo.gov
   Telephone: (202) 512-1800
   Fax: (202) 512-2104

2. **The National Technical Information Service**
   5301 Shawnee Road
   Alexandria, VA 22312-0002
   Internet: www.ntis.gov
   1-800-553-6847 or, locally, (703) 605-6000

A single copy of each NRC draft report for comment is available free, to the extent of supply, upon written request as follows:

Address: **U.S. Nuclear Regulatory Commission**
Office of Administration
Digital Communications and Administrative Services Branch
Washington, DC 20555-0001
E-mail: distribution.resource@nrc.gov
Facsimile: (301) 415-2289

Some publications in the NUREG series that are posted at the NRC's Web site address www.nrc.gov/reading-rm/doc-collections/nuregs are updated periodically and may differ from the last printed version. Although references to material found on a Web site bear the date the material was accessed, the material available on the date cited may subsequently be removed from the site.

## Non-NRC Reference Material

Documents available from public and special technical libraries include all open literature items, such as books, journal articles, transactions, *Federal Register* notices, Federal and State legislation, and congressional reports. Such documents as theses, dissertations, foreign reports and translations, and non-NRC conference proceedings may be purchased from their sponsoring organization.

Copies of industry codes and standards used in a substantive manner in the NRC regulatory process are maintained at—

**The NRC Technical Library**
Two White Flint North
11545 Rockville Pike
Rockville, MD 20852-2738

These standards are available in the library for reference use by the public. Codes and standards are usually copyrighted and may be purchased from the originating organization or, if they are American National Standards, from—

**American National Standards Institute**
11 West 42nd Street
New York, NY 10036-8002
Internet: www.ansi.org
(212) 642-4900

Legally binding regulatory requirements are stated only in laws; NRC regulations; licenses, including technical specifications; or orders, not in NUREG-series publications. The views expressed in contractor prepared publications in this series are not necessarily those of the NRC.

The NUREG series comprises (1) technical and administrative reports and books prepared by the staff (NUREG–XXXX) or agency contractors (NUREG/CR–XXXX), (2) proceedings of conferences (NUREG/CP–XXXX), (3) reports resulting from international agreements (NUREG/IA–XXXX),(4) brochures (NUREG/BR–XXXX), and (5) compilations of legal decisions and orders of the Commission and the Atomic and Safety Licensing Boards and of Directors' decisions under Section 2.206 of the NRC's regulations (NUREG–0750).

U.S.NRC
United States Nuclear Regulatory Commission
*Protecting People and the Environment*

NUREG/CR-7132

# Application of Radar-Rainfall Estimates to Probable Maximum Precipitation in the Carolinas

Manuscript Completed: June 2021
Date Published: June 2022

Prepared by
R. J. Caldwell, J. England, Jr., V.Sankovich

U.S. Department of the Interior
Bureau of Reclamation
Technical Service Center
Water and Environmental Resources Division
Flood Hydrology and Emergency Management Group
Denver, Colorado 80225

Elena Yegorova, NRC Project Manager

NRC Job Code N6570

Office of Nuclear Regulatory Research

# ABSTRACT

Probable Maximum Precipitation (PMP) is a widely-used concept in the design and assessment of critical infrastructure such as dams and nuclear facilities. In the Southeastern United States, PMP estimates are from Hydrometeorological Report 51 (HMR 51). The database of extreme storms used in HMR51 was last updated in the late 1970s. This study focuses on warm-season tropical cyclones in the Carolinas region of the Southeast United States, as these systems are the critical maximum rainfall mechanisms that result in extreme floods. We investigate ten tropical cyclones that impacted the Carolinas during the period 1996-2007. The major focus is to identify if these recent storms challenge the PMP values from HMR 51, in order to assess the adequacy of existing PMP estimates and the need for potentially updating the PMP estimates in a North Carolina-South Carolina pilot region.

The availability of modern, gridded datasets and increasing computing power provide the impetus to improve on existing PMP methods. We utilize the Multisensor Precipitation Reanalysis (MPR) dataset from NCDC, that covers a test region of the Carolinas for the period 1996-2007 and is available at high spatial and temporal resolution. During the period 1996-2007, many tropical cyclones impacted the two states, including Hurricane Floyd in 1999 and seven different storms in 2004, among others. Depth-Area Duration (DAD) calculations and in place storm maximization were performed for ten recent storms. Maximization of these storms also employed modern gridded datasets of moisture-related variables. Transposition, orographics, and envelopment were excluded from the analysis, in order to show in place impacts of new extreme storm data on existing PMP design estimates. Maximized DAD values from the new storms were compared with HMR 51 PMP and three of the largest events that are the basis for HMR 51.

The results suggest that Hurricanes Floyd (1999) and Fran (1996) approach or exceeded HMR 51 PMP at larger area sizes. Hurricane Floyd exceeded the PMP at durations of 24 and 72 hours, while Fran exceeded PMP at a 6-hour duration. The results of the current study should be considered preliminary but suggest an increase in HMR51 PMP estimates for large area sizes may be warranted along the Carolina coasts, based on in place maximization of Floyd and Fran over the Carolinas. The research also provides insight into the sensitivity of the method to several factors, including representative storm moisture, radar biases and grids, and precipitable water. Long-term trends in moisture availability were also investigated using Sea Surface Temperatures (SST) and dewpoints $T_d$ as proxies. Under the pretense of climate change and variability, the potential exists for storm moisture availability and long-term moisture climatologies used in storm maximization factors to increase or change over time. In general, limited significant trends in SSTs were identified along the East Coast or in the Gulf of Mexico. Based on the initial analysis conducted as part of this pilot study, if current SST trends continue, there will likely be little impact on in place moisture maximization factors and PMP. Future work in the Carolinas should consider a focus on the development of methodologies for transposing storms and adjusting these storms based on orographics, and improving the methods developed and used in this project.

# FOREWORD

This report (NUREG/CR-7132) documents work sponsored by the U.S. Nuclear Regulatory Commission (NRC) as part of the RES project "Research to Develop Guidance on Probable Maximum Precipitation (PMP) Estimates for the Eastern United States". The original objective of the project was to provide the NRC with data and analyses to assess whether PMP estimates for the Eastern United States contained in Hydrometeorological Report 51 (HMR 51) published by the National Oceanic and Atmospheric Administration (NOAA) in 1978, could be exceeded if information on more recent storms is considered. However, due to limited resources, the research focused on a pilot region in the Carolinas[1]. The work and recommendations presented in this report will be considered by the NRC as it revises Regulatory Guide 1.59, "Design Basis Floods for Nuclear Power Plants", which was last updated in 1978.

NUREG/CR-7132 focuses on precipitation from warm-season tropical cyclones, as these systems are the critical maximum rainfall mechanisms that result in extreme floods in the Carolinas region of the Southeast United States. The report investigates ten tropical cyclones that impacted the Carolinas during the period 1996-2007, including Hurricanes Fran (1996) and Floyd (1999). The major focus is to identify if these recent storms challenge the PMP values from HMR 51, in order to assess the adequacy of existing PMP estimates and the need for potentially updating the PMP estimates in the Carolinas. The results suggest that an increase in HMR51 PMP estimates for large storm area sizes may be warranted along the Carolina coasts, following further consideration of analysis sensitivities and PMP probabilities.

The report does not make detailed, site-specific recommendations or draw conclusions regarding PMP estimates used for licensing of specific power plants. It would not be appropriate to draw conclusions about the adequacy of flood protection for existing plants based on the work presented in this report since precipitation is only one aspect of flood hazard assessment. It should be noted that, as part of its overall response to the March 2011 Fukushima accident, the NRC has issued a request for information to all power reactor licensees and holders of construction permits under 10 CFR Part 50 on March 12, 2012. The March 12, 2012 50.54(f) letter includes a request that respondents reevaluate flooding hazards at nuclear power plant sites using updated flooding hazard information and present-day regulatory guidance and methodologies.

[1] Reducing the project scope to focus on the Carolinas pilot region does not compromise the applicability of the study. The pilot region has experienced several very large precipitation events in recent years. Analysis of these storms provides a sufficient basis for assessing the possibility that recent storms can challenge the existing PMP estimates for other regions provided in the HMRs.

# TABLE OF CONTENTS

# LIST OF FIGURES

# LIST OF TABLES

# EXECUTIVE SUMMARY

The database of extreme storms used in HMR51 was last updated in the late 1970s. Since that time, numerous extreme rainfall events have occurred across the eastern US, though many have not been analyzed or compared to the existing PMP values. In addition, the availability of modern datasets (e.g., gridded data) and ever-growing computing power provide the impetus to improve on existing methods for computing PMP. The current study capitalizes on these benefits of modern technology to process new storms for inclusion in the current and future PMP-related studies. One such modern dataset is the MPR data available from NCDC. This dataset covers a test region of the Carolinas for the period 1996-2007 and are available at high spatial (2.5 mi x 2.5 mi ; 4 km x 4 km) and temporal (hourly) resolution.

In the Carolinas, the primary meteorological phenomena responsible for extreme rainfall events are tropical cyclones. During the period 1996-2007, many tropical cyclones have impacted the two states, including Hurricane Floyd in 1999 and seven different storms in 2004, among others. Reclamation evaluated the historical gauge records and spreadsheets provided by HPC to select a total of 10 storms for investigation in the current study. MPR for each of these storms was analyzed and DADs computed using an automated software package developed in-house in open source scripting languages. Maximization of these storms also employed modern gridded datasets of moisture-related variables (e.g., SST, PW) to determine the IPMF. The current study did not consider transposition; and, hence, also did not adjust for orographics effects. Envelopment of maximum rainfalls from new storms was also neglected. The DADx values computed were then compared with DADx values from various tropical cyclone events included in HMR51 and with HMR51 PMP directly.

The current research suggests that Hurricanes Floyd (1999) and Fran (1996) approached or exceeded PMP at larger area sizes. Hurricane Floyd exceeded the PMP at durations of 24 and 72 hours, while Fran exceeded PMP at a 6-hour duration. The results of the current study should be considered preliminary but suggest an increase in HMR51 PMP estimates are warranted along the Carolinas coast. The research also provided insight into the sensitivity of the method to: (i) the selection of the CPP; (ii) data quality issues in radar and gauge precipitation measurements; and, (iii) the type of data used for determining IPMFs (e.g., SST and PW). We investigated each of these limitations to highlight the potential caveats and addressed the variability through comparisons with PMP grids and past storms from HMR51. Long-term trends in moisture availability were also investigated using SST and $T_d$ as proxies. In general, limited significant trends were identified along the East Coast or in the Gulf of Mexico.

Future work in the Carolinas should consider a focus on the development of methodologies for transposing storms and adjusting these storms based on orographics. Precipitation potential over the mountainous terrain in the western Carolinas may be enhanced due to additional lift, particularly in upslope-preferred regions along the eastern escarpment of the Appalachians. In contrast, the same region is also farthest from the oceanic moisture sources, which may limit the effects of orographics. Finally, the netCDF format of the MPR data has an additional variable that prescribes an hourly variance value, based on the deviation between precipitation gauge reports and MPR estimated precipitation value at each grid cell. In subsequent studies, if MPR data were available for other locations, the variance grids could be applied in the evaluation of uncertainty in the estimation of DADx using the current methodology.

# ABBREVIATIONS AND ACRONYMS

| | |
|---|---|
| AEP | Annual Exceedance Probability |
| AWA | Applied Weather Associates |
| CAD | Cold air damming |
| CFRB | Cape Fear River Basin |
| COOP | NCDC Cooperative Center |
| CPP | Core precipitation periods |
| DAD | Depth Area Duration |
| ET | Extratropical transition |
| FI | Flood Index |
| FRT | Extratropical cyclone near a front |
| GCIP | Global Energy and Water Cycle Experiment Continental-Scale International Project |
| GCM | Global climate model |
| HMR | Hydrometeorological Report |
| HPC | Hydrometeorological Prediction Center |
| HYSPLIT | Hybrid Single Particle Lagrangian Integrated Trajectory Model |
| ICOADS | International Comprehensive Ocean-Atmosphere Data Set |
| IPMF | In-place maximization factors |
| MPR | Multisensor Precipitation Reanalysis |
| MPE | Multisensor precipitation estimation algorithm |
| NA | North Atlantic |
| NARR | North American Regional Reanalysis |
| NAS | National Academy of Sciences |
| NASA | National Aeronautics and Space Administration |
| NC | North Carolina |
| NCDC | National Climatic Data Center |
| NCEP | National Centers for Environmental Prediction |
| NHDS | NOAA Hydrologic Data Systems Group |
| NOAA | National Oceanic and Atmospheric Administration |
| NLCD | National Land Cover Database |
| NRC | U.S. Nuclear Regulatory Commission |
| NRC | National Research Council |
| NWIS | U.S. National Geographic Survey National Water Information System |
| NWS | National Weather Service |
| OH | NCDC Office of Hydrology |

| | |
|---|---|
| PMF | Probable Maximum Flood |
| PMP | Probable Maximum Precipitation |
| PRE | Predecessor rain events |
| PW | Precipitable water |
| RAMS | Regional Atmospheric Modeling System |
| RES | Office of Nuclear Regulatory Research |
| SA | South Atlantic |
| SACSMA | Sacramento Soil Moisture Accounting model |
| SC | South Carolina |
| SE US | Southeast United States |
| SNOTEL | Natural Resources Conservation Service Snowpack Telemetry |
| SST | Sea surface temperature |
| TC | Tropical cyclone |
| USACE | U.S. Army Corps of Engineers or Corps |
| WSI | Weather Services International Corporation |

# 1 INTRODUCTION

Extreme storm rainfall data are essential in the assessment of potential impacts to design precipitation amounts, which are used in flood design criteria for dams and nuclear power plants (Prasad et al., 2011). Probable Maximum Precipitation (PMP) from National Weather Service (NWS) Hydrometeorological Report 51 (HMR51; Schreiner and Riedel 1978) is currently used for design rainfall estimates in the eastern U.S. These design estimates are based on a U.S. Army Corps of Engineers storm Depth-Area Duration (DAD) catalog (USACE, 1973) that is nearly 40 years old (England et al., 2011) that includes storms from the period of 1889 to 1972. In the past several decades, several extreme precipitation events have occurred, such as Hurricane Floyd (1999), Tropical Storm Jerry (1995), and Hurricane Gaston (2004) that have the potential to alter the PMP values across the Southeastern United States, including North and South Carolina. Unfortunately, these and other large precipitation-producing storms have not been analyzed or archived with the detail required for application in design studies.

## 1.1 Authorization

This work was completed by the Bureau of Reclamation (Reclamation) for the Nuclear Regulatory Commission (NRC), Office of Nuclear Regulatory Research (RES), via an Interagency Agreement. The work was performed under NRC Agreement RES-08-127, Job Code N6570. A pilot study region, including the states of North and South Carolina, was used. This report documents work from Task 2 of the NRC agreement, including new storm data collection and analysis. England et al. (2011) provide a literature review conducted as Task 1 of the agreement. Caldwell et al. (2011) synthesize PMP results with uncertainties, as part of Task 3 of the agreement.

## 1.2 Background

Since the mid-1970s, advances in technology have provided the ability to analyze new storms based on digital data (e.g., radar) that is now available in gridded format. In addition, digital versions of formerly analog weather maps and text precipitation gauge data are now easily accessible online. Increases in computational power allow the procedures for processing individual storm datasets to be automated and iterative investigation of the methodology to be performed without large investments of time and labor. For example, several methods have been employed to generate DAD curves from radar-rainfall data (Durrans et al., 2002; AWA, 2008; Clemetson and Melliger, 2010). Durrans et al. (2002) directed a study under the auspices of the NWS to generate depth-area relationships in the Arkansas-Red River Basin River Forecast Center domain. The method by Clemetson and Melliger (2010) of the USACE employs GIS software and an Excel spreadsheet to generate DAD plots. The availability of gridded precipitation and open source software packages allows this method to be easily converted to automated scripts for application in the current study.

## 1.3 Objectives

This study focuses on warm-season tropical cyclones (TCs) in the Carolinas region of the Southeast United States (SE US), as these systems are the critical maximum rainfall mechanisms in the SE US that result in extreme floods. The current study seeks to evaluate the potential of the more recent events, like those mentioned above, to reach or exceed current values of PMP that were based on datasets last updated in the mid-1970s. The study objectives of this part of the work include: extreme storm data collection, focusing on radar products; DAD

computations; analysis of individual storms; in-place moisture maximization of storms; and comparisons to PMP. The present study is limited to the following aspects: ‘standard’ PMP maximization concepts (WMO, 2009) are used; in-place analysis of existing storms is performed; orographic enhancement, transposition and envelopment of storms were not considered; and a limited temporal and spatial catalog of extreme storms is developed.

In the following sections, a total of ten storms are examined using modern datasets and methodologies, relative to point measurements used in past studies that provide enhanced spatial and temporal resolution. In addition, as with the DAD computations from Clemetson and Melliger (2010), the potential exists to develop software to process storms mechanistically and efficiently prior to in-depth analysis. Section 2 provides a detailed background on TC precipitation, including the hydrometeorological environments conducive for extreme rainfall events. We provide a synopsis of the datasets used in Section 3 and a full description of the methodology in Section 4. An example of the analysis performed for each of the top ten storms is shown in Section 5 using Hurricane Floyd as a template. Utilizing the newer methods and data requires consideration of potential limitations and evaluation of the newer storms within the context of historical storms used in HMR51. Discussion of issues and limitations, evaluation of the various techniques, and comparison to HMR51 storms and PMP values are presented in Section 6. In addition, a brief investigation of potential implications of climate change on PMP computations is provided. Section 7 includes a brief synopsis of findings and suggestions for future research.

# 2 EXTREME RAINFALL OVERVIEW

North Carolina (NC) and South Carolina (SC) regularly experience impacts from TCs when these storms cross land along the northern Gulf Coast and Atlantic seaboard. Commonly, these storms pass near or across the NC/SC region. The highest likelihood of storms impacting the region occurs during the months of August through October, with greatest threats during September (CSC, 2011; NHC, 2011). It is possible that these storms can occur in succession over a period of several weeks. For example in 2004, Hurricanes Frances, Ivan, and Jeanne all tracked across the SE US in only 20 days, with a total of seven TCs impacting NC/SC in the 60 days between 1 August and 29 September.

Tropical systems can provide either relief from water shortages through recharge of groundwater and surface water storage or can lead to severe flooding with significant damage and loss of life (Rappaport et al., 1999; Feldt, 2009). The NWS (2008) highlighted the extreme rainfall and flooding threat from TCs in a local NWS forecast area surrounding central NC. That document reports rainfall rates of up to 15 cm (6 in) per hour along with maximum rainfall amounts of 109 cm (43 in) in 24 hours with Tropical Storm Claudette that occurred over Alvin, TX in 1979. Hurricane Gaston (2004) dropped 15 to 30 cm (6 to 12 in) of rainfall near Richmond, VA, in only 8 hours, with 26 cm (10.5 in) of rainfall in Kingstree, SC (Franklin, 2005). Radar-rainfall estimates from the storm indicated totals up to 38 cm (15 in) across the eastern Carolinas. Hurricane Dora (1964) and Tropical Storm Fay (2008) dumped over 58 cm (23 in) of rainfall across northern Florida and southern Georgia (Jamski et al., 2009). The following sections describe the physical mechanisms responsible for the generation of extreme rainfall events from tropical systems and the storm selection methods used in the current study for NC/SC.

## 2.1 TC Precipitation Climatology

TC-induced rainfall contributes significantly to the annual precipitation budget over the Carolinas. Several studies have evaluated the contribution of TC rainfall using sites across various regions in the eastern half of the United States. Gleason (2006) found that 8 to 16 percent of annual precipitation that fell along coastal regions was related to TC events, with highest contributions in NC and SC of over 20 percent during the period of August to October, peaking in September. Similarly, Noguiera and Keim (2010) identified September as the primary month of TC precipitation in the eastern United States, with more than 15 cm (5.9 in) along the coastline from Texas to Virginia, making up over 30 percent of the monthly rainfall in eastern NC. Knight and Davis (2007) found that TCs contribute as much as 15 percent of the TC-season rainfall in the Carolinas. Knight and Davis (2007) also identified an increase in TC rainfall during the period 1980-2004, though the increase was more closely related to more storms rather than wetter storms. An east-west gradient across NC in percentages exists as the Appalachian Mountains act as a barrier to moisture transport from the Atlantic Ocean. A local study at the State Climate Office of NC, using 350 sites in NC alone, suggested percentages of 8 to 13 percent of warm-season precipitation were due to TCs (McKemy, 2011). The quantification of the contribution of TCs to extreme rainfall has also been examined using satellite-derived products. One study by Shepherd et al. (2009) showed that the largest number of extreme precipitation days during the period 1998 to 2006 occurred in September and October. The extreme precipitation days were correlated with TC days, with major hurricanes producing the largest magnitudes and storms/depressions contributing more to the overall seasonal total precipitation.

## 2.2 TC Precipitation Generation

Within a TC, the mechanisms responsible for the generation of precipitation, particularly enhanced or extreme rainfall, have been well documented in recent years. In general, TC precipitation is related to the speed of motion, size, strength, and relative positions of various synoptic and mesoscale features. The massive rainfall totals during Hurricane Floyd in 1999 across eastern NC was a significant driver for much of the research; NC State University researchers developed proposals as part of the Collaborative Science, Technology, and Applied Research program and held several workshops to address the need for improved forecasts of warm-season precipitation events, including TCs (Croke et al., 2005; Croke, 2006; Xie and Keeter, 2006). Croke et al. (2005) and Croke (2006) divided 28 TC events affecting NC since 1953 into heavy (>0.59 in ; >15 mm) and light events (<0.59 in ; <15 mm) and used 12 of those events to develop synoptic and mesoscale composites of weather conditions conducive to enhancement of precipitation in the region. They found storm intensity, translation speed, distance from the State of NC, and storm characteristics at landfall were not dominant factors in producing heavy rainfall. Instead, enhanced precipitation was more closely related to the position of synoptic and mesoscale features. Specifically, the presence of an upper-level low over the southern Plains, upper-level divergence ahead of the cyclone, moisture flux inland from the Atlantic prior to the storm, and the development of cold air damming and a coastal front were found to be the primary drivers of heavy rainfall related to TCs.

Cold air damming (CAD) occurs when high pressure positioned over the Northeast United States provides a source of cooler and generally drier air down the east side of the Appalachians. The gradient of temperature, pressure, and density between the airmass over land and the offshore Gulf Stream creates a region of convergence and lift, called the coastal front. As moist, warm air is transported inland ahead of tropical systems, the warm air glides up and over this cold pool, enhancing the lift and moisture available for precipitation production. This process is called isentropic lift and has been shown to be related to enhanced precipitation during TC events (DeLuca et al., 2004; Hartfield, 2006; Beasley and Ryan, 2009; Ryan and Beasley, 2009).

The approach of a trough from the southern Plains states provides the impetus for TCs to undergo what is known as extratropical transition (ET). TCs are generally warm core systems, with warm temperatures throughout the vertical from the surface to the mid-levels of the atmosphere. This also makes them efficient producers of precipitation as warmer air physically can hold more water than cooler air. Upper-level troughs are characterized by cold pools aloft. As the cold pool aloft impinges on a TC from the west, the instability increases as the warm air near the surface becomes relatively more buoyant compared to the warm core structure of a tropical system. For example, despite the moderately quick forward motion of Hurricane Floyd (1999), interaction of the storm with an approaching trough enhanced the extent and intensity of the rainfall and assisted in the development of the surface cold pool or CAD over the Carolinas (Atallah and Bosart, 2003; Atallah et al., 2007).

## 2.3 TC Precipitation Distribution

Using the information from prior studies on synoptic and mesoscale forcing of precipitation related to TCs, Konrad II and Perry (2009) evaluate the relationship between the forcings and

the amount of precipitation produced by dividing the storms into four classes. Class 1 and 2 storms were defined as small and weak systems that mainly occur during the months of June to August. The Class 1 and 2 storms are associated with lighter precipitation than the other two classes. The heaviest rainfall events occur with Classes 3 and 4. Class 3 storms cover a large spatial area and lack the presence of a nearby frontal system. As there is no associated frontal system, isentropic lift is minimal and the heaviest rainfall is generally located along the center of the track. More than 50 percent of Class 3 storms are hurricanes prior to landfall and occur after the peak of the tropical season on September 10th. Each of the Class 3 storms make landfall on the Atlantic seaboard. High values of precipitable water (PW) and low-level moisture flux are common with Class 3 storms. Class 4 storms differ from Class 3 in that there is interaction with a frontal boundary and isentropic lift is enhanced, displacing the precipitation at least 70 percent farther from the center of track than other classes. These storms are typically ET storms with over 75 percent of Class 4 storms occurring after September 10th. Despite having high precipitation totals, these storms move up to 40 percent faster than other storm classes. Hurricane Floyd (1999) might be considered a Class 4 storm.

In addition to the mechanisms responsible for the generation of heavy rainfall in TCs, significant research has also been performed to determine the factors responsible for the distribution of this rainfall. The distribution of rainfall is important for defining the shape of design storms for hydrologic impact assessments. Matyas (2009) described a GIS-based methodology for defining the shape of storms relative to various metrics of environmental conditions using radar reflectivity data. The general consensus is that vertical shear and storm motion are important contributors to rainfall asymmetries (Cline, 2003; Rogers et al., 2003; Chen et al., 2006). Cline (2003) also found orographics to be a dominating factor in the Carolinas as the generally north-south oriented Appalachians create a region of potentially enhanced upslope flow. Haggard et al. (1973) examined the probability of orographically-enhanced rainfall over the Appalachians related to tropical systems. During ET, the main region of precipitation tends to fall to the left of track and the storm becomes tilted westward toward the cooler air aloft. For systems that interact with a surface boundary, for example a coastal front, the precipitation will tend to shift toward that boundary (Gonski, 2006). In the case of Hurricane Floyd, ET and coastal frontogenesis were both occurring, resulting in a large broad area of enhanced rainfall across eastern NC. At the mesoscale, several studies investigated the role of local cold pools in Tropical Storm Hanna (2008). Smith and Blaes (2009) and Eastin (2009) showed that evaporative cooling resulted in enhancement of low-level boundaries, convergence, and thus rainfall.

## 2.4 Other TC Precipitation Research

Often times there are predecessor rainfall events (PREs) ahead of TCs that prime a region for potential flooding. Precipitation prior to the arrival of a storm can saturate soils and fill rivers and streams to capacity. From a scientific perspective, PREs are defined as precipitation amounts of at least 100 mm (3.94 in) in 24 hour well in advance of the TC (Bosart and Galarneau, Jr., 2009). Bosart and Galarneau, Jr. (2009) found that at least one-third of all TCs are associated with PREs. These events are typically driven by the leading edge of the tropical moisture plume that coincides with the region where the lift associated with the upper level jet stream is maximized. The position of the upper-level trough and amplitude of the flow pattern across North America are modulating factors in the occurrence and magnitude of PREs (Jurewicz, Sr., et al., 2009). Tropical Storm Erin (2007) and Tropical Storm Rita (2005) are two examples of PREs with 200-250 mm (7.87 – 9.84 in) of rainfall preceding the passage of the TCs (Moore et al., 2009).

Other research has focused on the development of tools for predicting TC rainfall but will not be described fully here. Of primary note are climatological aides which use analog storms from objective guidance (Roth, 2009), satellite-derived tools to identify regions of enhanced tropical rainfall potential (Kusselson et al., 2009), and stochastic simulation software which uses storm tracks, observed rainfall, and parameterized physics to estimate TC-induced rainfall (Grieser et al., 2009).

## 2.5 Storm Selection

Reclamation identified the top 24 precipitation-producing TCs that affected the Southeast region since the mid-1970s (Table 2-1). A qualitative approach was used to identify the largest events; main factors included maximum point precipitation amounts, TC information and climatology, widespread precipitation, flooding and flood-related impacts, and proximity to the Southeast region. Only 12 of the 24 storms have gridded multi-sensor precipitation reanalysis (MPR; Nelson et al., 2010) data available. Section 3 provides additional details on data sets utilized, including MPR. The top ten storms, from those 12 storms with MPR, were qualitatively selected for analysis based on the size of the innermost isohyet, precipitation pattern, and record-setting rainfall reports. Danny 1997 and Hermine 1998 were not analyzed.

The top ten storms were discriminated further based on track type (Table 2-1; Figure 2-1), as the path of the storm is closely correlated to the synoptic meteorological conditions. The tracks of the ten storms were lumped into five individual types: coastal; stalled offshore; direct; west of Appalachians; and east of Appalachians. Coastal storms (Figure 2-1a) generally approach the coast from the south and are turned to the northeast by an approaching mid- or upper-level trough from the west. These storms also have the potential to interact with the approaching trough and to begin ET, a process that is highlighted in the introduction as conducive to enhanced precipitation production. As described earlier, the position of the Gulf Stream off the coast of NC/SC can also produce a region of baroclinicity (where temperature and pressure gradients drive variations in atmospheric density) between a cooler and drier onshore airmass and much warmer and moist airmass over the Gulf Stream. This atmospheric environment often leads to the formation of a coastal front that progresses inland along with the TC, providing additional convergence and lift at the surface to enhance rainfall. An example of this is found in Srock and Bosart (2009) during Tropical Storm Marco in 1990. Storms which are stalled offshore (Figure 2-1b), present a different mechanism for heavy rainfall generation, as the storms have often been lifted north initially by an approaching trough but were never fully captured in the westerly flow. The storms then stall and move erratically and slowly offshore, sending copious moisture onshore in TC banding features. The greatest risk for large rainfall from these storms is driven by the stationary nature and repeated rainfall over the same areas over a long duration.

**Table 2-1 Top 24 Precipitation Producing TCs affecting the Carolinas (1979-2008)**

| Year | Approximate Dates | Storm | Primary State | Secondary State(s) | MPR |
|---|---|---|---|---|---|
| 1979 | 2 – 7 September | David | NC, SC | VA | |
| 1981 | 15 – 20 August | Dennis | NC | | |
| 1984 | 9 – 15 September | Diana | NC | | |
| 1985 | 26 – 28 September | Gloria | NC | VA,PA | |
| 1989 | 21 – 24 September | Hugo | SC | NC | |
| 1990 | 8 – 14 October | Marco/Klaus | SC | GA,NC | |
| 1994 | 13 – 18 August | Beryl | SC | NC,GA,FL | |
| 1994 | 1 – 4 October | TD 10A | SC | GA,FL | |
| 1995 | 2 – 8 June | Allison | NC, SC | GA | |
| 1995 | 22 – 29 August | Jerry | SC | GA,NC | |
| 1995 | 3 – 7 October | Opal | NC | AL | |
| 1996 | 4 – 8 September | Fran | NC | VA | X |
| 1997 | 17 – 26 July | Danny | NC | SC,AL | X* |
| 1998 | 26 – 29 August | Bonnie | NC | VA | X |
| 1998 | 1 – 6 September | Earl | SC | FL,GA | X |
| 1998 | 13 – 23 September | Hermine | FL | SC | X* |
| 1999 | 28 August – 8 September | Dennis | NC | VA | X |
| 1999 | 14 – 17 September | Floyd | NC | SC | X |
| 2004 | 3 – 11 September | Frances | NC | SC,FL,GA | X |
| 2004 | 25 August – 1 September | Gaston | SC | NC,VA | X |
| 2004 | 13 – 26 September | Ivan | NC | FL,AL | X |
| 2005 | 5 – 16 September | Ophelia | NC | SC | X |
| 2006 | 30 August – 4 September | Ernesto | NC | VA | X |
| 2008 | 17 – 29 August | Fay | NC | GA,FL | |

* Storms with MPR available that were not analyzed in the current study.

**Table 2-2 Top 10 Storms Selected for Analysis and Track Type**

| Storm | Year | Dates | Track Type |
|---|---|---|---|
| Bonnie | 1998 | 26 - 29 August | Coastal |
| Dennis | 1999 | 28 August - 8 September | Stalled Offshore |
| Earl | 1998 | 1 - 6 September | East of Appalachians |
| Ernesto | 2006 | 30 August - 4 September | Coastal |
| Floyd | 1999 | 14 - 17 September | Coastal |
| Fran | 1996 | 4 - 8 September | Direct |
| Frances | 2004 | 3 - 11 September | West of Appalachians |
| Gaston | 2004 | 25 August - 1 September | Coastal |
| Ivan | 2004 | 13 - 26 September | West of Appalachians |
| Ophelia | 2005 | 5 - 16 September | Stalled Offshore |

Direct landfalling storms (Figure 2-1c) travel through an atmospheric weakness in the flow, generally with upper-level high pressure over New England and upper-level low over the Lower Mississippi or Tennessee Valley regions. An example of this type of storm, not included in the current study, is Hurricane Hugo (1989) that produced very high winds but low rainfall totals over the SE US. The storms that make direct landfalls generally travel at moderate to fast translation speeds and heaviest precipitation occurs east of track and adjacent to the Appalachians in regions where the easterly flow enhances orographic lift.

Finally, the east and west of Appalachian storm tracks (Figure 2-1d and Figure 2-1e) are typically also Gulf of Mexico landfalling storms. Again, these storms are characterized by enhanced orographic precipitation along the eastern escarpment of the Appalachians. The recurvature from the Gulf Coast to the northeast indicates the potential for ET and, hence, further enhancement of the rainfall. Some storms that make landfall along the Gulf Coast, particularly the east of Appalachian storms, may have been “left behind” by the trough as in the stalled offshore scenarios. In these cases, the storms are often much weaker, but due to the slow movement and ample moisture supply from both the Atlantic and Gulf of Mexico, the potential exists for significant rainfall. For additional information on the mechanisms for tropical cyclone motion, Chu (2011) provides an excellent discussion in Chapter 4 of the online version of the tropical Cyclone Forecasters’ Reference Guide.

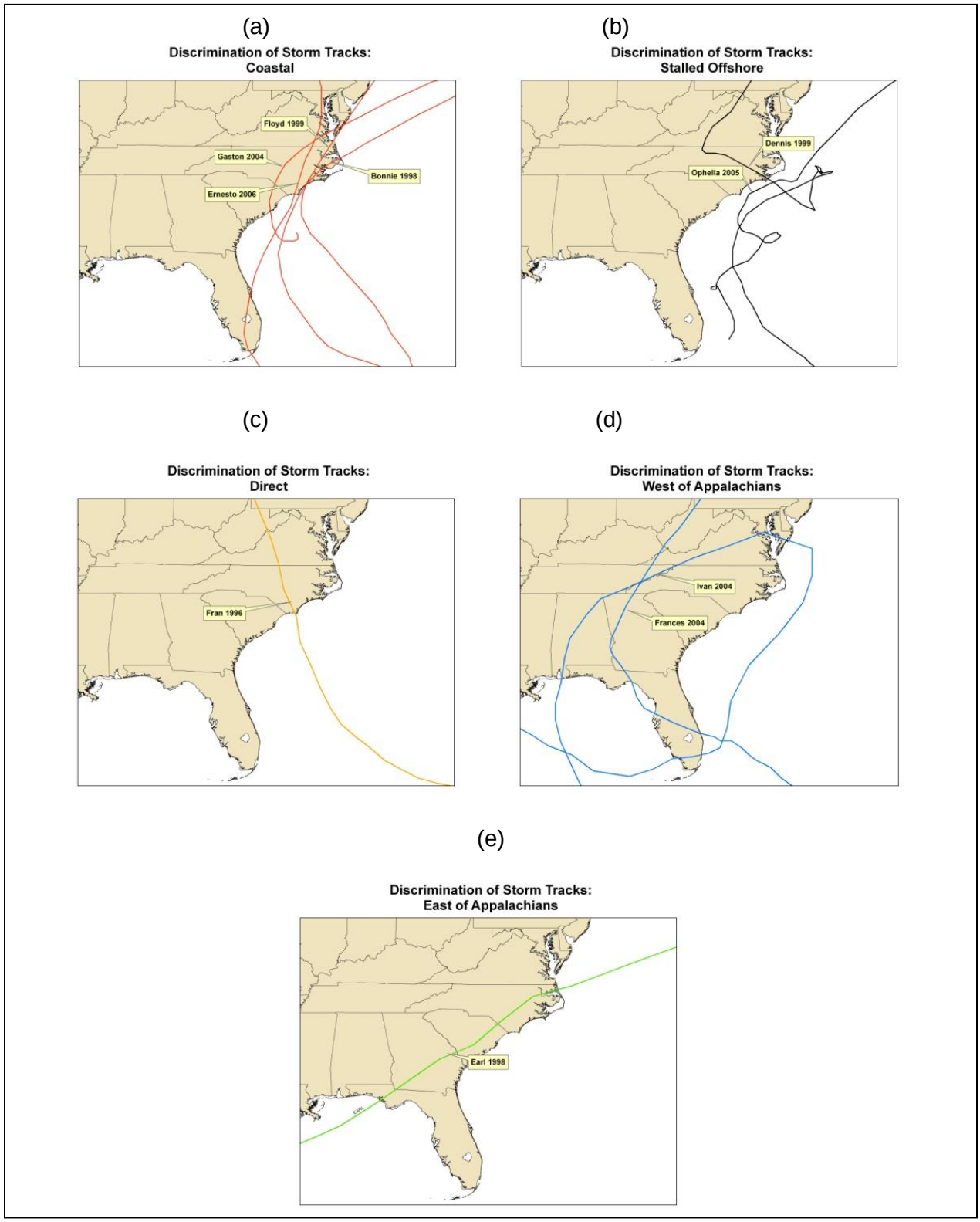


**Figure 2-1 Storm Track Discrimination for the Top 10 Storms**

Based on the limited number of storms analyzed in the current study, the location of maximum point precipitation is closely related to the type of storm track and synoptic forcing mechanisms (Figure 2-2). The direct, stalled offshore, and coastal storms produce highest rainfall totals along the coast, nearest to the source of moisture and during the time when intensity was highest as it passed near or across the Carolina coastlines. Storms that made landfall along the Gulf Coast generally had highest precipitation totals in the piedmont and mountainous terrain across the western Carolinas. The individual point maximum storm total precipitation values are presented in Section 4 (Table 4-1). Each of the 10 storms had maximum point rainfall totals in excess of 25 cm (10 in), with Floyd (1999) and Frances (2004) having observations of greater than 58 cm (23 in).

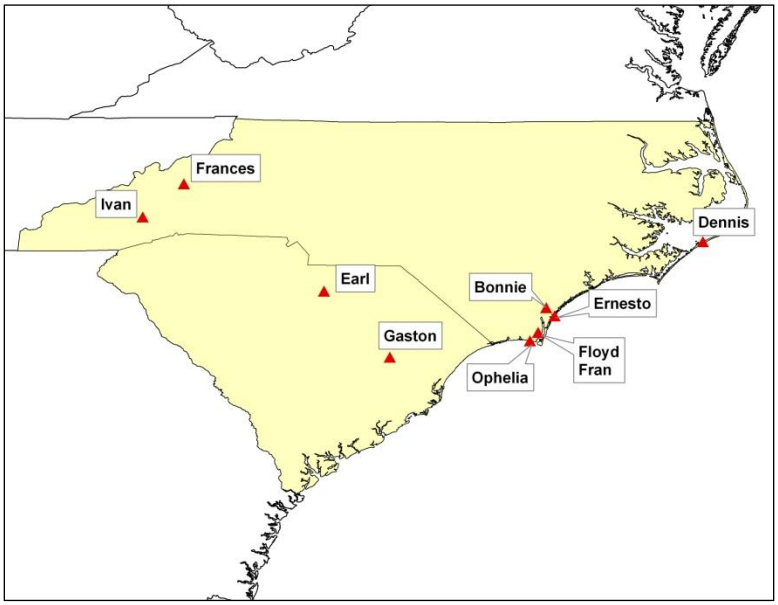


**Figure 2-2 Sites are primarily concentrated near the coast for storms approaching from the Atlantic. Storms making landfall along the Gulf of Mexico produced highest rainfall totals in the piedmont and mountain regions**

# 3 METEOROLOGICAL DATA

Various meteorological data were gathered and synthesized for use in the storm analyses in the current project. First, general information was downloaded and used to describe the individual storms, including the synoptic evolution, definition of start and end dates of precipitation, and the point maximum precipitation values for each storm. Subsequently, radar-estimated precipitation data were downloaded and processed to generate high spatial and temporal resolution grids of storm total and various storm duration rainfall. Finally, additional datasets were required to determine in-place maximization factors (IPMFs) for each storm, including: sea surface temperature (SST) and PW. Although not included in the current study, meteorological data were also collected for other storms of interest (see Section 3.10). A synthesis of data and synoptic discussion for each storm is presented in Appendix A.

## 3.1 TC Tracks

TC tracks were downloaded from GeoCommons for the period 1851-2008 in shapefile format (http://geocommons.com/overlays/15782). These data were uploaded to the site by staff at the National Oceanic and Atmospheric Administration (NOAA) Coastal Services Center (CSC) and contain the following metadata for each storm: name, category, winds, time/date, latitude/longitude, and barometric pressure. Additional information on TCs in the Atlantic Basin can be found at the National Hurricane Center website (http://www.nhc.noaa.gov). The TC data were used for discrimination of the storm tracks described in Section 2. In addition, the tracks for the top ten storms were overlaid on the storm total precipitation maps for reference and to identify the location of the maximum precipitation relative to the track. While limited analysis was performed in the current project to identify relationships between forward speed and storm strength at the time each storm affected the Carolinas, this dataset would also allow that type of in-depth examination in the future.

## 3.2 Radar

The National Climatic Data Center (NCDC; http://www.ncdc.noaa.gov) offers online viewing of national mosaic reflectivity images at daily or sub-daily time steps for the period 1 April 1995 to present. These images are provided by Weather Services International Corporation (WSI) and the National Aeronautics and Space Administration (NASA) though the Global Energy and Water Cycle Experiment Continental-Scale International Project (GCIP). The instantaneous images of radar were used in conjunction with TC dates provided by the Hydrometeorological Prediction Center (HPC) to determine approximate start and end dates of precipitation for each of the top ten storms.

## 3.3 Surface Weather Maps

Daily surface weather maps provide a snapshot of the synoptic conditions, generally around 7am EST (12 UTC), each day. Historical maps are available for the period 1871-2002 from the NOAA Central Library (http://docs.lib.noaa.gov/rescue/dwm/data_rescue_daily_weather_maps.html). The hard copy maps were digitized using funding from the NOAA Climate Data Modernization Program. Since 2002, the HPC provides electronic daily weather maps online at http://www.hpc.ncep.noaa.gov/dailywxmap/index.html. In general, these maps show details on barometric pressure, temperature, precipitation, wind, and moisture (e.g., dewpoint temperature ($T_d$)) at the surface. The web-based maps from HPC also provide a map showing 500-hPa heights and

temperatures. The surface maps are used to evaluate the synoptic conditions present for each of the top ten storms and to further refine the start and end dates of precipitation (when necessary). The synoptic discussions provided with each of the top 10 storms (Appendix A) are based on these maps. Intermediate time periods through the storm duration are not available and, therefore, identification of the mesoscale forcing mechanisms responsible for localized heavy rainfall centers is not explicitly performed for the discussions.

## 3.4 HPC TC Precipitation

NOAA Hydrometeorological Prediction Center provides information on individual TCs. David Roth of the HPC has spent an inordinate amount of time and effort in developing a detailed TC rainfall climatology (http://www.hpc.ncep.noaa.gov/ tropical/rain/tcrainfall.html). Total storm rainfall and daily rainfall totals for available sites during each storm have been compiled into Excel spreadsheets and were made available by HPC for the NRC project. For each significant precipitation-producing storm, the website provides a brief synoptic discussion and general isohyetal maps for a wealth of storms for the period 1968 to present. Daily rainfall totals were used to define the preliminary start and end dates for each TC before refinement with NCDC instantaneous radar and surface weather maps. In addition, the maximum point storm total rainfall amounts for each storm were extracted from the database for use as reference locations in computing back-trajectories (Section 4.3).

## 3.5 Hourly/Daily Point Precipitation

The NOAA Hydrologic Data Systems Group (NHDS) provides access to historical data used for the calibration of hydrologic models and development of hydrometeorological techniques. The inventory of historical data at NHDS is a copy of other agencies' data that consists of: NCDC Cooperative Observer (COOP) and Surface Airway Observation (SAO) stations; Natural Resources Conservation Service Snowpack Telemetry (SNOTEL) sites; and United States Geological Survey National Water Information System (NWIS) data. The historical data are available in raw format or NWS Office of Hydrology (OH) datacard format. These data are used operationally at the River Forecast Centers during calibration of the Sacramento Soil Moisture Accounting (SACSMA) model. Both hourly and daily precipitation data are available from the site, but the current study focused on gathering and use of the hourly data for direct comparison with hourly MPR. The hourly data are available for the period 1948 to present and were extracted for a total of 65 sites in the Carolinas (Figure 3-1). These data were used in the development of mass curves and in determining the mean bias of the radar over individual storm durations.

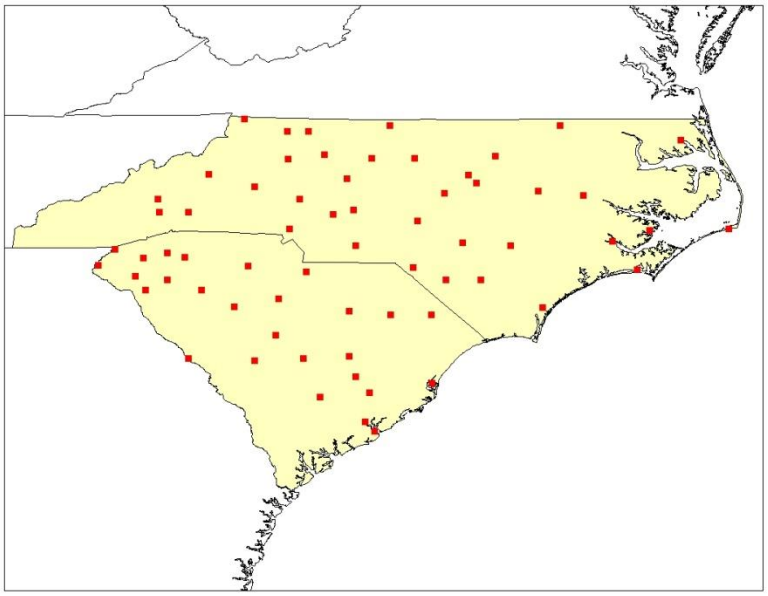

**Figure 3-1 Locations of the 65 hourly precipitation sites from NHDS. Number of potential sites in NC and SC were 38 and 27, respectively. Only sites with non-zero storm total accumulations were used for comparisons**

## 3.6 Multisensor Precipitation Reanalysis

The MPR dataset is created to replace the Stage III precipitation estimation product produced at the NWS River Forecast Centers. The MPR is created using the multisensor precipitation estimation (MPE) algorithm, an expression designed to merge radar and rain gauge observations of precipitation. Data are available from 1996 to 2007 at one hour increments for a study region of NC and SC, as shown in Figure 3-2 (Nelson et al., 2010). This dataset is extremely useful and critical for extreme rainfall estimation and PMP comparisons, because hourly precipitation is provided on 2.5 mi x 2.5 mi (4 km x 4 km) grids, which are subsequently aggregated to determine precipitation depths at longer durations with high spatial resolution (Section 4). The resulting accumulated grids at various temporal resolutions are used to generate DAD relationships. The domain of the MPR project is closely aligned with the focus region of the NRC NC-SC pilot project, and serves as the primary basis for evaluating the top ten TCs during the period.

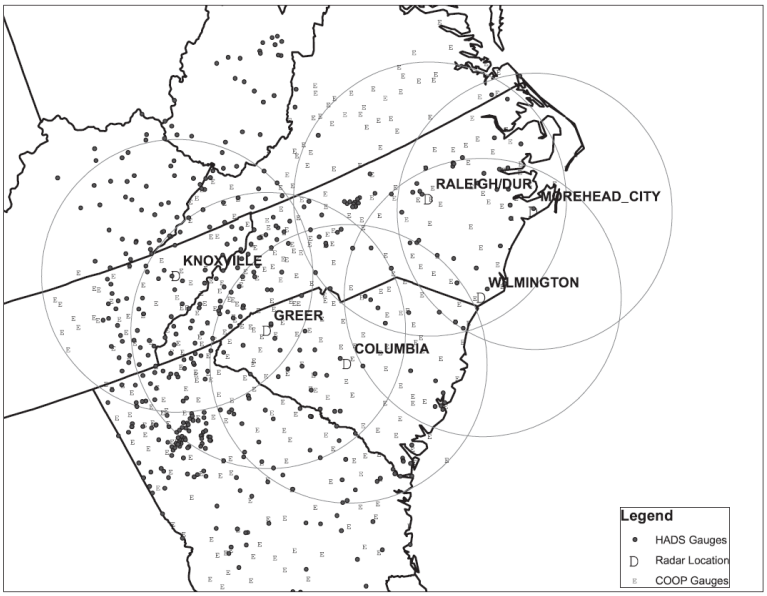


**Figure 3-2 Radar locations and range rings of 230 km (143 mi) (Nelson et al., 2010). Rain gauges used in MPR calibration and bias computations are also shown**

## 3.7 Sea Surface Temperatures

The International Comprehensive Ocean-Atmosphere Data Set (ICOADS) Release 2.5 (Woodruff et al., 2005; Woodruff et al., 2011) is the most extensive collection of surface marine data spanning the past three centuries. Monthly values are available for the period January 1960 to present on a 1- x 1-degree latitude-longitude global grid. Multiple variables are available within this dataset including monthly mean and standard deviation of SST, wind, pressure, air temperature, and other relevant surface fluxes and observations. The ICOADS data are provided in netCDF format by the National Oceanic and Atmospheric Administration/Office of Atmospheric Research/Earth Systems Research Laboratory/Physical Sciences Division (NOAA/OAR/ESRL/PSD) in Boulder, Colorado, using online download (http://www.esrl.noaa.gov/psd/data/gridded/ data.coads.1deg.html). To convert from the netCDF format, the SST monthly mean and standard deviation grid values used in this project require adding an offset of 327.65 and 322.65, respectively, and adjusting for a scale factor of 0.01.

The NOAA high-resolution, blended analysis of daily SST and ice dataset is available on a 0.5- x 0.5-degree latitude-longitude grid for the period 1981 to present from the NOAA/OAR/ESRL/PSD in Boulder, CO (Reynolds et. al., 2007) via download (http://www.esrl.noaa.gov/psd/data/gridded/ data.noaa.oisst.v2.highres.html). Daily and long-term means, errors, and anomalies were available for download in netCDF format. The daily SSTs were sub-sampled to a 1- x 1-degree latitude-longitude grid using the Geospatial Data Abstraction Library (GDAL) to allow for comparison with the coarser-resolution ICOADS monthly data. To convert from the netCDF format, the SST daily values require adjustment using a scale factor of 0.01.

The monthly SST data are used in this project to compute a maximum SST value for each month, defined as the monthly mean plus two standard deviations (an approximate of the 1-in-100 year event). Daily SST data are used to extract a storm representative SST. Each SST value is then converted to a PW value. Additional details on the procedures used to generate these values and for extraction are provided in Section 4. The monthly SST data are also used to calculate trends using the Kendall-Theil slope for the period of record (Helsel and Hirsch, 1992; Granato, 2006). Kendall-Theil is a robust, non-parametric method resistant to the effects of outliers and non-normality in residuals. The slope is computed as the median of all possible pair-wise slopes between points. The Kendall tau is a measure of correlation and is used to test for significance of trend.

## 3.8 Precipitable Water

The National Center for Environmental Prediction/National Centers for Atmospheric Research (NCEP/NCAR) Reanalysis 1 dataset provides daily and monthly values of various atmospheric variables for the period January 1948 to present, including integrated PW (Kalnay et. al., 1996). The NCEP/NCAR reanalysis project uses a state-of-the-art analysis/forecast system to perform data assimilation using historical meteorological data. Both daily and monthly data are downloaded from the NOAA/OAR/ESRL/PSD in Boulder, CO, in netCDF format on a 2.5- x 2.5-degree latitude-longitude grid. Similar to the SST grids, the monthly PW grids are used to generate a maximum PW value as mean plus two standard deviations; the daily grids are used for calculating a storm representative PW value. The PW grids are substituted when the methodology with SST fails to produce results and for comparison of past storms prior to 1981 when daily SST data are unavailable.

## 3.9 Specific Humidity

The NCEP/NCAR Reanalysis 1 dataset provides daily and monthly values of various atmospheric variables for the period January 1948 to present, including specific humidity (Kalnay et. al., 1996). The NCEP/NCAR reanalysis project uses a state-of-the-art analysis/forecast system to perform data assimilation using historical meteorological data. The monthly data are downloaded from the NOAA/OAR/ESRL/PSD in Boulder, CO, in netCDF format on a 2.5- x 2.5-degree latitude-longitude grid. The monthly specific humidity grids are converted to grids of $T_d$ using Teten's formula from Stull (1988). The $T_d$ data are used to calculate trends using the Kendall-Theil slope for the period of record, in the same manner as was performed using the monthly ICOADS SST data.

## 3.10 Other Storm Data Collected

For the additional storms listed in Table 2-2 that did not have MPR available, and for the Rapidan, VA, storm of 1995 (Smith et al., 1996), various meteorological datasets, such as 500 hPa charts and daily precipitation analyses, were gathered and archived separately. Table 3-1 provides an accounting of these supplemental datasets collected. These storms could be considered as part of future extreme rainfall studies in the Southeast.

**Table 3-1 Top 10 Storms Selected for Analysis and Track Type**

| Storm | Surface Map | NCDC Radar | Additional Maps |
|---|---|---|---|
| Alberto 1994 | X | | |
| Allison 1995 | X | X | |
| Beryl 1994 | X | | |
| Danny 1997 | X | X | |
| David 1979 | X | | |
| Dennis 1981 | X | | |
| Diana 1984 | X | | |
| Fay 2008 | X | X | X |
| Gloria 1985 | X | | |
| Hermine 1998 | X | X | |
| Hugo 1989 | X | | |
| Jerry 1995 | X | X | |
| Marco/Klaus 1990 | X | | |
| Opal 1995 | X | | |
| Rapidan, VA 1995 | X | X | |
| TD #10A 1994 | X | | |

# 4 METHODOLOGY

The procedure for processing each of the individual storms involves the manipulation of hourly gridded precipitation data to generate two-dimensional, latitude-longitude grids at various durations for computation of DAD relationships and curves. In addition, comparisons of the hourly accumulations from point measurements (i.e., rain gauge sites) to the gridded precipitation values were performed using mass curves. The general methodology for precipitation processing is presented in Figure 4-1. Once the DAD curves were calculated, each storm was maximized in place using moisture maximization techniques from HMR 57 (Hansen et al., 1994) and HMR 59 (Corrigan et al., 1999) to estimate PMP (see Figure 4-2). This section describes the methodology and software used to process the input data presented in Section 3. Some further details on processing steps are included in Appendix B, with software listed in Appendix C.

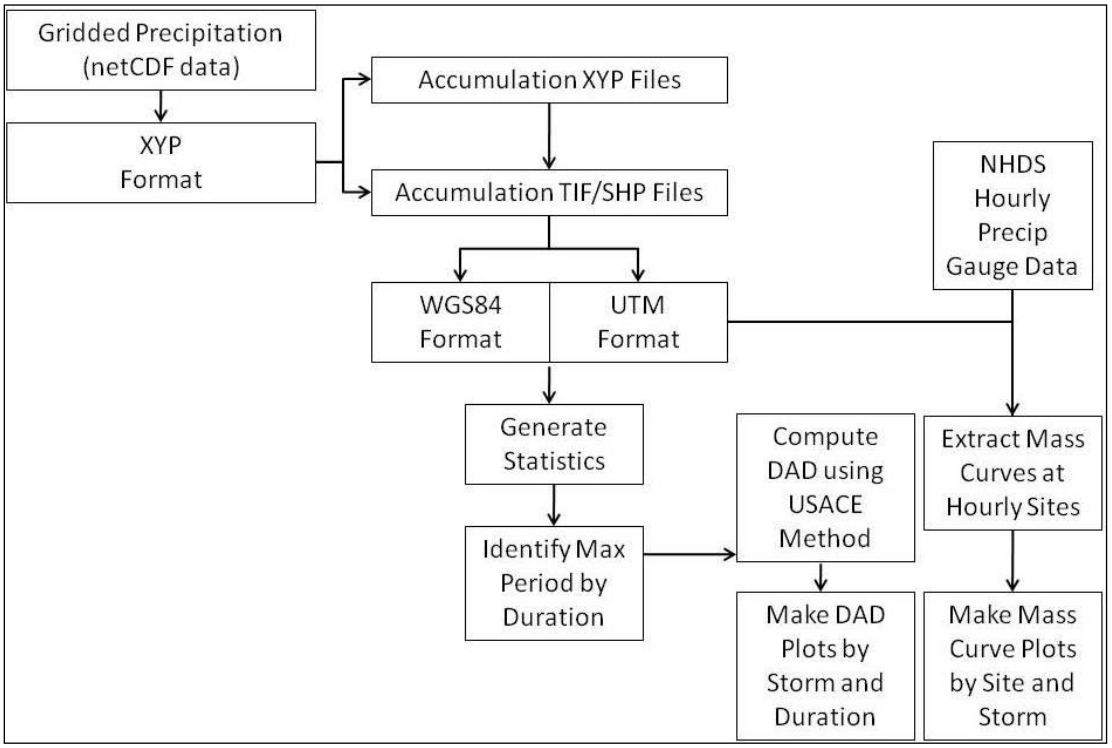


**Figure 4-1 Flow chart depicting the procedure for processing gridded precipitation data**

## 4.1 Precipitation Processing

Start and end dates for each of the TCs were initially extracted from the HPC TC precipitation website. Since these dates were all-inclusive for all affected states/regions, the NEXRAD radar images from NCDC were evaluated at three-hour intervals to determine the appropriate dates of rainfall impacts in the Carolinas. Start and end times were prescribed as 0000 UTC and 2300 UTC on the start and end dates, respectively. The result was a set of start and end time stamps used to define the storm total accumulation period.

For each storm period, the hourly precipitation estimates provided by MPR were accumulated by hour using GDAL and shell scripts to generate 6-hour, 12-hour, 24-hour, 72-hour, and storm total precipitation amounts, with output in text and gridded (tiff) formats. Grids were output in both geographic (World Geodetic System 1984; WGS 84) and projected coordinates (Universal Transverse Mercator Zone 17 North; UTM Zone 17N). The grid resolutions were 0.05 degrees latitude-longitude in geographic coordinates, or 4 km (2.5 mi) in UTM. Maximum and mean values for each grid were identified and used to select the core precipitation periods (CPPs) for all durations. For CPPs that were not "stacked", or overlapping in time, the maximum value during the stacked period was selected instead.

Using the hourly point precipitation data from NHDS, the gridded storm total precipitation files were compared to accumulated storm total gauge data over the storm total accumulation period. In addition, mass curves were generated using the same point precipitation sites. Subsequently, the same point locations were used to extract the cell values for each hour from the MPR using the command xyz-vs-gdal.py. Mass curve plots were generated using R, an open source statistical programming language (see Appendices B and C for details).

## 4.2 DAD Calculations

Basic DAD methodologies and computation approaches are described in England et al. (2011). There are very few approaches that utilize gridded data for DAD estimation; software is not readily available. The USACE developed a methodology to generate DAD curves from gridded precipitation data (Clemetson and Melliger, 2010) using ArcGIS and Microsoft Excel. Due to the computational expense of processing storms individually using this method, Reclamation extracted the concepts and methodology behind the USACE programs and developed open source scripts in shell and GDAL to perform the DAD analysis in batch mode.

To compute the DAD, the CPP accumulation grid at each duration for each storm was converted to ASCII text format, then counts of the number of cells above a threshold precipitation value (typically incrementally by one inch from one inch to the floor of the maximum value) and the mean value of those cells is computed and output to a DAD summary file. Since the MPR is available on a 4x4 km (2.5 x 2.5 mi) grid, the number of cells is easily converted to an area size. The resulting summary files were ingested into R software to generate plots of DAD for each storm and duration.

## 4.3 Moisture Maximization

HMR51 (Schreiner and Riedel, 1978) outlined a methodology for generating storm IPMFs based on moisture availability using the reference and maximum dew point temperature at 1000-hPa as a proxy for determining PW content of the atmosphere. HMRs 57 and 59 introduced the concept of using SST values as the proxy for PW, since many of the coastal storms in the western U.S. have moisture source regions over the Pacific Ocean (Hansen et al., 1994; Corrigan et al., 1999). Similarly, for the current project, TC moisture in the SE US typically originates from the Gulf of Mexico or Atlantic Ocean. Therefore, it is appropriate for this study to utilize the SST concepts from HMR 59 to estimate PW for the SE US TC events, rather than land-based $T_d$ observations. The flow chart for converting SST to PW and generating IPMFs is shown in Figure 4-2.

Potential moisture source regions for each storm were determined by first identifying the location of maximum storm total precipitation from HPC's spreadsheets of TC precipitation for each of the top 10 storms. Precipitation statistics for the top 10 storms are provided in Table 4-1. Using the online HYSPLIT model tool from the NOAA Air Resources Laboratory (Draxler and Rolph, 2011; Rolph, 2011), back-trajectories were generated using a matrix method with the point maximum location serving as the center and eight addition points placed at 1-degree latitude-longitude spacing zonally, meridionally, and diagonally about the center point. The moisture inflow into each storm was assumed to be at 500 meters (0.31 mi) above ground level. The time to start each HYSPLIT run was selected as the start time of the 24-hour CPP identified in the MPR DAD analysis. Back-trajectories of length 24 hours were computed using NCEP/NCAR reanalysis data as input. The HYSPLIT online toolbox provides output in an image and text file format; the text file contains the position information for the origination location of each of the nine initial parcels in the matrix, which is assumed to represent the potential moisture source regions.

Using the output origination locations, the daily SST values from the gridded analyses are extracted using GDAL to approximate the representative SST for each storm. ICOADS maximum monthly SSTs are used to determine the maximum SST value at the same points. The maximum SST is defined as the mean plus two standard deviations (or approximately the 1-in-100 year event) for the warmest month within 15 days of the date of the back trajectory origination date, which follows the same assumptions made in HMRs 57 and 59. Warmest months were determined using the regional mean monthly SST from the NCEP/NCAR reanalysis for the area of 20 to 50 N latitude and 90 to 70 W longitude (Figure 4-3).

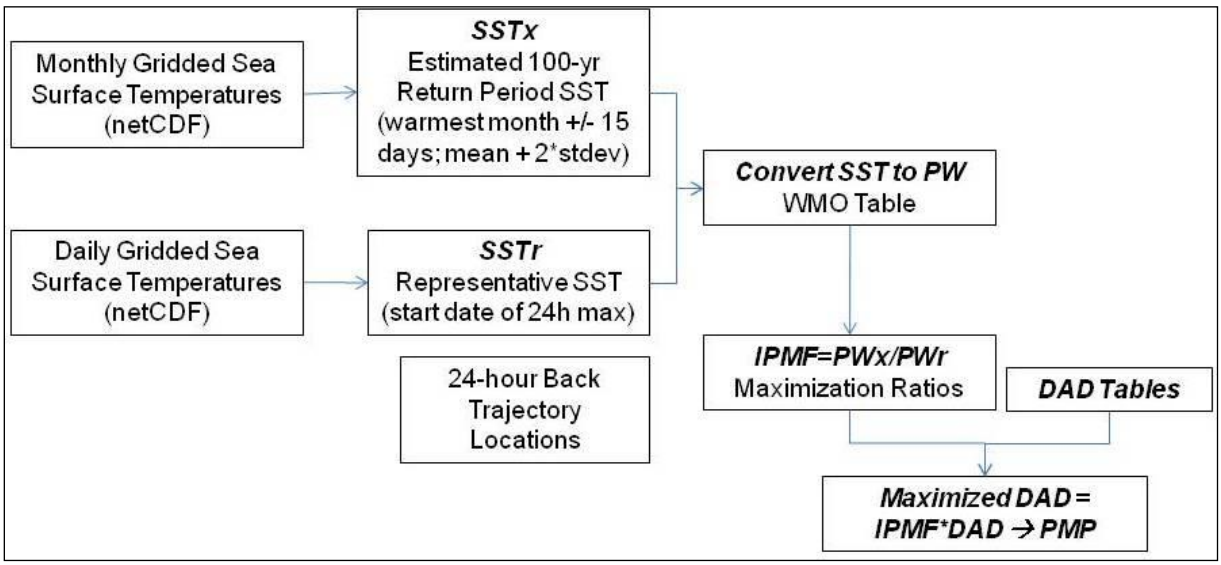


**Figure 4-2 Flow chart depicting the procedure for generating IPMFs**

**Table 4-1 Maximum precipitation statistics for the top 10 storms affecting the Carolinas**

| Storm | Site | Location * | Elevation (ft) * | Point Max (in) | Grid Max (in) | CPP Start Time | SST/PW Month |
|---|---|---|---|---|---|---|---|
| Bonnie | Wilmington 7N, NC | 34.3N, 77.9W | 30 | 14.61 | 6.96 | 26 August 1998 06 UTC | August |
| Dennis | Ocracoke, NC | 35.1N, 76.0W | 4 | 19.91 | 24.69 | 6 September 1999 08 UTC | August |
| Earl | Kershaw, SC | 34.5N, 80.6W | 300 | 10.14 | 7.84 | 3 September 1998 08 UTC | August |
| Ernesto | Wrightsville Beach, NC | 34.2N, 77.8W | 6 | 14.61 | 16.22 | 31 August 2006 15 UTC | August |
| Floyd | Southport 5N, NC | 34.0N, 78.0W | 20 | 24.06 | 32.61 | 15 September 1999 13 UTC | August |
| Fran | Southport 5N, NC | 34.0N, 78.0W | 20 | 12.65 | 20.80 | 5 September 1996 12 UTC | August |
| Frances | Mount Mitchell, NC | 35.8N, 82.3W | 6240 | 23.57 | 16.72 | 7 September 2004 12 UTC | August |
| Gaston | Kingstree, SC | 33.7N, 79.8W | 66 | 10.98 | 10.09 | 1 September 2004 00 UTC | August |
| Ivan | Cruso, NC | 35.4N, 82.8W | 2935 | 17.00 | 22.21 | 16 September 2004 22 UTC | September |
| Ophelia | Oak Island WTP, NC | 33.9N, 78.1W | 15 | 17.50 | 18.18 | 14 September 2005 12 UTC | August |

* Elevation and location are approximated when values were unavailable from HPC. Location rounded to nearest 0.1 degree.

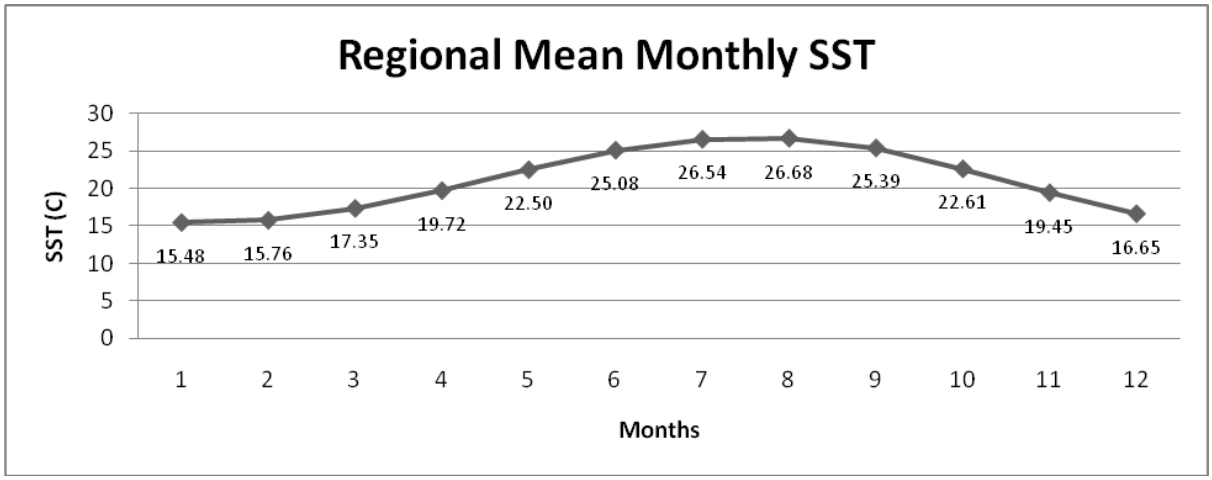


**Figure 4-3 Monthly average SST from NCEP/NCAR Reanalysis for the period 1948 to 2010 for the region 20N to 40N latitude and 90W to 70W longitude**

Once storm-representative SST and maximum SST values were computed, values from the PW tables in the WMO (2009) PMP report were tabulated and a polynomial model of PW was fit against temperature in degrees Celsius (Figure 4-4) to facilitate interpolation of table values. Using the resultant equation (see Figure 4-4 inset), estimates of PW (y) are computed from the representative and maximized SST values (x). The maximized PW may then be divided by the representative PW to obtain the IPMF.

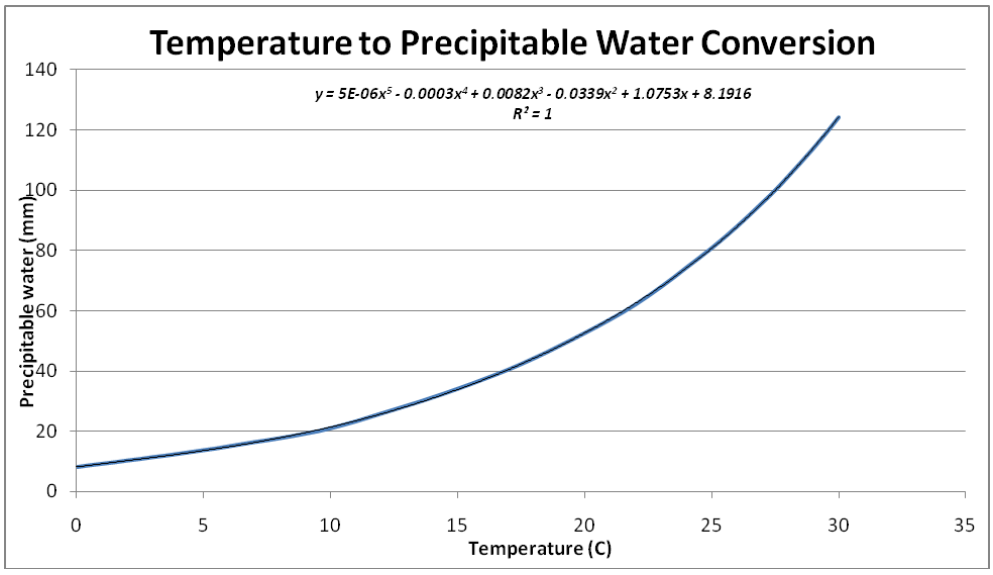


**Figure 4-4 Method for converting temperature values to PW using tabulated values from Table A.1.3 in WMO (2009)**

To evaluate the sensitivity of the IPMF to a representative site location, and to identify potential uncertainty and variability in the current methodology, the representative and maximized PW values from each storm were recomputed using all available combinations. For example, if only two source locations had been used, the representative PWs (e.g., r1 and r2) could be combined with the maximized PWs (e.g., m1 and m2) such that the resulting exhaustive combinations would include four potential ratios (e.g., m1/r1, m2/r1, m1/r2, and m2/r2). Using R statistical software, the resultant IPMFs for all combinations were plotted as boxplots. Basic statistics (i.e., mean, median, minimum, and maximum) of IPMF were also computed for each storm (Figure 4-5).

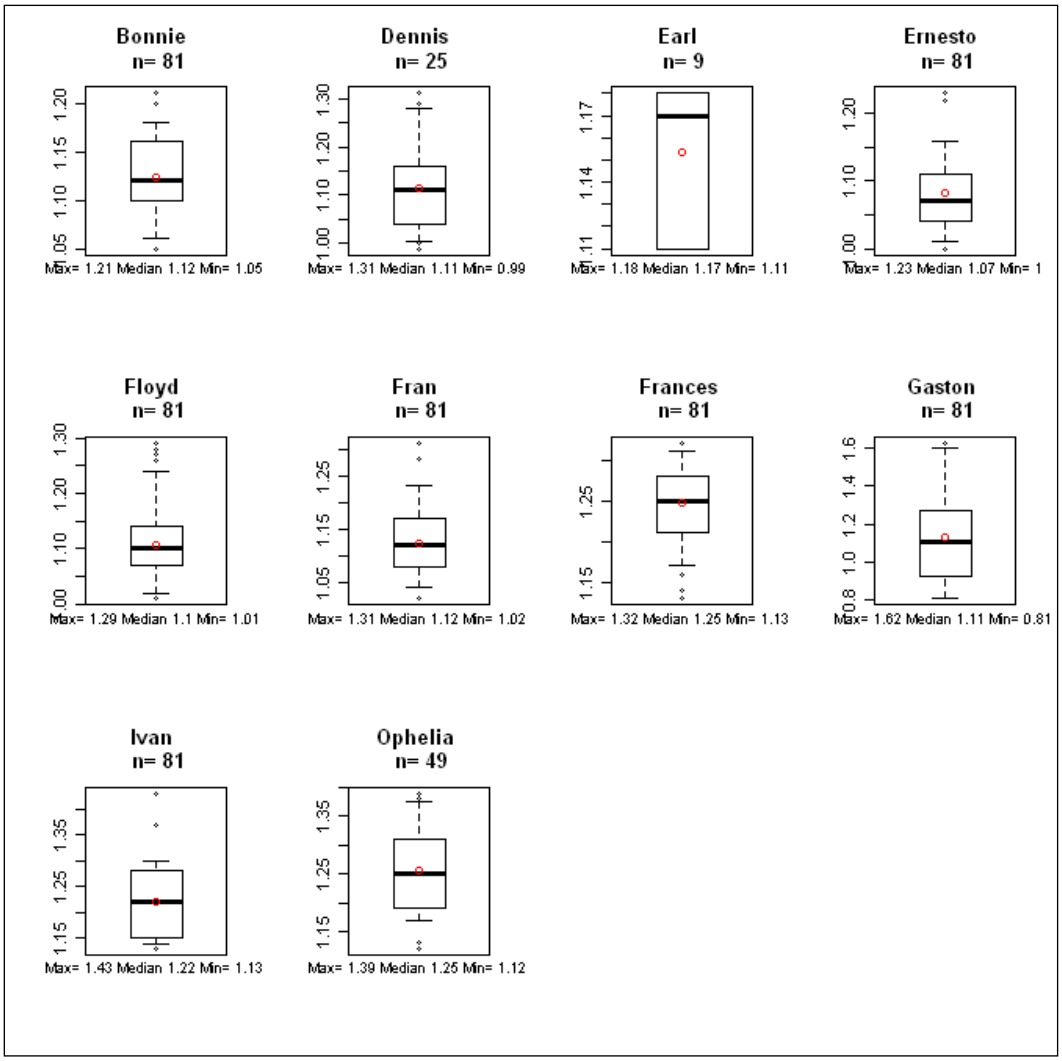


**Figure 4-5 Boxplots of IPMFs for the top 10 newly analyzed storms using gridded SST (except Gaston, which uses NCEP/NCAR gridded PW). Values less than 1.00 are assumed to be 1.00. Whiskers represent 5th and 95th percentiles, box represents interquartile range, solid black line represents median, and red dot represents the mean. Hollow points in black indicate outliers. The value of n represents the number of combinations from HYSPLIT back-trajectories**

For Hurricane Gaston, the source locations from the HYSPLIT model runs were located solely over land areas. To keep with the current methodology, NCEP/NCAR reanalysis values of PW at the daily and monthly time scale were used to generate IPMFs for each storm, using the same conceptual model as with the SST data. A preliminary analysis of the sensitivity of the method to input dataset (e.g., SST vs. PW) showed similar ranges of IPMF (Figure 4-5 and Figure 4-6).

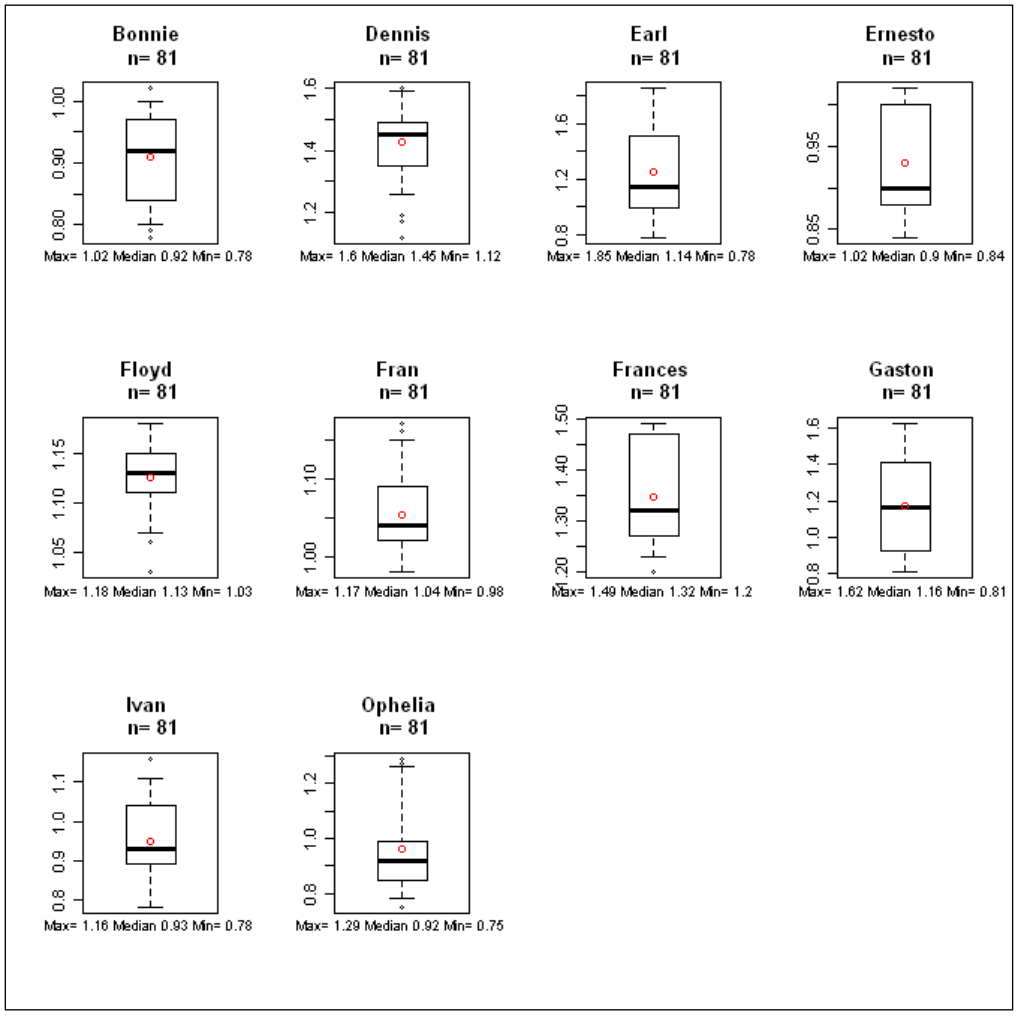


**Figure 4-6 Boxplots of IPMFs for the top 10 newly analyzed storms using NCEP/NCAR gridded PW. Values less than 1.00 are assumed to be 1.00. Whiskers represent 5th and 95th percentiles, box represents interquartile range, solid black line represents median, and red dot represents the mean. Hollow points in black indicate outliers. The value of n represents the number of combinations from HYSPLIT back-trajectories**

The availability of gridded SST data is limited prior to 1960; however, gridded PW data from NCEP/NCAR is available since 1948, which would allow extension of this method to extreme precipitation events from HMR51, particularly the Yankeetown, FL, storm in 1950. In order to

evaluate the method for generating IPMFs from PW grids, three TC events from HMR51 were analyzed using the gridded PW data. The three storms included: (a) Tyro, VA (Hurricane Camille, 1969), (b) Zerbe, PA (Agnes, 1972), and (c) Yankeetown, FL (Hurricane Easy, 1950). The IPMFs obtained from the Appendix in HMR51 for the three test cases were compared to results from the current moisture maximization scheme (see Section 6).

## 4.4 Maximized DAD (DADx) Computations

An in-place storm maximization, DADx, is determined by multiplying the observed storm DAD curves by the appropriate IPMF (Figure 4-2). It is important to note that the current methodology neglects the effects of orographics and does not attempt to perform storm transposition; each of the storms was maximized solely in place. In addition, envelopment of individual storm maximized values for the pilot region is neglected, because the focus of the study is on examination of potential impacts of individual storms on HMR51 PMP.

The definition for PMP is “the greatest depth of precipitation for a given duration meteorologically possible for a design watershed or a given storm area at a particular location at a particular time of year, with no allowance made for long-term climatic trends” (WMO 2009). By calculating the IPMFs using multiple combinations, a range of potential values is provided, with the maximum value used to estimate the greatest potential depth of precipitation. Initial results, as presented in Section 6, indicate that rainfall estimates using the maximum IPMF from several recent TCs approach previously defined PMP from HMR51. To evaluate the sensitivity of the results to other selected IPMFs, we also calculate the DADx using the median value of the IPMFs for those select storms in Section 6.

# 5 INDIVIDUAL STORM ANALYSIS

A storm analysis, including discussions of synoptic environment and DAD computations, is performed for each of the top ten events presented in Section 2 (Table 2-2). For simplicity in the discussions for each of the top ten storms, the reference to intensity is given by the maximum category on the Saffir-Simpson scale reached by the storm during its lifetime. Storm intensity at the time of impact on a particular region is not necessarily indicative of the threat of heavy rainfall; forward speed and storm trajectory are more important predictors of extreme rainfall potential. As an example of the type of results provided for each of the individual storms in the top ten list, the case of Hurricane Floyd is presented, which impacted eastern NC during the period 14 – 17 September 1999 (Figure 5-1). Storm discussions and DAD results for each of the top ten storms are provided in Appendix A. Details on processing steps are included in Appendix B. A directory of electronic files, including data, results and shell scripts for each storm, is presented in Appendix C.

## 5.1 Synoptic Discussion

Hurricane Floyd started as a disorganized tropical wave in the eastern Atlantic Ocean and moved westward on the southern side of a broad high pressure. The tropical wave reached tropical depression status approximately 1000 miles (1600 km) east of the Lesser Antilles on 6 September and tropical storm status on 8 September. The cyclone slowly strengthened over the next few days to become Hurricane Floyd on 10 September around 200 miles (320 km) east-northeast of the Leeward Islands. Floyd then moved on a northwest path to the north of the eastern Caribbean islands then turned westward and strengthened as the storm took aim at the Bahamas. A mid- to upper-level trough over the eastern U.S. eroded the subtropical ridge over the western Atlantic and Floyd turned north then northeast paralleling the coast of Florida. Hurricane Floyd made landfall near Cape Fear, NC on 16 September (Figure 5-1). The brief synopsis was derived directly from NHC preliminary reports (http://www.nhc.noaa.gov/).

Prior to Floyd's landfall, air temperatures across the Carolinas ranged from highs in the 80s, with 60s and 70s in the rain cooled air. Dewpoints during the morning hours were generally in the 60s with several coastal locations in the low 70s (Figure 5-2). A stationary front was positioned along the spine of the Appalachians with surface convergence enhanced by northwest winds west of the front and northeast winds east of the frontal system. As Floyd approached the Carolinas, the frontal system shifted eastward to a position along the coastal plain. The airmass to the west over the Ohio Valley was also much cooler and drier with dewpoints in the 40s. Isentropic upglide and frontal enhancement through convergence of winds at the surface led to widespread rainfall across the eastern Carolinas and Virginia (Figure 5-2 and Figure 5-3). More stable air to the west and southwesterly shear from the mid-level trough limited the westward extent of rainfall.

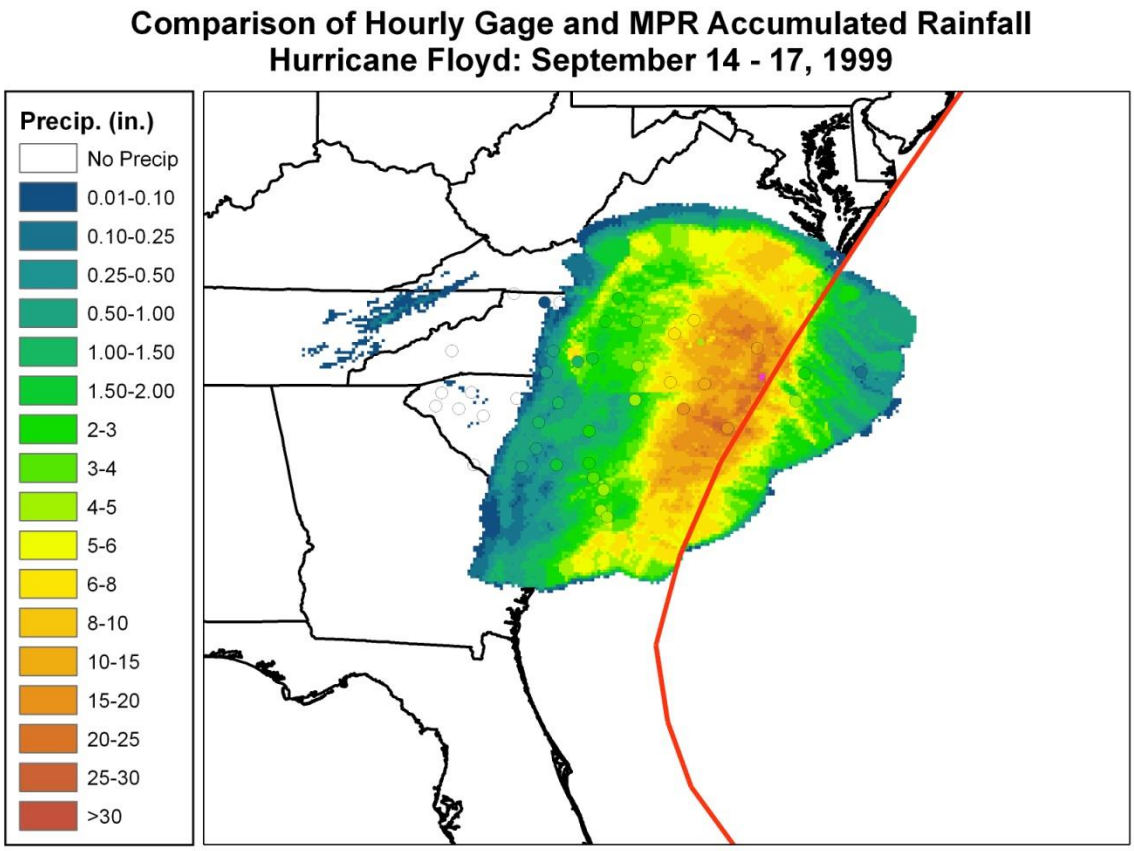


**Figure 5-1 Storm total precipitation (based on MPR) for Hurricane Floyd with best storm track from NOAA shown in red. Hourly precipitation gauge accumulations are overlaid to indicate differences between gauge and radar estimates**

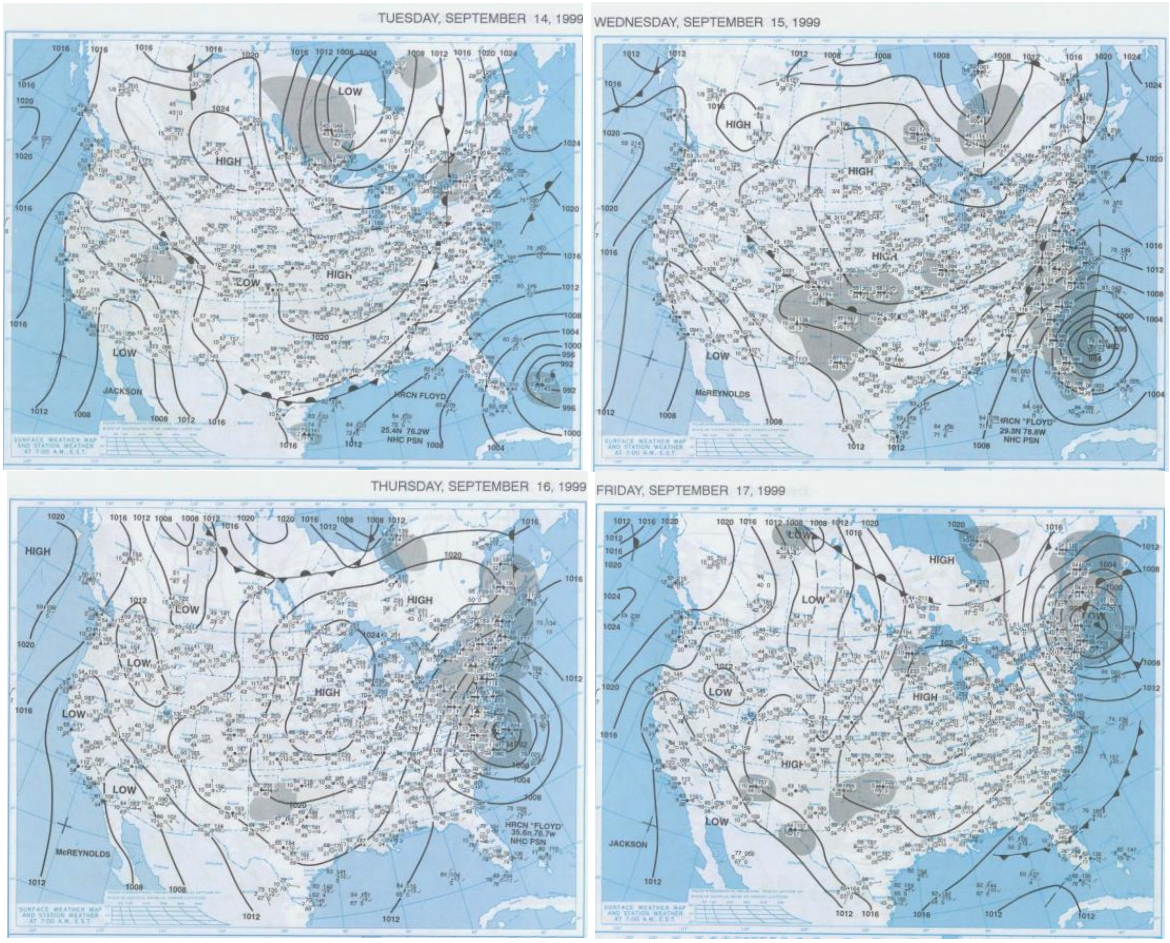


**Figure 5-2 Surface weather maps valid at 7 a.m. EST for the period 9/14/1999 to 9/17/1999. Source: NOAA Central Library, http://docs.lib.noaa.gov/rescue/dwm/ data_rescue_daily_weather_maps.html**

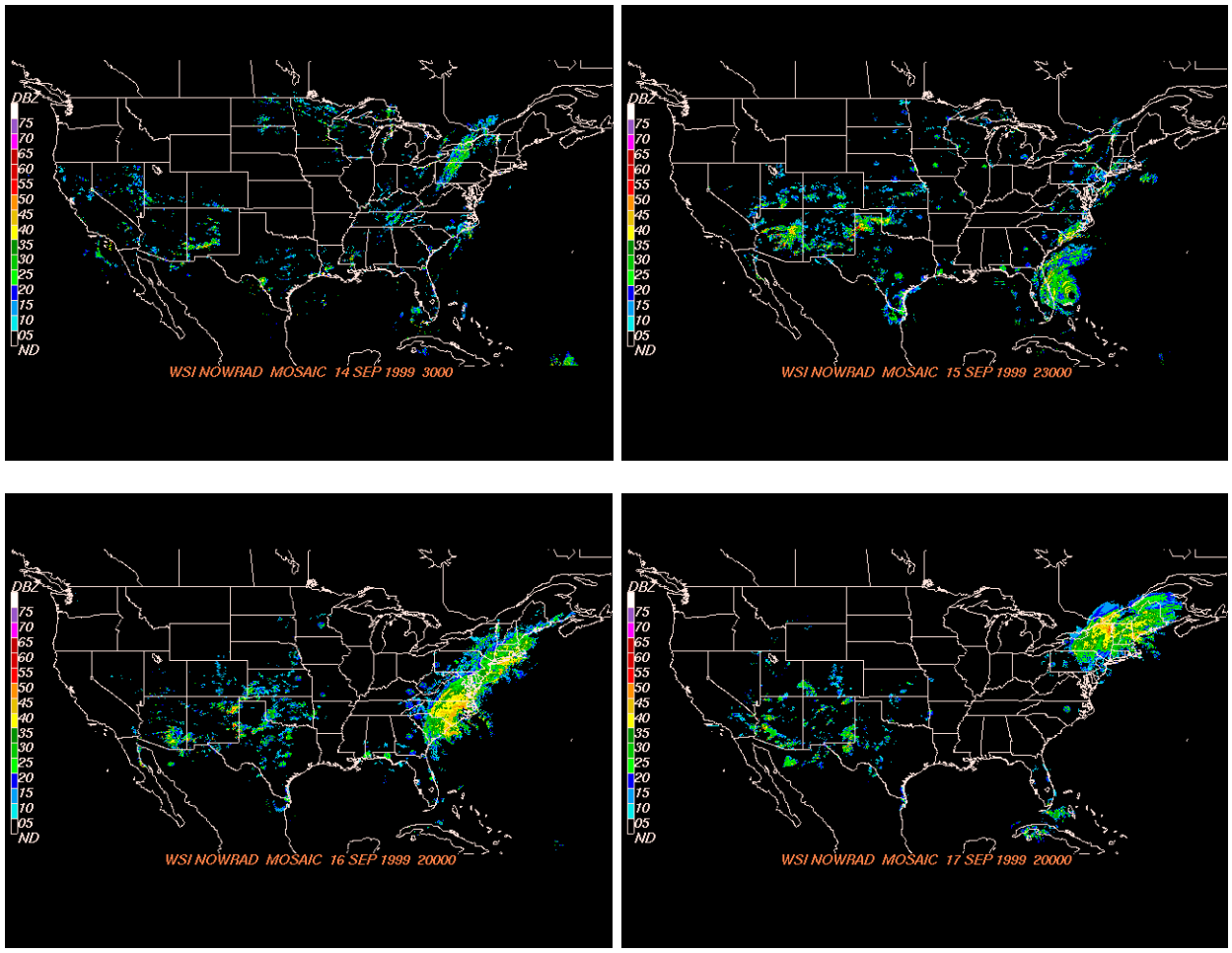


**Figure 5-3 National mosaic NEXRAD reflectivity images for the period 9/14/1999 to 9/17/1999. Imagery is valid at closest available time to 0000 UTC each day. Source: National Climatic Data Center, https://www.ncdc.noaa.gov/nexradinv/**

## 5.2 DAD Analysis

The synoptic analysis allowed the selection of 14 – 17 September as the storm total accumulation period for Hurricane Floyd. Subsequently, the radar-estimated precipitation was summed across various durations. DAD curves, calculated at 6, 12, 24, and 72 hours, were maximized based on the HYSPLIT analysis, and then compared to PMP values from HMR51. The mean positions of the maximum radar pixel value at each of the durations were determined and then used to extract the PMP value from gridded contours from HMR51 at the various durations and area sizes. The extracted values were then overlaid on the DAD curves to evaluate the magnitude of this storm relative to HMR51 PMP (Figure 5-4). Hurricane Floyd was found to exceed PMP from HMR51 at area sizes greater than 3861 $mi^2$ (10,000 $km^2$) at 24- and 72-hour durations, and to approach PMP at large area sizes for 6- and 12-hour durations. Results for the remaining top ten storms are described in Section 6, with DAD curves presented in Appendix A.

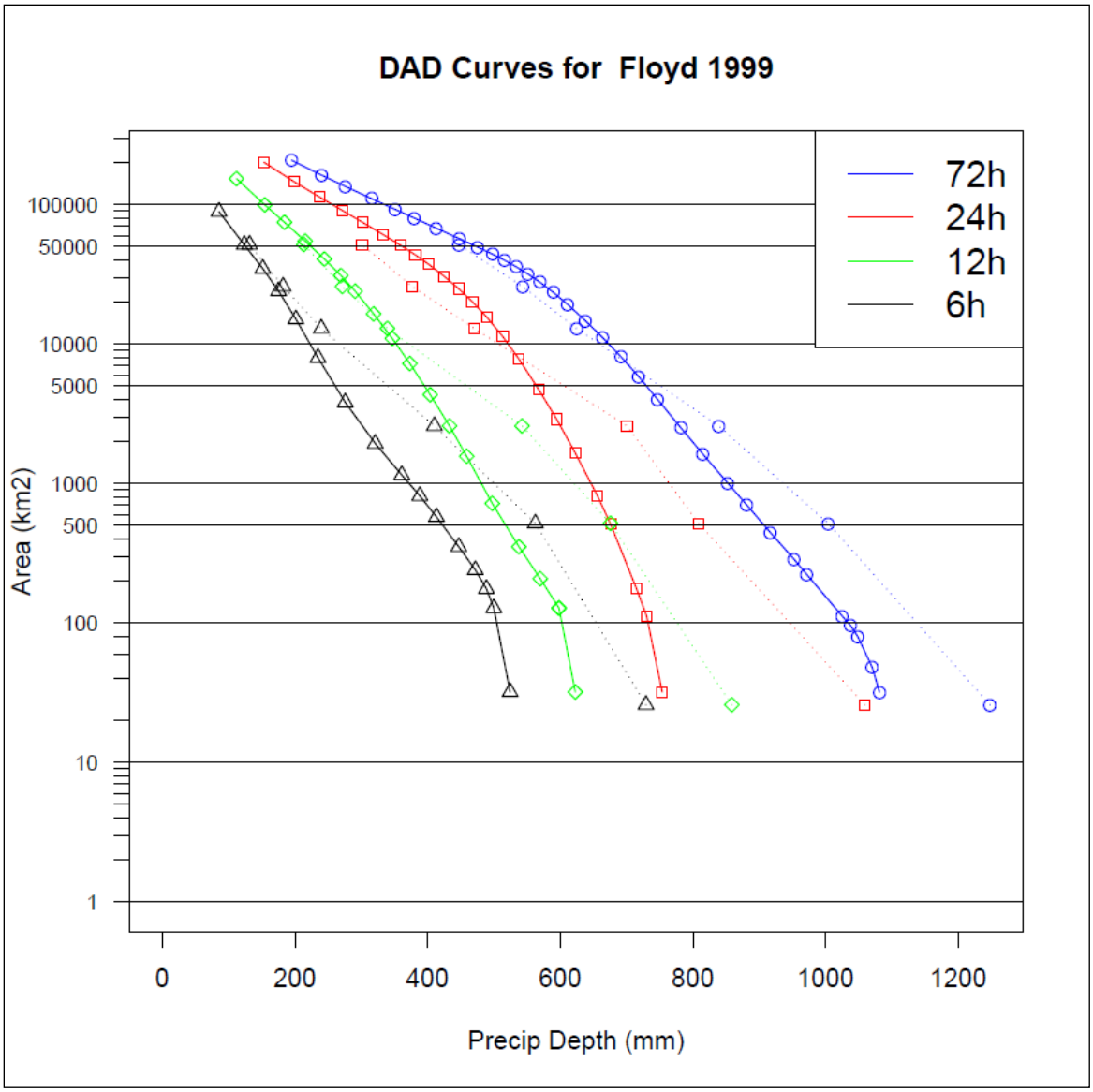


**Figure 5-4 Comparison of DADx curves for Hurricane Floyd (solid) and PMP values extracted from HMR51 (dotted)**

# 6 RESULTS

Due to the implementation of newer methods and datasets for the current study, Reclamation investigated performance of some aspects of these methods through several sensitivity experiments. First, three storms from HMR51 were selected to assess the sensitivity of the HYSPLIT simulations to the selection of CPP and to evaluate the prudence of using gridded data, specifically, NCEP/NCAR PW, in determining the IPMF. Second, there was some concern that precipitation extraneous to the TC or radar-specific issues along the domain boundary might influence estimates of DAD and PMP. Therefore, we ran multiple experiments using a "clipping" polygon to remove or include the MPR from the computations. Recognition of the potential implications this may have on the analysis is important to the interpretation of results.

Comparison of the new data from storms of interest, using in place maximized amounts (DADx) to existing data from HMR51 was performed. Two primary storms of interest, Floyd 1999 and Fran 1996, were selected for presentation as each exceeded PMP at various durations and area sizes. Direct comparison of the DADx values from the current study with PMP extracted from HMR 51 and with other individual tropical storms will elucidate the exceedances. The DADx results from the eight other new storms indicated amounts less than HMR 51 (Appendix A). This section also includes a review of the caveats and limitations of using radar-based gridded precipitation datasets, along with some of the advantages. An initial evaluation of long-term trends in moisture availability using gridded SST and $T_d$ data is presented, in order to examine potential increases and climate change effects on maximum precipitation estimation.

## 6.1 Evaluation of Moisture Maximization Technique

As described earlier in Section 3, no daily SST data were available prior to 1981; therefore, for three TCs from HMR51 (Table 6-1), the PW values from NCEP/NCAR reanalysis were used, as with Hurricane Gaston. Since these storms are from years prior to 1972, the availability of meteorological data for each is limited. For each storm, we determine the CPP based on mass curves available in Pertinent Data Sheets from the USACE Extreme Storm Catalog (e.g. Figure 6-1) and relative to features on surface weather maps (e.g. Figure 6-2). Due to the coarse temporal resolution of surface weather maps, these data were considered inferior to the mass curves; however, it is possible that for other storms the mass curves may be unavailable and surface maps (or daily gages) may be the only source for selecting a CPP. For the three storms from HMR51, the CPP varied by storm on the order of 12 to 24 hours.

**Table 6-1 Storm information for 3 TC events from HMR51 used to evaluate moisture maximization technique**

| Site (HMR51 No./Name) | Location | CPP (surface map) | CPP (mass curve) | IPMF (HMR51) | PW Month |
|---|---|---|---|---|---|
| Yankeetown, FL (85/Easy) | 29.0N, 82.7W | 06 September 1950 12 UTC | 05 September 1950 12 UTC | 1.10 | August |
| Tyro, VA (99/Camille) | 37.8N, 79.0W | 19 August 1969 12 UTC | 20 August 1969 00 UTC | 1.05 | July |
| Zerbe, PA (100/Agnes) | 40.8N, 76.7W | 22 June 1972 12 UTC | 22 June 1972 00 UTC | 1.21 | August |

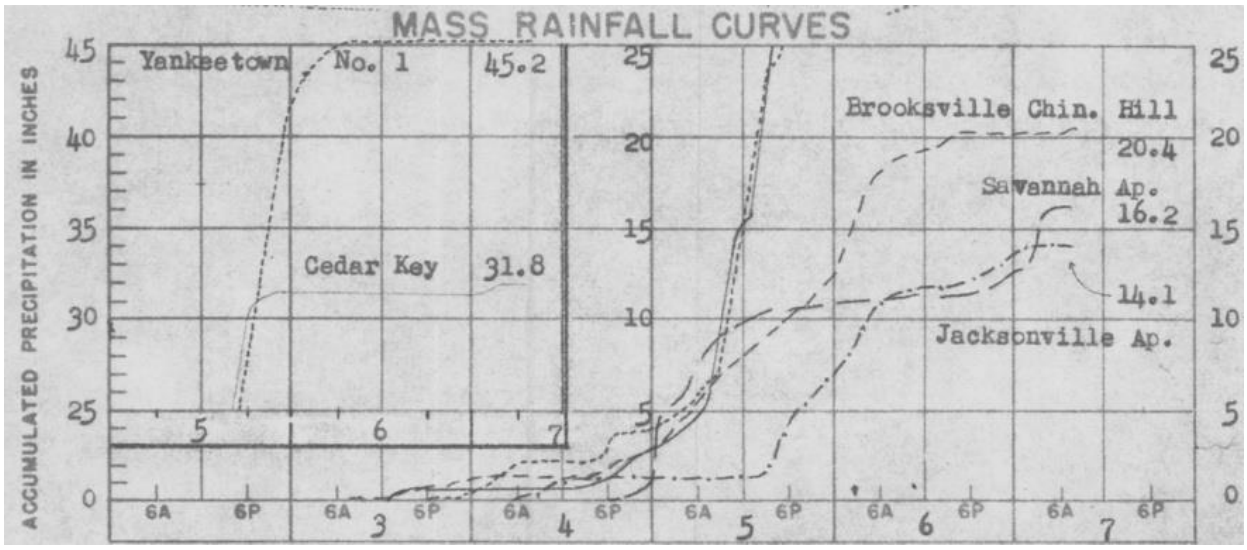


**Figure 6-1 Mass curve for Yankeetown, FL, storm September 3 – 7, 1950. CPP indicated as starting around 6am on September 5, 1950 for a majority of gauges**

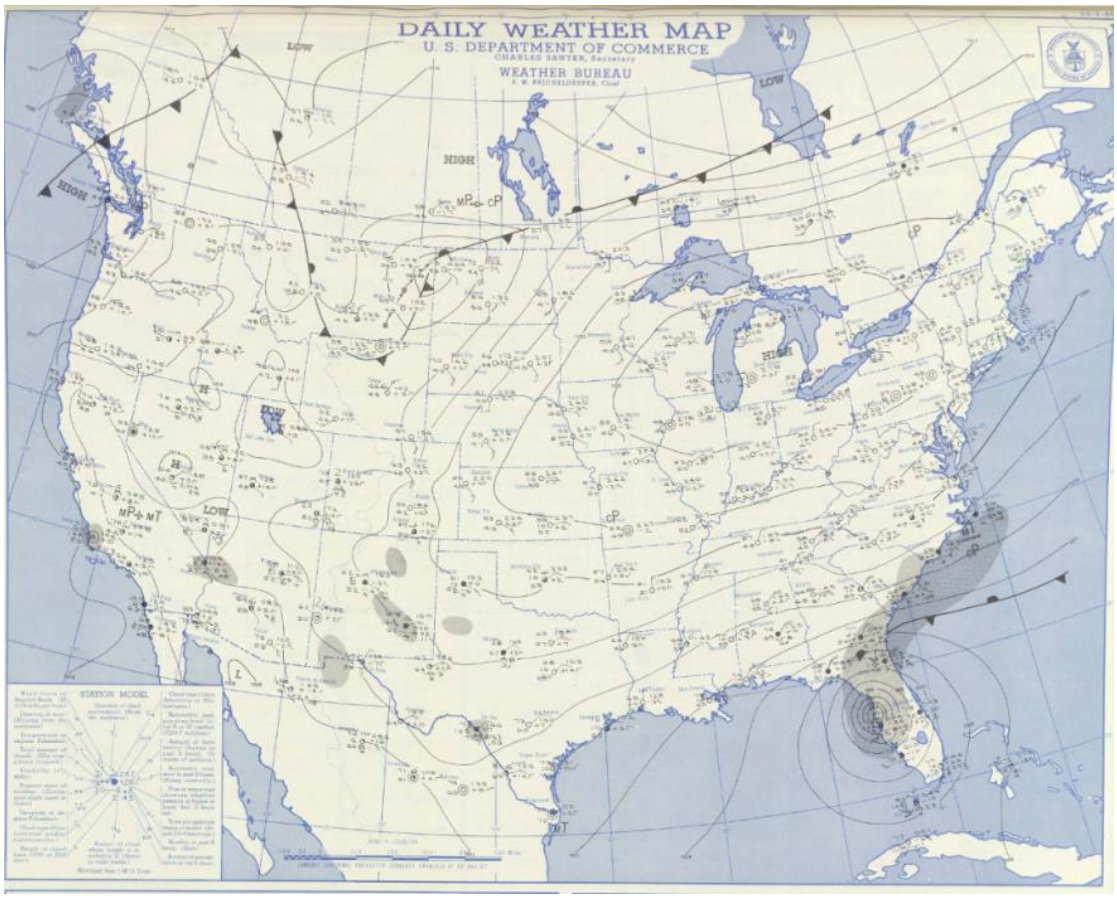


**Figure 6-2 Daily weather map from September 6, 1950 at 1200 UTC for the Yankeetown, FL, storm. Storm center is still located south of the maximum location of precipitation; therefore, this time per available surface maps was selected as the start time for the CPP**

Using the HYSPLIT model, back-trajectories were computed for each storm using the point location of maximum rainfall from each event as the center location and the matrix methodology described earlier. As can be seen in Figure 6-3, the source locations of moisture for the Yankeetown, FL storm are highly variable depending on the method used to select CPP. For this case, the mass curve approach yielded a much more consolidated source region over the Florida Straits and Cuba. In contrast, the surface map approach provided source regions from the Gulf of Mexico and Atlantic Ocean over or near the Gulf Stream. As such, boxplots of the IPMFs for each method indicate that the Yankeetown storm has generally higher values of IPMF using the surface map approach, potentially due to sampling of the PW grids over the Gulf Stream (Figure 6-4). From HMR51, IPMFs for Yankeetown, Tyro, and Zerbe are 1.10, 1.05, and 1.21, respectively (Table 6-1). Using the mass curve approach and maximum IPMF values yields results within ~10 percent of those derived in HMR51.

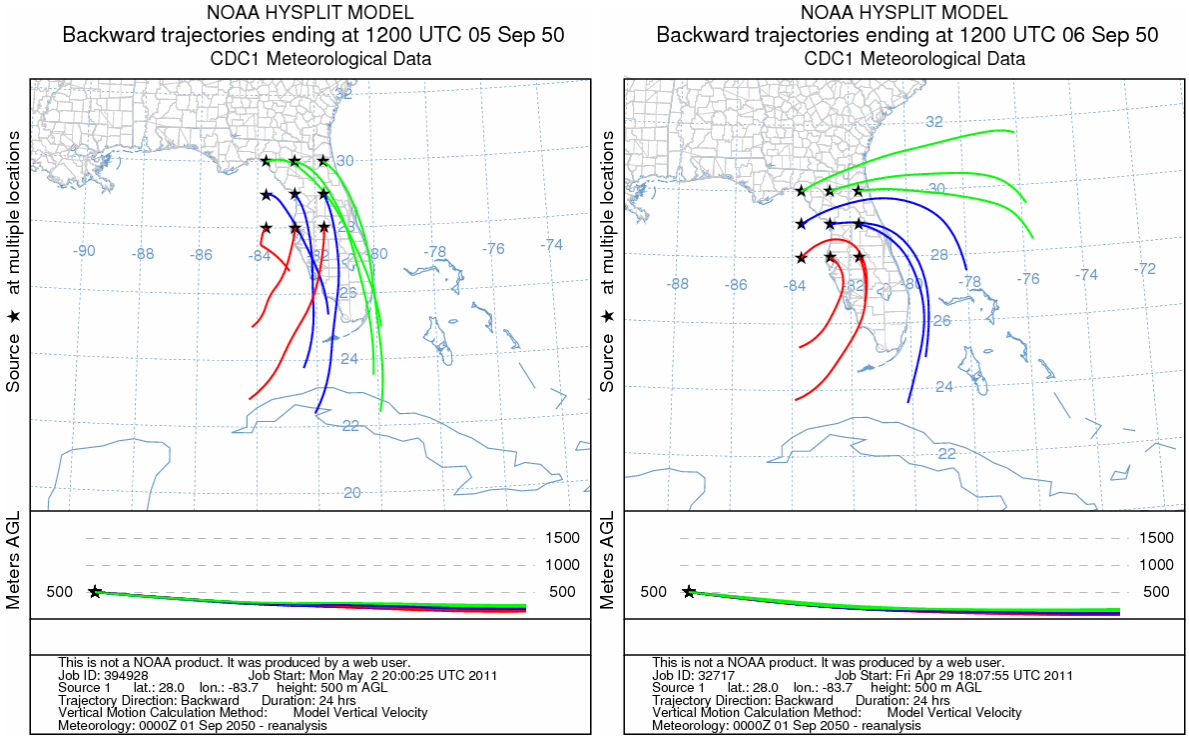


**Figure 6-3 Sensitivity of Yankeetown, FL, event to selection of start time for HYSPLIT model run. CPP start time selected by using mass curves (left; 1200 UTC September 5, 1950) and surface weather maps (right; 1200 UTC September 6, 1950). Mass curves were ultimately used to determine start of the CPP**

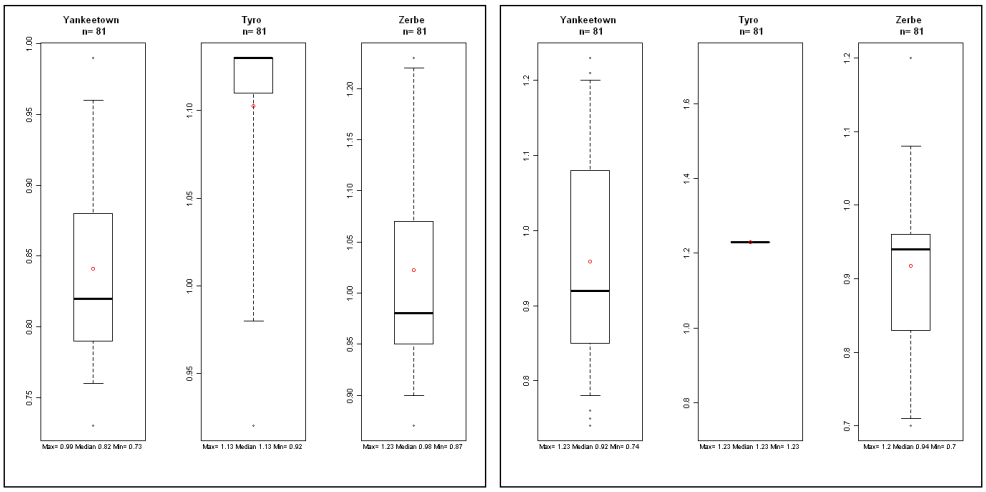


**Figure 6-4 Boxplots of IPMFs for the three HMR51 storms for CPP from mass curves (left) and surface weather maps (right). Maximum values of IPMF range from 0.99 to 1.23, depending on the CPP selected. Values less than 1.00 are assumed to be 1.00. Whiskers represent 5th and 95th percentiles, box represents interquartile range, solid black line represents median, and red dot represents the mean. Hollow points in black indicate outliers**

## 6.2 Evaluation of Storm Clip Regions

For each of the storms, a 50-km (31 mi) buffer was applied to a two-state shapefile of NC and SC to remove radar-based data artifacts from the accumulations. The intent was to isolate the precipitation errors while including enough precipitation offshore and across state boundaries to generate a reasonable and representative value of DADx. The NC-SC buffer region enabled a focus on this pilot region, so that in place storm maximization amounts are limited to NC and SC, within the MPR data domain (Figure 3-2). Storm centers and amounts outside of this domain are not considered as part of the present work. Additional efforts would be needed to examine extreme storm rainfall centers in other locations associated with some of these TCs, notably Floyd in Virginia and New Jersey, and Fran in northern Virginia.

The USACE methodology for calculating DAD uses a delineating contour to determine the region of storm-specific precipitation, typically the one inch contour. For most of the TCs, the precipitation shield was along track and not extraneous to the primary circulation feature; however, for Hurricane Fran, a secondary precipitation center with values in excess of 10 inches (>300 mm) occurred over western NC. To determine the potential impact of values away from the storm on DAD computations, a clipping region was defined to additionally exclude this precipitation from the calculations (Figure 6-5).

A comparison of DADx curves for Hurricane Fran with 50-km (31 mi) buffer clipping (non-cropped) and with an additional clipping to exclude the western NC precipitation (cropped) was performed (Figure 6-6). Primary differences occur at area sizes greater than 50,000 $km^2$ at 72-hour duration and are generally less than 15 mm (0.59 in). Exclusion of the rainfall exterior to the main storm precipitation region results in slightly lower values of PMP at those area sizes.

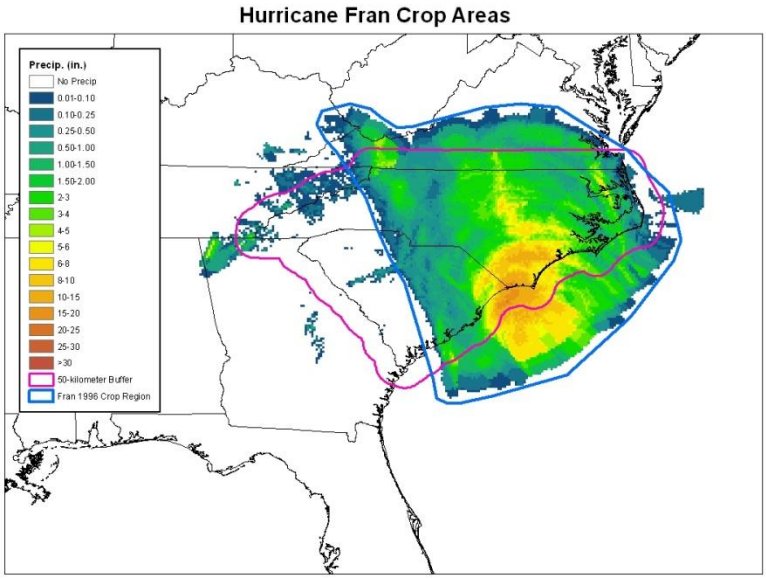


**Figure 6-5 Crop areas used to examine the impact of extraneous precipitation outside of the main precipitation region. The 50-km (31 mi) buffer (magenta) was used to clip the gridded precipitation for all storms. The Fran 1996 crop region (blue) was subsequently used to clip precipitation in the western Carolinas from the analysis that was not directly associated with the tropical system. The 24-hour maximum precipitation period for Fran 1996 is shown. This correlates well with the spatial extent of precipitation directly associated with the TC**

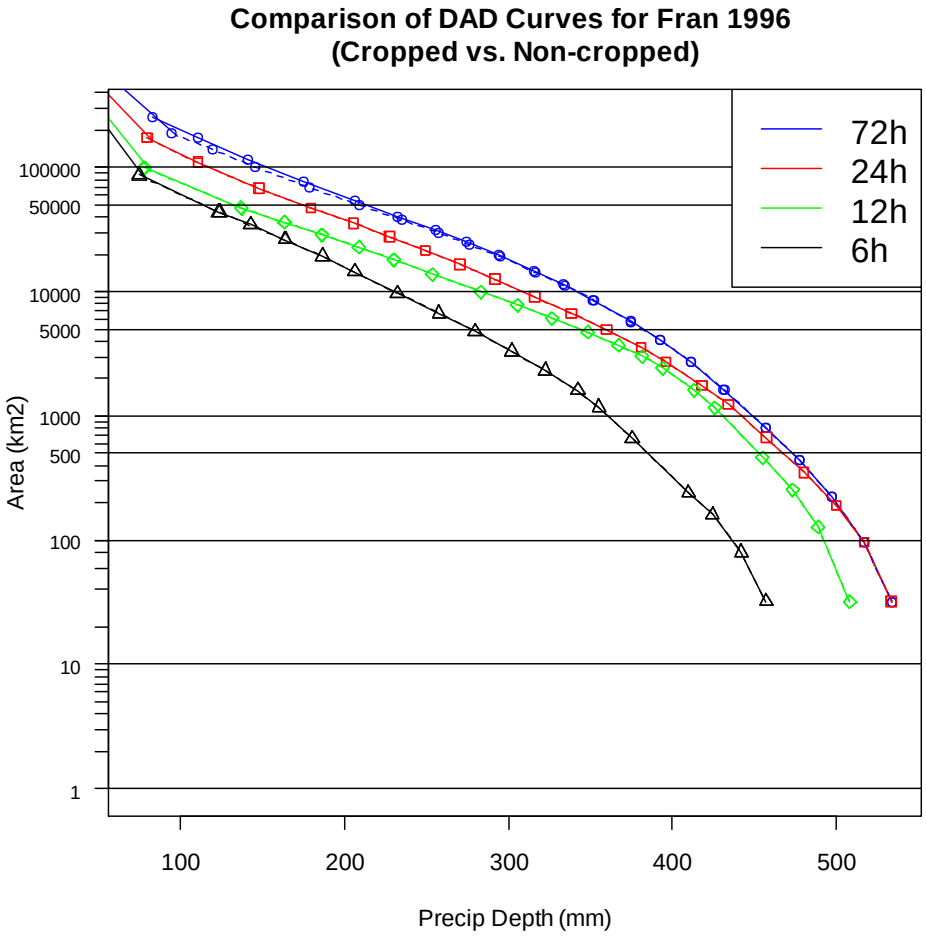


**Figure 6-6 Comparison of DADx curves for Fran 1996 for the cropped (solid) and non-cropped (dashed) experiments**

As described, an initial buffer zone was created around the two-state area of the Carolinas to exclude any potential issues with radar (as can be seen in Figure 6-5 offshore). To investigate the sensitivity of removing this data, the DADx curves for Hurricane Floyd were recalculated without removing data outside the 50-km (31 mi) buffer (non-cropped) and differences were examined. Primary differences occur at area sizes greater than 50,000 km$^2$ and are generally less than 30 mm (1.18 in). Inclusion of the region outside of the buffer results in slightly higher values of PMP at those area sizes (Figure 6-7).

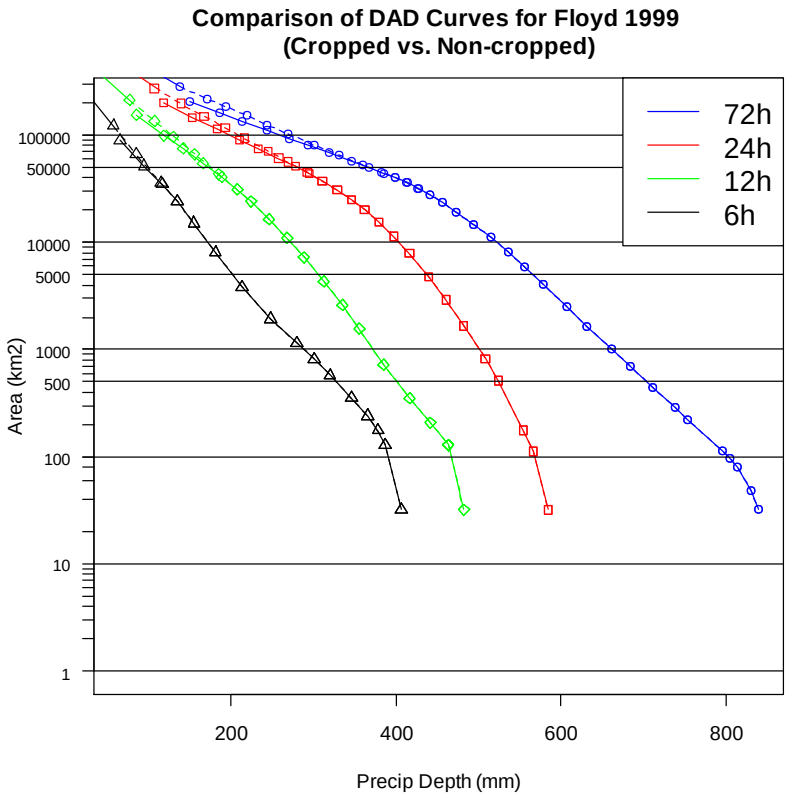


**Figure 6-7 Comparison of DADx curves for Floyd 1999 for the cropped (solid) and non-cropped (dashed) experiments**

## 6.3 Comparisons of New Storms to HMR51 PMP

For each storm, the DADx curves were overlaid with the extracted PMP values from the HMR51 grids (England et al., 2011) for each duration and area size. Evaluation of these plots for each storm indicated that only two storms approached PMP based on the current methodology: Hurricane Floyd 1999 and Hurricane Fran 1996. Hurricane Floyd showed exceedances at area sizes generally greater than 10,000 mi2 at durations of 24 and 72 hours with values approaching PMP at the same area sizes at 6 and 12 hours (Table 6-3; Figure 6-8). Differences at 72-hour duration for Hurricane Floyd generally fall within the +/- 10 percent errors prescribed by HMR51; however, at 24-hours for exceptionally large area sizes (> 10,000 $mi^2$), the differences exceed 10 percent. Hurricane Fran also showed exceedances, but only at 6-hour duration for area sizes of more than 1,000 $mi^2$ (2,500 $km^2$) (Table 6-3; Figure 6-8). The percent difference between HMR51 and DADx from MPR exceeded 12 percent at 5000, 10000, and 20000 $mi^2$. These results suggest that HMR51 PMP estimates need to be increased for large area sizes, based on in place maximization of Floyd and Fran over the Carolinas.

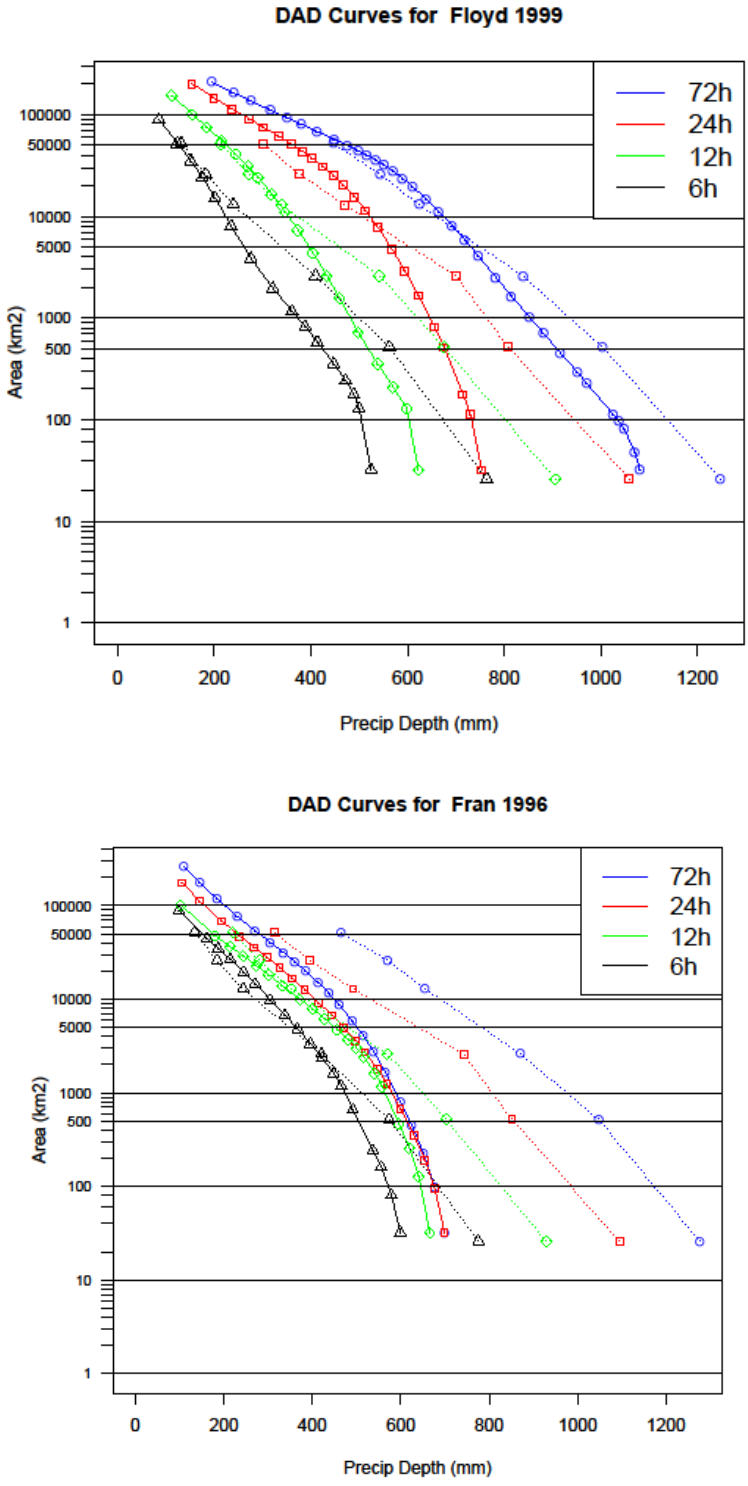


**Figure 6-8 Comparison of DADx curves from MPR (solid) and HMR51 (dashed) for Floyd 1999 (left) and Fran 1996 (right). Exceedance of HMR51 PMP values are evident where solid lines cross dashed lines of the same color**

**Table 6-2 Comparison of PMP values from HMR51 grids and 24-hour and 72-hour DADx from MPR for Floyd 1999. Floyd exceeds PMP at area sizes greater than 5000 mi² ( ~12950 km²) for 24-hour duration**

| Floyd1999 | | 24h | | | 72h | | |
|---|---|---|---|---|---|---|---|
| Area (km²) | Area (mi²) | HMR51 (mm) | MPR (mm) | % diff | HMR51 (mm) | MPR (mm) | % diff |
| 25.9 | 10 | 1084.59 | 755.40 | -43.58 | 1279.64 | 1085.44 | -17.89 |
| 51.8 | 20 | 840.78 | 675.41 | -24.48 | 1046.30 | 906.62 | -15.40 |
| 2590 | 1000 | 731.55 | 601.39 | -21.64 | 873.40 | 779.99 | -11.98 |
| 12950 | 5000 | 485.41 | 504.01 | 3.69 | 651.87 | 650.61 | -0.19 |
| 25900 | 10000 | 388.75 | 443.13 | 12.27 | 567.97 | 578.20 | 1.77 |
| 51800 | 20000 | 309.86 | 357.37 | 13.29 | 462.52 | 467.33 | 1.03 |

**Table 6-3 Comparison of PMP values from HMR51 grids and 6-hour DADx from MPR for Fran 1996. Fran exceeds PMP at area sizes greater than 965 mi² (2500 km²) for 6-hour duration**

| Fran 1996 | | 6h | | |
|---|---|---|---|---|
| Area (km²) | Area (mi²) | HMR51 (mm) | MPR (mm) | % diff |
| 25.9 | 10 | 763.76 | 601.47 | -26.98 |
| 51.8 | 20 | 561.59 | 506.74 | -10.82 |
| 2590 | 1000 | 408.53 | 415.47 | 1.67 |
| 12950 | 5000 | 237.21 | 281.65 | 15.78 |
| 25900 | 10000 | 181.59 | 216.70 | 16.20 |
| 51800 | 20000 | 131.31 | 150.27 | 12.62 |

## 6.4 Comparison of New Storms to HMR51 Storms

Based on the results from Section 6.3, the PMP values for three tropical storms from HMR51 (Table 6-4) were compared with DADx for Hurricanes Floyd and Fran. Hurricane Easy was of particular interest since it anchors the PMP values across the southeastern United States. Figure 6-9 and Figure 6-10 show the comparison of Hurricane Floyd to two of the storms: Hearne, TX and Yankeetown, FL. The Ewan, NJ storm was of short duration; HMR51 did not provide PMP values at durations of 24 or 72 hours for this event. Similar to the plots in Section 6.3, Hurricane Floyd DADx exceeded PMP relative to each of the storms at 24 hours above ~2700 $mi^2$ (~7000 $km^2$). The Hearne, TX, storm was very similar at area sizes below ~ 1930 $mi^2$ (~5000 $km^2$). For the 72-hour duration, Hurricane Floyd DADx values are larger than the Hearne, TX storm at areas less than 75 $mi^2$ (200 $km^2$) but fall between the two storms at larger area sizes greater than 3860 $mi^2$ (10000 $km^2$). This would suggest that the Hearne, TX storm drives the PMP values at 72-hour duration for larger area sizes. Figure 6-11 shows the plots for Hurricane Fran for 6-hour duration. MPR-derived DADx curves for Fran indicate that the three storms from HMR51 have smaller PMP values except at small area sizes less than 115 $mi^2$ (300 $km^2$). Non-tropical storms that are more convective in nature may be the primary forcing for large values of PMP at short durations at those small area sizes. Floyd and Fran are very large, extreme storms. The comparisons of these new storms to the three record storms, used to determine PMP in HMR51, suggest that Floyd and Fran would be influential on setting potentially new (and larger) PMP estimates in the Southeast.

**Table 6-4 Storm information for 3 TCs events from HMR51 used in PMP comparisons**

| Site | Event Dates | Storm Type |
|---|---|---|
| Yankeetown, FL (85) | 03 – 07 September 1950 | Hurricane Easy |
| Hearne, TX (7) | 27 June – 01 July 1899 | Weak tropical low |
| Ewan, NJ (67) | 01 September 1940 | Tropical storm |

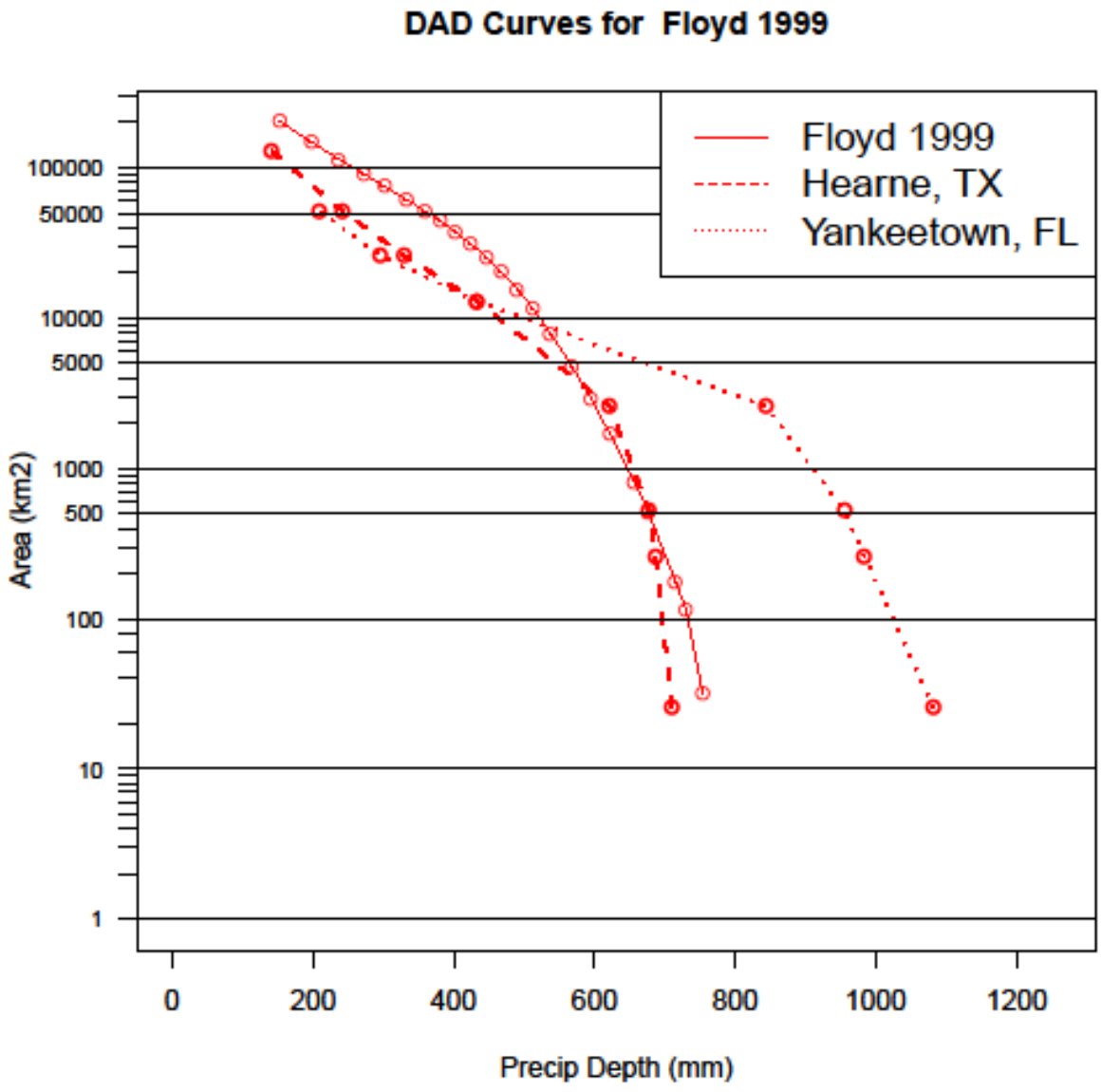


**Figure 6-9 Comparison of 24-hour DADx curve for Floyd 1999 with two tropical storms from HMR51. Floyd 1999 exceeds each of these storms at area sizes greater than 2700 mi$^2$ (~7000 km$^2$)**

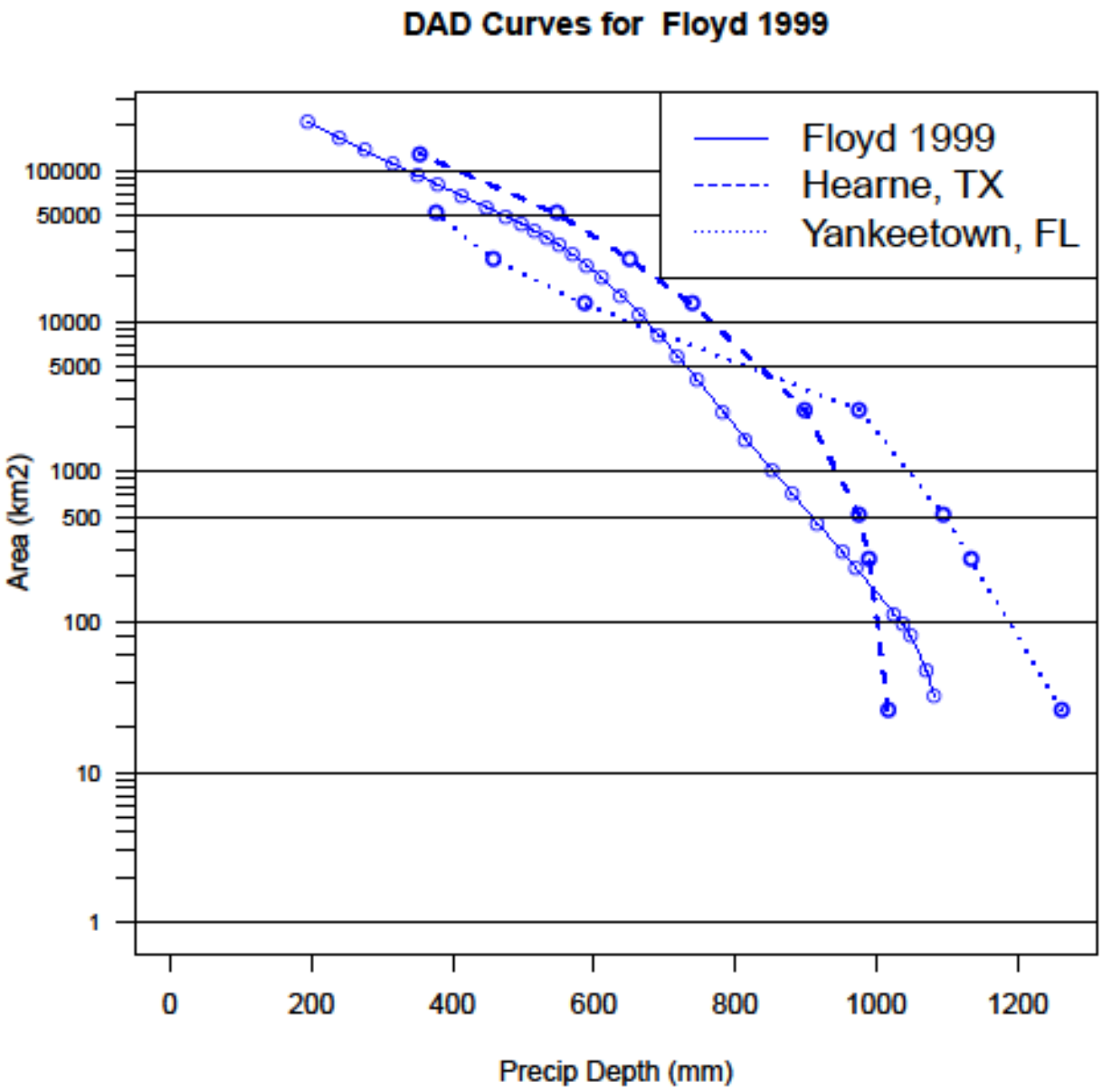


**Figure 6-10** **Comparison of 72-hour DADx curve for Floyd 1999 with two tropical storms from HMR51. Floyd 1999 exceeds the Hearne, TX storm at area sizes below 75 mi$^2$ (200 km$^2$) and generally falls between the two curves at large area sizes greater than 3860 mi$^2$ (10000 km$^2$)**

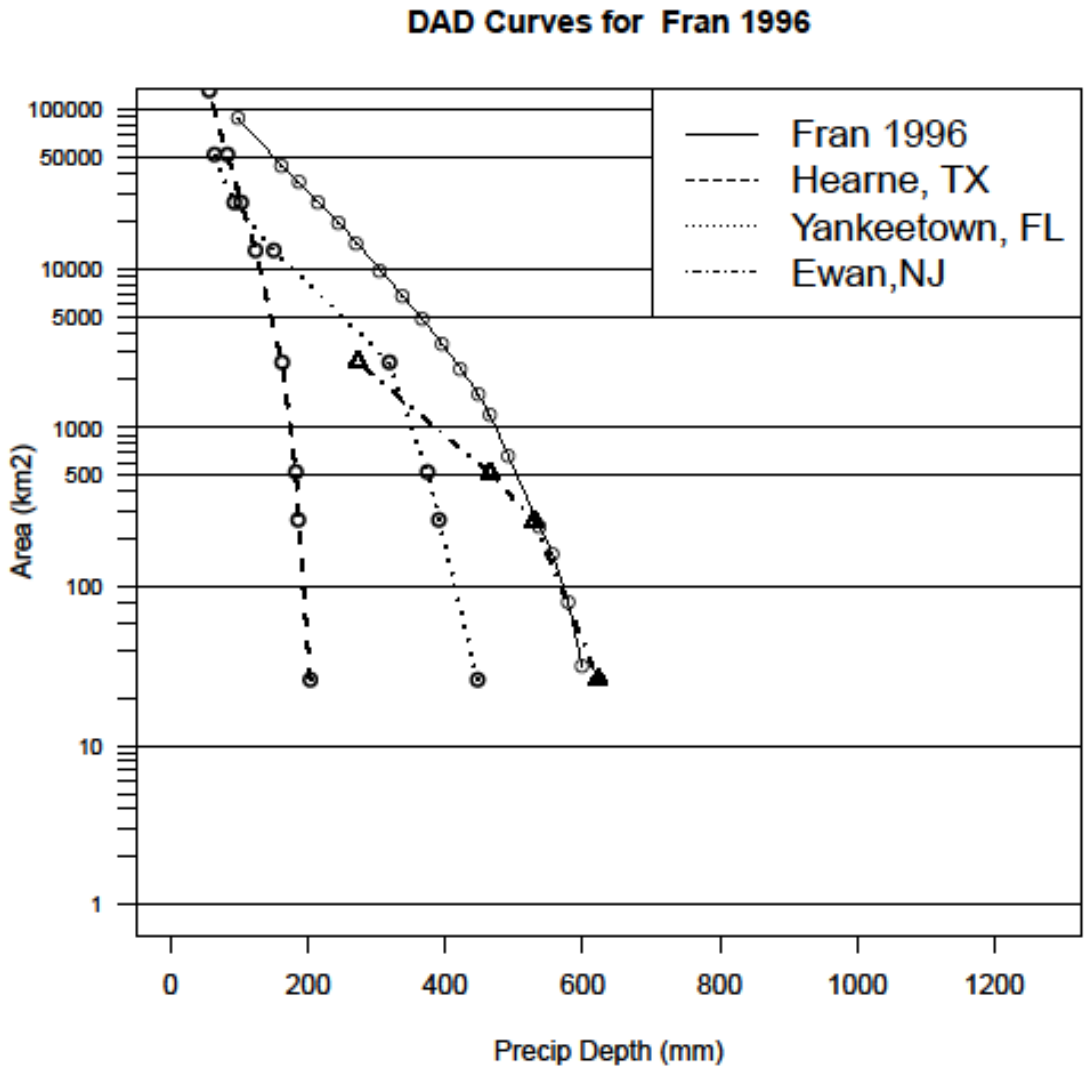


**Figure 6-11 Comparison of 6-hour DADx curve for Fran 1996 with three tropical storms from HMR51. Fran 1996 exceeds each of these storms at area sizes above 115 mi$^2$ (300 km$^2$)**

## 6.5 Radar-related Issues and Caveats

While radar estimates of precipitation provide the benefits of enhanced spatial and temporal resolution, the radar estimates are also riddled with significant issues (Baeck and Smith, 1998; Mizzell, 1999; Smith et al., 1996; Ulbrich and Lee, 2002). Radars operate by sending out a pulse at a given wavelength and then measure the time to return along with the power of signal which is converted to reflectivity (Z). Reflectivity (Z) is then related to precipitation rate (R) by using a power function, or Z-R relationship, such that $Z=aR^b$, where a and b are empirically derived constants based on the type of precipitation (e.g., stratiform, convective, etc.). Individual National Weather Service offices have the ability to change these Z-R relationships

operationally; however, often times the precipitation mechanism may be different across the 150 mi (240 km) range of the radar with stratiform and convective precipitation occurring simultaneously (Ulbrich and Lee, 2002). The pulse sent by the radar is emitted at various angles from the receiver to ensure capturing the signal at various heights. Generally, only the 0.5-degree signal is used to determine the rainfall rate. At large/short distances from the radar, the pulse can miss the rainfall entirely by going over/under the region of precipitation. In addition, the radar can have significant issues above the freezing level where hail and wet snow generate reflectivities that correspond to much higher rain rates than observed (Smith et al., 1996). An excellent discussion on the capabilities, limitations, and potential improvements to radar estimates of rainfall can be found at http://www.srh.noaa.gov/mrx/research/precip/precip.php.

The MPR dataset provided by NCDC for the Carolina study region was adjusted based on a mean field bias. Bias calculations for radar estimates are determined based on ground truth, or precipitation gauge data. These biases are averaged across the individual radar range and applied uniformly at all radar pixels; therefore, some areas may ultimately be under-estimated while others are over-estimated. Unfortunately, precipitation gauges exhibit their own set of issues (Sieck et al., 2007). During high wind events, precipitation gauges have been shown to under-estimate the actual precipitation as displacement away from the gauge occurs and rain falling into the collection apparatus is blown out. In addition, tipping bucket gauges collect rain in specific increments and heavy rainfall can overwhelm the tipping mechanism resulting in further under-estimation. Tropical storms present both of these weather conditions along with severely high winds that can completely destroy or remove communications from these gauges for a period of time. In addition, it is assumed that the individual gauge represents the region of 2.5 mi x 2.5 mi (4 km x 4 km) of the radar pixel, which introduces a sampling issue such that the point total is likely not truly representative of the precipitation occurring over a 10 $mi^2$ (16 $km^2$) area.

**Table 6-5 Comparison of gauge (g) and radar-estimated (r) precipitation. Ratio is calculated as r/g such that values less/greater than 1 indicate under/overestimates by radar, respectively**

| Storm | Gauge (mm) | MPR (mm) | Ratio |
|---|---|---|---|
| Bonnie | 71.0738 | 36.17 | 0.51 |
| Dennis | 79.7122 | 83.4479 | 1.05 |
| Earl | 65.9051 | 41.6814 | 0.63 |
| Ernesto | 68.5875 | 67.1569 | 0.98 |
| Floyd | 103.793 | 102.147 | 0.98 |
| Frances | 111.006 | 114.26 | 1.03 |
| Fran | 59.5086 | 72.4056 | 1.22 |
| Gaston | 46.4617 | 45.1394 | 0.97 |
| Ivan | 48.2801 | 55.7489 | 1.15 |
| Ophelia | 38.7985 | 37.5308 | 0.97 |

For each of the 10 storms, the NHDS hourly precipitation gauges were used to extract the hourly precipitation from the MPR grids. Comparison of those grids showed a variety of biases across the Carolinas domain (Table 6-5). For example, for Hurricane Floyd, there were 41 of the 65 sites with storm total precipitation greater than zero. For each of these sites the differences by hour were plotted in Figure 6-12 (left panel). Maximum differences exceed 100 mm (> 3.94 in) between individual gauges and radar estimates. It should be noted that radar estimates are areal averages over a 4km x 4km (1.54mi x 1.54mi) grid cell and, therefore, may not represent a point total rainfall accurately. In addition, displacement of rainfall totals by a single grid cell in radar estimates may influence the bias computations. There are 10 locations where differences are greater than zero (radar over-estimates), 19 locations where differences are less than zero (radar under-estimates), and 12 locations where differences equal zero (radar performs well). The mean bias across time indicates a brief period of under-estimation across all sites from hours 40 through 60. This time period corresponds to the same period in which a majority of the heaviest rainfall was occurring across eastern NC (e.g., Figure 6-12 (right panel)).

Future work may involve the inclusion of additional rain gauges in the generation of MPR data. While gauges do have issues, these issues are usually able to be identified and corrected more easily than radar biases. McGehee et al. (2009) showed improved areal precipitation estimates for Tropical Storm Fay when using additional rainfall inputs from the Community Collaborative Rain, Hail, and Snow (CoCoRaHS) network. During TS Fay, precipitation observations were 635, 300, and 685 mm (25, 11.8, and 27 in) from radar estimates, satellite estimates, and CoCoRaHS measurements, respectively. The importance of dense point gauge measurements in capturing the spatial and temporal distribution of rainfall during extreme events is highlighted in their case study.

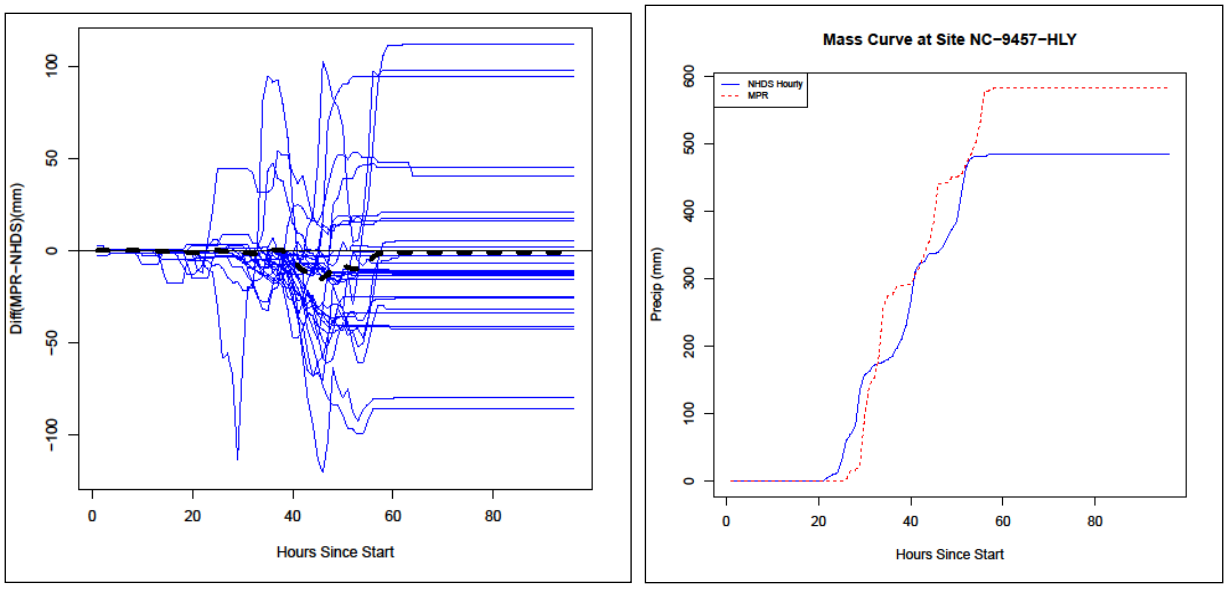


**Figure 6-12 Plots of the differences between MPR and 41 NHDS hourly gauges for Floyd (left) and an example mass curve comparison for Wilmington International Airport, NC, for Floyd (right)**

## 6.6 Implications of Recent Trends

The calculation of IPMFs is directly related to the respective values of maximum and representative $T_d$ and/or SSTs (for this section "temperatures" will denote either $T_d$ or SST), depending on the method selected for determining PW. Under the pretense of climate change and variability, the potential exists for these values to change over time. For example, if the temperatures associated with TCs are generally constant with time while the overall trend in maximum temperatures is increasing, then the IPMFs will become larger as the denominator is becoming relatively smaller compared to the numerator in the IPMF equation described in Section 4 (Figure 4-2). As a preliminary investigation into temperature trends across the region, we calculated monthly mean $T_d$s from the NCEP/NCAR specific humidity values at 1000-hPa and extracted the monthly SST values from the ICOADS dataset used earlier. The discussion below will focus on potential source regions for extreme precipitation events in the Carolinas, namely the Atlantic, Gulf of Mexico, and Caribbean, along with land-based locations (for $T_d$ only) across the southeastern United States. Trends in $T_d$ and SSTs were estimated using techniques outlined in Section 3.7. Retrospective, moving-window decadal and period-of-record time periods were used in the analysis.

Long-term trends (1948 to 2010) in $T_d$s across the Carolinas generally show no significant trends during the tropical season, except offshore where positive trends of less than +0.1 C/yr are noted (Figure 6-13). The most recent period (1991 to 2010) shows similar warming over the oceans during the months of July through October (Figure 6-13). A recent cooling trend is evident over the Carolinas in July. Some long-term cooling trends are also noted during the months of February through May over the Carolinas and adjacent coastal waters. These cooling trends are enhanced in the most recent period of 1991-2010, suggesting much of the long term trend may be driven by recent changes in dewpoint temperatures. It is impossible to determine if this is an artifact of the reanalysis data, a temporary trend, or indication of a longer term signal.

Long-term trends (1960 to 2010) in SSTs during the tropical season show few grids with significant trends, but some evidence of localized warming exists in the Gulf of Mexico, Atlantic Ocean, and Caribbean (Figure 6-14). These trends are also seen in the most recent two decades since 1991 (Figure 6-14). Nearly all the trends in the vicinity of the Southeast range from -0.10 to +0.10 C/year and cluster near zero.

Since a majority of the storms analyzed in the current study used SST and $T_d$ values from the month of September for both representative and maximum PW, Figure 6-15 provides a zoomed depiction of each decadal and long-term trend. The long-term trend (1961-2010) in $T_d$s during September indicates increasing $T_d$s across the Lower Mississippi River Valley that is being attenuated in recent decades by no significant trend. The long-term trend in SST off the coast of NC shows increasing trends roughly in the vicinity of the Gulf Stream; however, more recently the trends are generally insignificant at 90 percent confidence and show a dipole of cooling and warming temperatures offshore.

The general implication, based on the initial analysis conducted as part of this pilot study, would be that if current trends continue, there will likely be little impact on the IPMFs. Source regions for moisture near the Carolinas indicate little or no trend in either $T_d$ or SST, with most of the significant trend regions over the SE US and adjacent coastal waters being driven by trends earlier in the period of record during the mid-20$^{th}$ century.

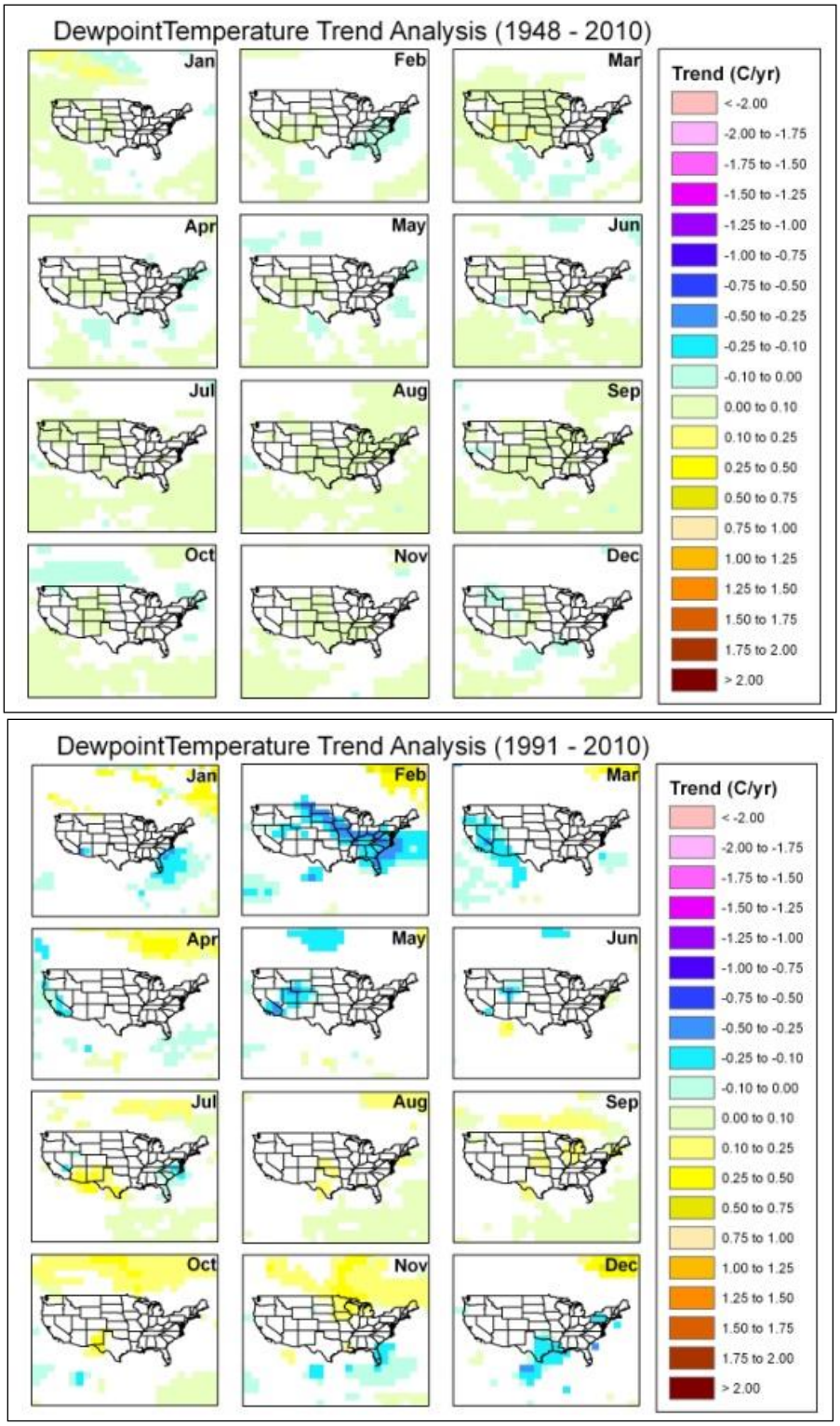


**Figure 6-13 Td trend analysis using NCEP/NCAR reanalysis data. Significant trends (alpha > 0.10) from two different periods, 1948-2010 (top) and 1991-2010 (bottom), are shown to indicate contributions to long term trends from more recent data**

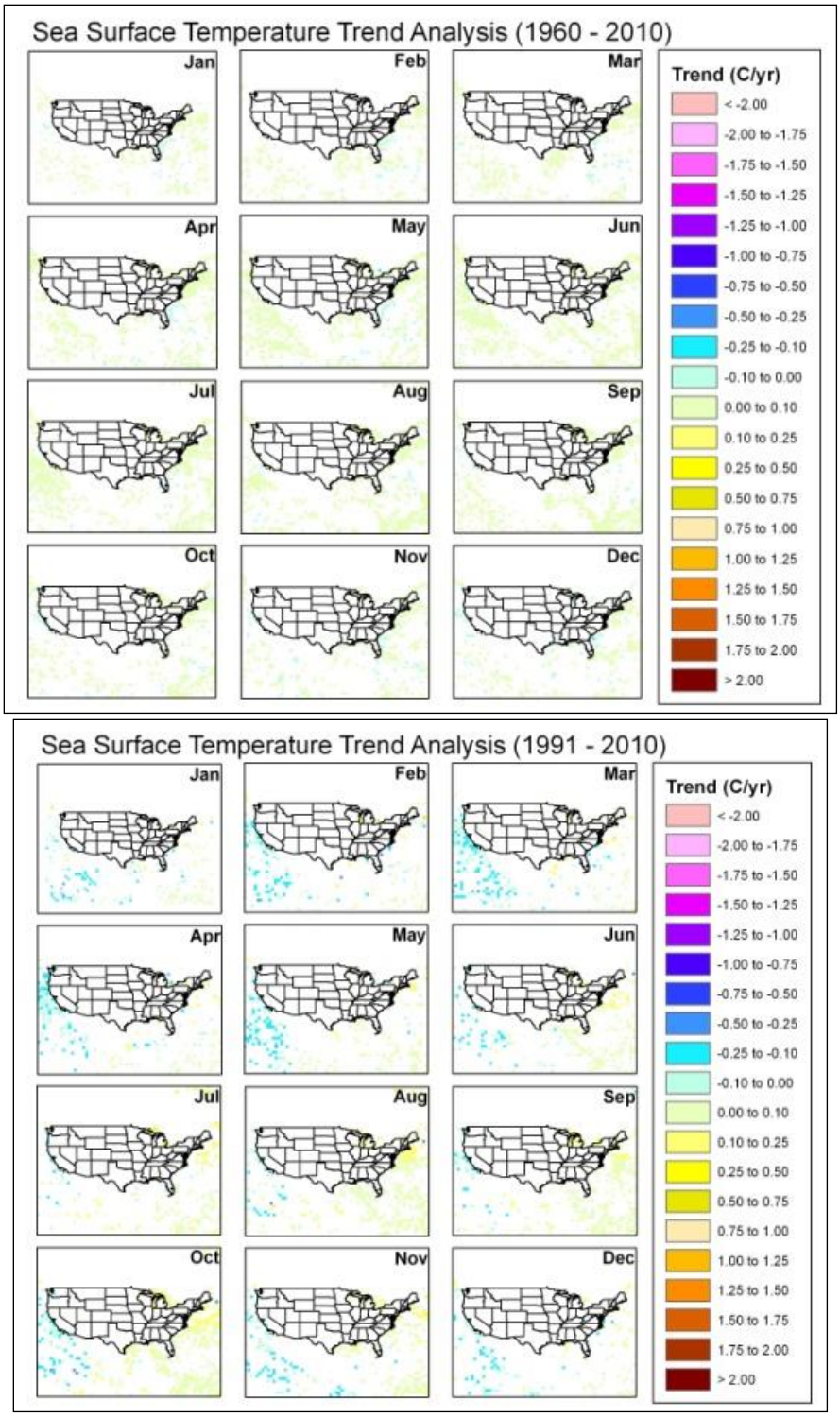


**Figure 6-14 SST trend analysis using ICOADS data. Significant trends (alpha > 0.10) from two different periods, 1960-2010 (top) and 1991-2010 (bottom), are shown to indicate contributions to long term trends from more recent data**

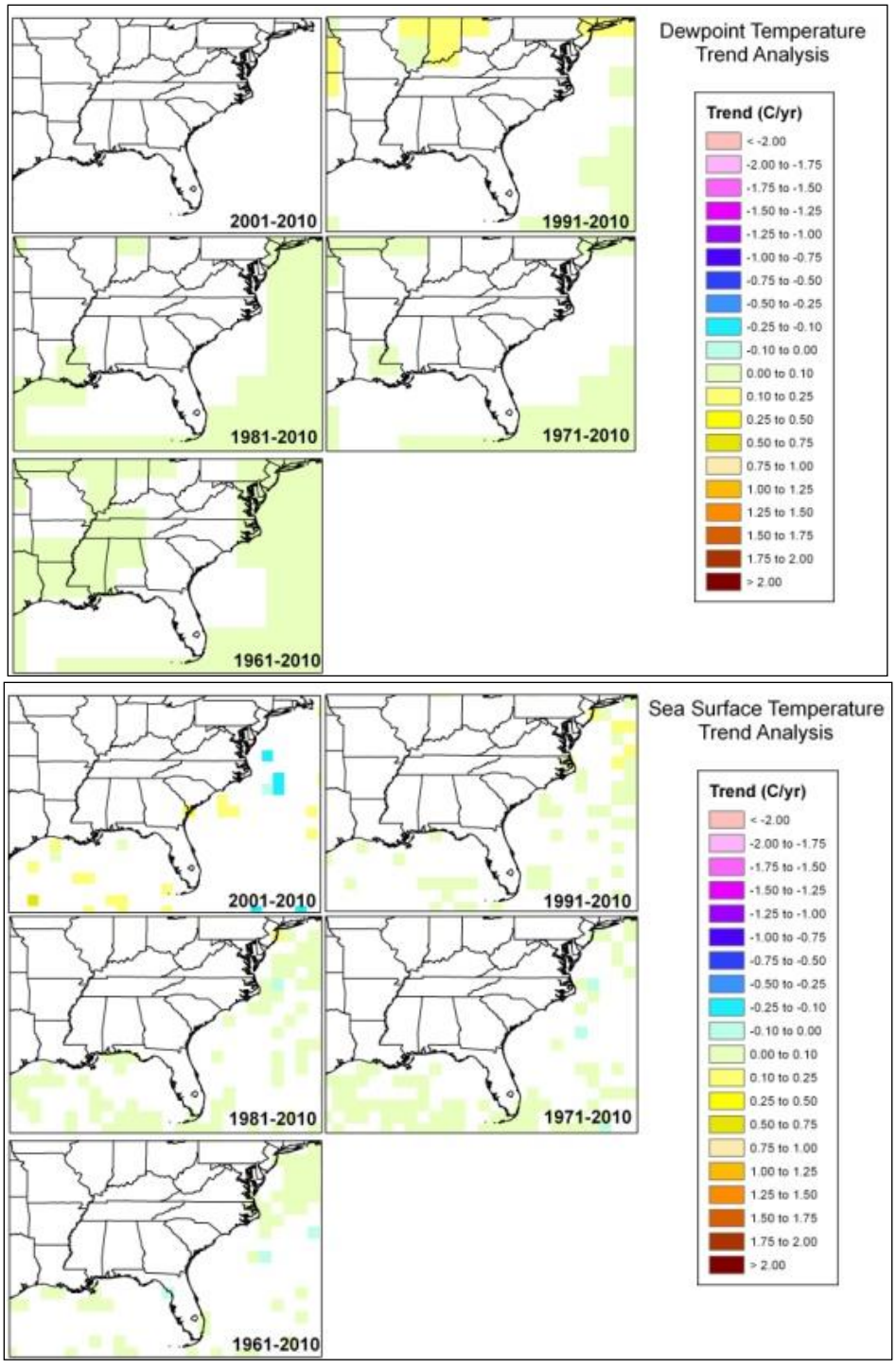


**Figure 6-15 Trend analysis for Td (top) and SSTs (bottom) for the month of September for each decade during the respective periods of record for NCEP/NCAR (1948-2010) and ICOADS (1960-2010). Only significant trends (alpha > 0.10) are shown**

# 7 SUMMARY

The database of extreme storms used in HMR51 was last updated in the late 1970s. Since that time, numerous extreme rainfall events have occurred across the eastern US, though many have not been analyzed or compared to the existing PMP values. In addition, the availability of modern datasets (e.g., gridded data) and ever-growing computing power provide the impetus to improve on existing methods for computing PMP. The current study capitalizes on these benefits of modern technology to process new storms for inclusion in the current and future PMP-related studies. One such modern dataset is the MPR data available from NCDC. This dataset covers a test region of the Carolinas for the period 1996-2007 and are available at high spatial (2.5 mi x 2.5 mi ; 4 km x 4 km) and temporal (hourly) resolution.

In the Carolinas, the primary meteorological phenomena responsible for extreme rainfall events are tropical cyclones. During the period 1996-2007, many tropical cyclones have impacted the two states, including Hurricane Floyd in 1999 and seven different storms in 2004, among others. Reclamation evaluated the historical gauge records and spreadsheets provided by HPC to select a total of 10 storms for investigation in the current study. MPR for each of these storms was analyzed and DADs computed using an automated software package developed in-house in open source scripting languages. Maximization of these storms also employed modern gridded datasets of moisture-related variables (e.g., SST, PW) to determine the IPMF. The current study did not consider transposition; and, hence, also did not adjust for orographics effects. Envelopment of maximum rainfalls from new storms was also neglected. The DADx values computed were then compared with DADx values from various tropical cyclone events included in HMR51 and with HMR51 PMP directly.

The current research suggests that Hurricanes Floyd (1999) and Fran (1996) approached or exceeded PMP at larger area sizes. Hurricane Floyd exceeded the PMP at durations of 24 and 72 hours, while Fran exceeded PMP at a 6-hour duration. The results of the current study should be considered preliminary, but suggest an increase in HMR51 PMP estimates are warranted along the Carolinas coast. The research also provided insight into the sensitivity of the method to: (i) the selection of the CPP; (ii) data quality issues in radar and gauge precipitation measurements; and, (iii) the type of data used for determining IPMFs (e.g., SST and PW). We investigated each of these limitations to highlight the potential caveats and addressed the variability through comparisons with PMP grids and past storms from HMR51. Long-term trends in moisture availability were also investigated using SST and $T_d$ as proxies. In general, limited significant trends were identified along the East Coast or in the Gulf of Mexico.

Future work in the Carolinas should consider a focus on the development of methodologies for transposing storms and adjusting these storms based on orographics. Precipitation potential over the mountainous terrain in the western Carolinas may be enhanced due to additional lift, particularly in upslope-preferred regions along the eastern escarpment of the Appalachians. In contrast, the same region is also farthest from the oceanic moisture sources, which may limit the effects of orographics. Finally, the netCDF format of the MPR data has an additional variable that prescribes an hourly variance value, based on the deviation between precipitation gauge reports and MPR estimated precipitation value at each grid cell. In subsequent studies, if MPR data were available for other locations, the variance grids could be applied in the evaluation of uncertainty in the estimation of DADx using the current methodology.

# 8 REFERENCES

## 8.1 References Cited


Applied Weather Associates (AWA), 2008: Site-Specific Probable Maximum Precipitation (PMP) Study for Nebraska. Prepared for Lower Platte North NRD, Wahoo, Nebraska by Applied Weather Associates, Monument, CO, 127 p. and Appendices A-I.

Atallah, E.H., and L.F. Bosart, 2003: The extratropical transition and precipitation distribution of Hurricane Floyd (1999). Mon. Wea. Rev., 131, 1063-1081.

Atallah, E., L. F. Bosart, and A. Aiyyer, 2007: Precipitation distribution associated with landfalling tropical cyclones over the eastern United States. Mon. Wea. Rev.,135, 2185–2206.

Baeck, M.L., and J.A. Smith, 1998: Rainfall estimation by the WSR-88D for heavy rainfall events. Wea. Forecasting, 13, 416-436.

Beasley, R., and M.S. Ryan, 2009: The effects of Hurricane Frances on north and central Georgia: Part I- Impacts. Conference on the Inland Impacts of Tropical Cyclones, American Meteorological Society/National Weather Association, Atlanta, GA, June 2009.

Bosart, L.F., and T.J. Galarneau, Jr., 2009: An overview of predecessor heavy rainfall events associated with landfalling tropical cyclones. Conference on the Inland Impacts of Tropical Cyclones, American Meteorological Society/National Weather Association, Atlanta, GA, June 2009.

Caldwell, R.J., Sankovich, V.L. and England, J.F. Jr., 2011: Synthesis of Extreme Storm Rainfall and Probable Maximum Precipitation in the Southeastern U.S. Pilot Region, for the Nuclear Regulatory Commission, Office of Nuclear Regulatory Research. Bureau of Reclamation, Denver, CO, December.

Chen, S.S., J.A. Knaff, and F.D. Marks, 2006: Effects of vertical wind shear and storm motion on tropical cyclone rainfall asymmetries deduced from TRMM. *Mon. Wea. Rev.,*134, 3190–3208.

Chu, J-H, 2011: TC Forecaster's Reference Guide. Naval Research Laboratory, Marine Meteorology Division, Monterey, CA, referenced online at http://www.nrlmry.navy.mil/~chu/.

Clemetson, D., and J. Melliger, 2010: Creating depth-area curves from GIS data. Draft Procedure, U.S. Army Corps of Engineers, Omaha District, April.

Cline, J.W., 2003: Recent tropical cyclones affecting North Carolina, unpublished thesis (M.S.), University of Miami.

Coastal Services Center (CSC), 2011: Historical Hurricane Tracks Tool, accessed online at http://www.csc.noaa.gov/digitalcoast/tools/hurricanes/index.html.

Corrigan, P., D.D. Fenn, D.R. Kluck, and J.L. Vogel, 1999: Probable Maximum Precipitation for California. Hydrometeorological Report No. 59, Hydrometeorological Design Study Center, National Weather Service, National Oceanic and Atmospheric Administration, U.S. Department of Commerce, Silver Spring, MD 392 p.

Croke, M.S., 2006: Examining planetary, synoptic and mesoscale features that enhance precipitation associated with landfalling tropical cyclones in North Carolina, unpublished thesis (M.S.), North Carolina State University.

Croke, M., L. Xie, M. Kaplan, G. Lackmann, and K. Keeter, 2005: Tropical cyclone landfall and precipitation. Local Presentation. National Weather Service, Raleigh, NC, accessed at http://www.meas.ncsu.edu/nws/www/workshops/.

DeLuca, D.P., L.F. Bosart, and D. Keyser, 2004: The distribution of precipitation over the Northeast accompanying landfalling and transitioning tropical cyclones. 20th Conference on Weather Analysis and Forecasting, Seattle, WA., Amer. Meteor. Soc.

*Draxler, R.R. and Rolph, G.D., 2011. HYSPLIT (HYbrid Single-Particle Lagrangian Integrated Trajectory) Model access via NOAA ARL READY Website (http://ready.arl.noaa.gov/HYSPLIT.php). NOAA Air Resources Laboratory, Silver Spring, MD.*

Durrans, S.R., L.T. Julian, and M. Yekta, 2002: Estimation of depth-area relationships using radar-rainfall data. J. Hydro. Eng., 7, 356-367.

Eastin, M.D., 2009: Surface observations of landfalling rainbands in Tropical Storm Hanna (2008). Conference on the Inland Impacts of Tropical Cyclones, American Meteorological Society/National Weather Association, Atlanta, GA, June 2009.

England, J.F. Jr., Sankovich, V.L. and Caldwell, R.J., 2011: Review of Probable Maximum Precipitation Procedures and Databases used to Develop Hydrometeorological Reports, for the Nuclear Regulatory Commission, Office of Nuclear Regulatory Research. Bureau of Reclamation, Denver, CO, December.

Feldt, J.J., 2009: Hydrologic impacts from inland-moving tropical systems: From welcome rainfall to devastating floods. Conference on the Inland Impacts of Tropical Cyclones, American Meteorological Society/National Weather Association, Atlanta, GA, June 2009.

Franklin, J.L., D.P. Brown, and C. McAdie, 2005: Hurricane Gaston. National Hurricane Center Tropical Cyclone Report, accessed online at http://www.nhc.noaa.gov/2004gaston.shtml.

Gleason, B., 2006: Characteristics of tropical cyclone rainfall in the United States. Preprints, 27th Conference on Hurricanes and Tropical Meteorology, Amer. Meteor. Soc.

Granato, G.E., 2006: Kendall-Theil Robust Line (KTRLine-version 1.0)- A Visual Basic program for calculating and graphing robust non-parametric estimates of linear regression coefficients between two continuous variables. U.S. Geological Survey Techniques and Methods 4-A7, Chapter 7, 37 pp.

Grieser, J., S. Jewson, and D. Lohmann, 2009: The RMS TC-Rain Model. Conference on the Inland Impacts of Tropical Cyclones, American Meteorological Society/National Weather Association, Atlanta, GA, June 2009.

Gonski, R., 2006: Tropical cyclone precipitation distribution of storms impacting the Carolinas from 2003-2005. Local Seminar, National Weather Service, Raleigh, NC.

Haggard, W.H., T.H. Bilton, and H.L. Crutches, 1973: Maximum rainfall from tropical cyclone systems which cross the Appalachians. J. Appl. Meteorol., 12, 50-61.

Hansen, E.M., D.D. Fenn, P. Corrigan, J.L. Vogel, L.C. Schreiner, and R.W. Stodt, 1994: Probable Maximum Precipitation-Pacific Northwest States, Columbia River (including portions of Canada), Snake River and Pacific Coastal Drainages. Hydrometeorological Report No. 57, National Weather Service, National Oceanic and Atmospheric Administration, U.S. Department of Commerce, Silver Spring, MD, 338 p.

Hartfield, G., 2006: Tropical cyclone precipitation distribution with landfalling North Carolina storms. Local Seminar, National Weather Service, Raleigh, NC.

Helsel, D.M. and R.M. Hirsch, 1992: Statistical Methods in Water Resources, Studies in Environmental Science 49, Elsevier, Amsterdam, 529 pp.

Jamski, M.A., R.J. Lanier, R.J. Verdi, 2009: A comparison of the inland impacts of Tropical Storm Fay (2008) and Hurricane Dora (1964). Conference on the Inland Impacts of Tropical Cyclones, American Meteorological Society/National Weather Association, Atlanta, GA, June 2009.

Jurewicz, Sr., M.L., M. Cote, L. Bosart, and D. Keyser, 2009: A study of predecessor rainfall events (PRE) in advance of tropical cyclones. Conference on the Inland Impacts of Tropical Cyclones, American Meteorological Society/National Weather Association, Atlanta, GA, June 2009.

Kalnay et al., 1996: The NCEP/NCAR 40-year reanalysis project, Bull. Amer. Meteor. Soc., 77, 437-470.

Knight, D.B., and R.E. Davis, 2007: Climatology of tropical cyclone rainfall in the southeastern United States. Physical Geography, 28, 126-147.

Konrad II, C.E., and L.B. Perry, 2009: Relationships between tropical cyclones and heavy rainfall in the Carolina region of the USA. Int. J. Climatol., DOI: 10.1002/joc.1894, 13 pp.

Kusselson, S., M. Turk, L. Zhao, S. Kidder, J. Forsythe, A. Jones, and E.E. Ebert, 2009: New satellite-derived tools for inland rainfall impacts from tropical cyclones. Conference on the Inland Impacts of Tropical Cyclones, American Meteorological Society/National Weather Association, Atlanta, GA, June 2009.

Matyas, C., 2009: A GIS-based analysis of the post-landfall shape properties of tropical cyclone rain fields. Conference on the Inland Impacts of Tropical Cyclones, American Meteorological Society/National Weather Association, Atlanta, GA, June 2009.

McGehee, C.H., M. Griffin, P. Knox, and L.A. Eaton, 2009: Improved areal precipitation estimates for Tropical Storm Fay due to Community Collaborative Rain, Hail, and Snow (CoCoRaHS) network observations. Conference on the Inland Impacts of Tropical Cyclones, American Meteorological Society/National Weather Association, Atlanta, GA, June 2009.

McKemy, D., 2011: Tropical Precipitation Statistics – Methodology. Local Study Document, State Climate Office of North Carolina, June 2009. https://climate.ncsu.edu/wp-content/uploads/2020/10/TropicalPrecip_NC.pdf

Mizzell, H., 1999: Comparison of WSR-88D derived rainfall estimates with gauge data in Lexington County, South Carolina. M.S. Thesis, University of South Carolina, Columbia, SC.

Moore, B.J., L.F. Bosart, and D. Keyser, 2009: A comparison of significant predecessor rain events associated with Tropical Cyclone Rita (2005) and Tropical Cyclone Erin (2007). Conference on the Inland Impacts of Tropical Cyclones, American Meteorological Society/National Weather Association, Atlanta, GA, June 2009.

National Hurricane Center (NHC), 2011: Tropical Cyclone Climatology, accessed online at http://www.nhc.noaa.gov/pastprofile.shtml.

National Weather Service (NWS), 2008: Notes on tropical cyclone precipitation distribution across central North Carolina. Local Document. National Weather Service, Raleigh, NC, accessed at http://www.erh.noaa.gov/rah/science/rah.tropical.cyclone.precipitation.distribution.pdf.

Nelson, B., D.J. Seo, and D. Kim, 2010: Multisensor precipitation reanalysis. J. Hydromet., 11, 666-682.

Noguiera, R.C. and B.D. Keim, 2010: Contributions of Atlantic tropical cyclones to monthly and seasonal rainfall in the eastern United States 1960-2007. Theor. Appl. Clim., 10.1007/s00704-010-0292-9.

Prasad, R., Hibler, L.F., Coleman, A.F., and Ward, D.L., 2011: Design-Basis Flood Estimation for Site Characterization at Nuclear Power Plants in the United States of America. Nuclear Regulatory Commission NUREG/CR-7046, PNNL-20091, prepared by Pacific Northwest National Laboratory, Richland, WA.

Rappaport, E.N., M. Fuchs, and M. Lorentson, 1999: The threat to life in inland areas of the United States from Atlantic tropical cyclones. Preprints, 23rd Conf. on Hurricanes and Tropical Meteorology, Dallas, TX, Amer. Meteor. Soc.

Reynolds, Richard W., Thomas M. Smith, Chunying Liu, Dudley B. Chelton, Kenneth S. Casey, Michael G. Schlax, 2007: Daily High-Resolution-Blended Analyses for Sea Surface Temperature. J. Climate, 20, 5473-5496.

Rogers, R., S. Chen, J. Tenerelli, and H. Willoughby, 2003: A numerical study of the impact of vertical shear on the distribution of rainfall in Hurricane Bonnie (1998). Mon. Wea. Rev., 131, 1527-1599.

Rolph, G.D., 2011. Real-time Environmental Applications and Display sYstem (READY) Website (http://ready.arl.noaa.gov). NOAA Air Resources Laboratory, Silver Spring, MD.

Roth, D., 2009: About CLIQR: A climatological aide to tropical cyclone rainfall forecasting. Conference on the Inland Impacts of Tropical Cyclones, American Meteorological Society/National Weather Association, Atlanta, GA, June 2009.

Ryan, M.S., and R. Beasley, 2009: The effects of Hurricane Frances on north and central Georgia: Part II- Meteorological Analysis. Conference on the Inland Impacts of Tropical Cyclones, American Meteorological Society/National Weather Association, Atlanta, GA, June 2009.

Schreiner, L.C., and J.T. Riedel, 1978: Probable Maximum Precipitation Estimates, United States East of the 105th Meridian. Hydrometeorological Report No. 51, National Weather Service, National Oceanic and Atmospheric Administration, U.S. Department of Commerce, Silver Spring, MD, 87 p.

Shepherd, J.M., A. Grundstein, and T.L. Mote, 2009: Quantifying the contribution of tropical cyclones to extreme rainfall along the coastal southeastern United States. Conference on the Inland Impacts of Tropical Cyclones, American Meteorological Society/National Weather Association, Atlanta, GA, June 2009.

Sieck, L.C., S.J. Burges, and M. Steiner, 2007: Challenges in obtaining reliable measurements of point rainfall. Water Resour. Res., 43, W01420, 23 pp.

Smith, J.A., M.L. Baeck, M. Steiner, and A.J. Miller, 1996: Catastrophic rainfall from an upslope thunderstorm in the central Appalachians: The Rapidan storm of June 27, 1995. Water Resour. Res., 32, 3099-3113.

Smith, B., and J. Blaes, 2009: Effects of dry air ridging on precipitation in Tropical Storm Hanna (2008). Conference on the Inland Impacts of Tropical Cyclones, American Meteorological Society/National Weather Association, Atlanta, GA, June 2009.

Srock, A.F., and L.F. Bosart, 2009: Heavy precipitation associated with southern Appalachian cold-air damming and Carolina coastal frontogenesis in advance of weak landfalling Tropical Storm Marco (1990). Mon. Wea. Rev., 137, 2448-2470.

Stull, R.B., 1988: An Introduction to Boundary Layer Meteorology. Kluwer, 666 pp.

Ulbrich, C.W., and L.G. Lee, 2002: Rainfall characteristics associated with the remnants of Tropical Storm Helene in Upstate South Carolina. Wea. Forecasting, 17, 1257-1267.

U.S. Army Corps of Engineers (USACE) (1973) Storm Rainfall in the United States, 1945 - 1973. Washington, D.C.

Woodruff, S.D., H.F. Diaz, S.J. Worley, R.W. Reynolds, and S.J. Lubker, 2005: Early ship observational data and ICOADS. Climatic Change, 73, 169-194

Woodruff, S.D., S.J. Worley, S.J. Lubker, Z. Ji, J.E. Freeman, D.I. Berry, P. Brohan, E.C. Kent, R.W. Reynolds, S.R. Smith, and C. Wilkinson, 2011: ICOADS Release 2.5: Extensions

and enhancements to the surface marine meteorological archive. *Int. J. Climatol.* 31 (7), 951-967, doi:10.1002/joc.2103.

World Meteorological Organization (WMO) (2009) Manual on Estimation of Probable Maximum Precipitation (PMP). WMO No. 1045, Geneva, 259 p.

Xie, L., and K. Keeter, 2006: Inland flooding from tropical cyclones. COMET Outreach Program Final Report, S04-44684.

## 8.2 Other Pertinent References

Al-Mamun, A., and A. Hashim, 2004: Generalised long duration probable maximum precipitation (PMP) isohyetal maps for peninsular Malaysia. J. Spatial Hydrology, 4, Spring 2004.

Burke, P., 2009: Tropical Storm Erin re-intensifies over Oklahoma. Conference on the Inland Impacts of Tropical Cyclones, American Meteorological Society/National Weather Association, Atlanta, GA, June 2009.

Chen, L.C., and A.A. Bradley, 2007: How does the record July 1996 Illinois rainstorm affect probable maximum precipitation estimates? J. Hydro. Eng., 12, 327-335.

Chen, L.C., and A.A. Bradley, 2006: Adequacy of using surface humidity to estimate atmospheric moisture availability for probably maximum precipitation. Wat. Res. Research, 42, W09410, 17 pp.

Davies-Jones, R., 2007: An efficient and accurate method for computing the wet-bulb temperature along pseudoadiabats. Mon. Wea. Rev., 136, 2764-2785.

Douglas, E.M., and A.P. Barros, 2003: Probable maximum precipitation estimation using multifractals: application in the eastern United States. J. Hydromet, 4, 1012-1024.

Hart, R. E., J. L. Evans and C. Evans., 2006: Synoptic composites of the extratropical transition life cycle of North Atlantic tropical cyclones: Factors determining post-transition evolution. Mon. Wea. Rev., 134, 553-578.

Hart, R. E., 2003: A cyclone phase space derived from thermal wind and thermal asymmetry. Mon. Wea. Rev., 131, 546-564.

Landsea, C.W., 1993: A climatology of intense (or major) Atlantic hurricanes. Mon. Wea. Rev., 121, 1703-1713.

Leverson, V.H., 1986: Rainfall characteristics of the Prescott, Arizone, storm of 23-24 September 1983. Mon. Wea. Rev., 114, 2344-2351.

Robinson, P.J., 1998: Monthly variations of dew point temperature in the coterminous United States. Int. J. Climatology, 18, 1539-1556.

U.S. Navy, 1981: Marine Climatic Atlas of the World. Vol. IX: World-wide Means and Standard Deviations, NAVAIR 50-1C-65, U.S. Government Printing Office, Washington, D.C., 169 pp.

# APPENDIX A STORM DISCUSSIONS

For each of the storms evaluated in the current study, we provide pertinent weather maps required to describe the synoptic conditions associated with each storm. In addition, the storm total accumulated MPR and hourly gauge data are shown for the top 10 storms. The storms are presented in alphabetical order by storm track type. A summary of the maximum precipitation periods for each of the events is provided at the end of Appendix A.

## A.1 Coastal Storm Tracks

### A.1.1 Hurricane Bonnie: August 26 – August 29, 1998

Hurricane Bonnie started as a tropical wave in the eastern Atlantic Ocean and moved on a generally west or west-northwest track on the southern side of a broad high pressure until it reached the Bahamas. The steering currents weakened as the high pressure to the north collapsed, causing Bonnie to move slowly northward along the U.S. East Coast. The ridge of high pressure then restrengthened and turned Bonnie to the northwest toward the Carolina coasts. Bonnie made landfall near Wilmington, NC, as a borderline Category 2/3 hurricane on 27 August 1998 (Figure A.1). A mid-level trough impinged on the hurricane from the northwest and turned Bonnie to the northeast and offshore into the North Atlantic. [Brief synopsis derived from NHC preliminary reports; http://www.nhc.noaa.gov/]

Air temperatures across the Carolinas ranged from highs in the mid- to upper 90s, with low 80s in the rain cooled air. Dewpoint temperatures during the morning hours ranged from the upper 60s to the mid-70s (Figure A.2). Surface winds ahead (north) of the storm were onshore along the NC coastal plain with northerly or northwesterly downslope flow across the western Carolinas to the west of Bonnie. A cold front also passed through the western Carolinas by the morning of 27 August, limiting the westward extent of precipitation. Isentropic upglide potentially enhanced rainfall to the north of Bonnie as a warm, moist Atlantic airmass was lifted over a cooler and drier dome of high pressure centered over the Ohio Valley. Heaviest precipitation was, therefore, confined along the track of Bonnie across the coast and nearby coastal plain in northeastern SC and eastern NC (Figures A.1 and A.3). DADx estimates for Hurricane Bonnie (based on MPR), with comparison to HMR51 PMP, are shown in Figure A.4.

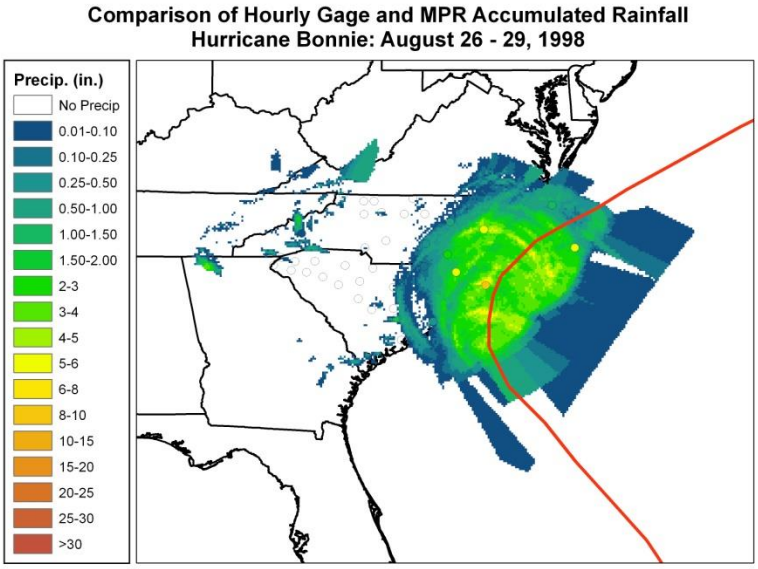


**Figure A.1** **Storm total precipitation for Hurricane Bonnie with best storm track from NOAA shown in red**

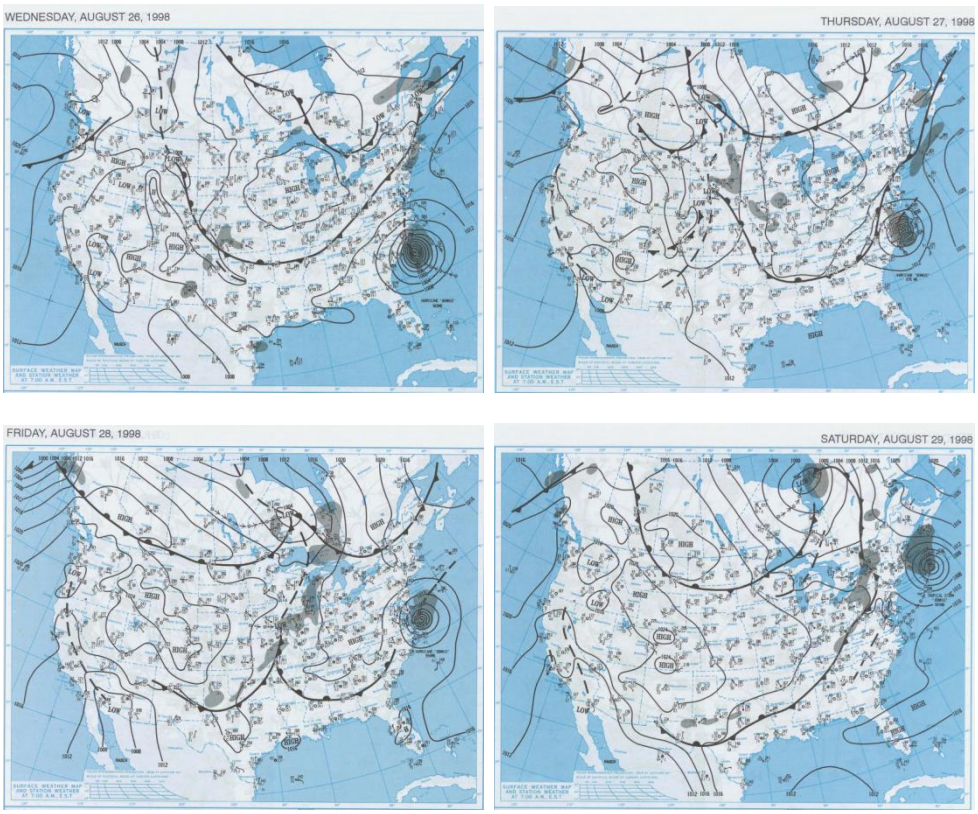


**Figure A.2** **Surface weather maps valid at 7 a.m. EST for the period August 26 – 29, 1998. Source: NOAA Central Library, https://library.noaa.gov/Collections/Digital-Collections/US-Daily-Weather-Maps**

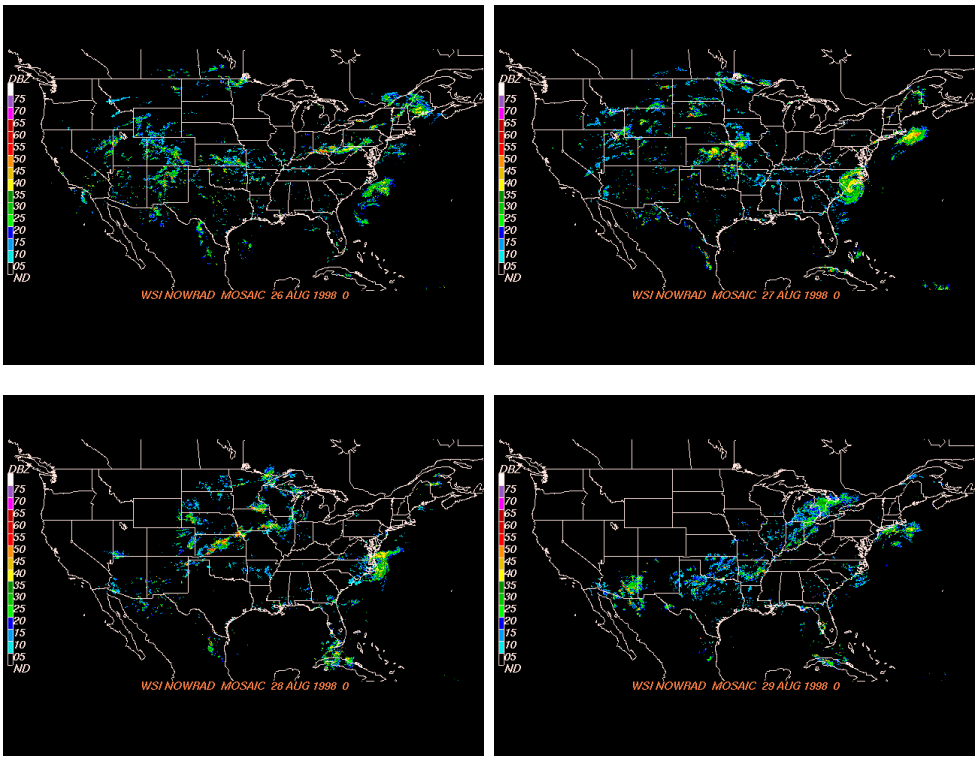


**Figure A.3** **National mosaic NEXRAD reflectivity images for the period August 26 – 29, 1998. Imagery is valid at closest available time to 0000 UTC each day. Source: National Climatic Data Center, https://www.ncei.noaa.gov/products/radar/next-generation-weather-radar**

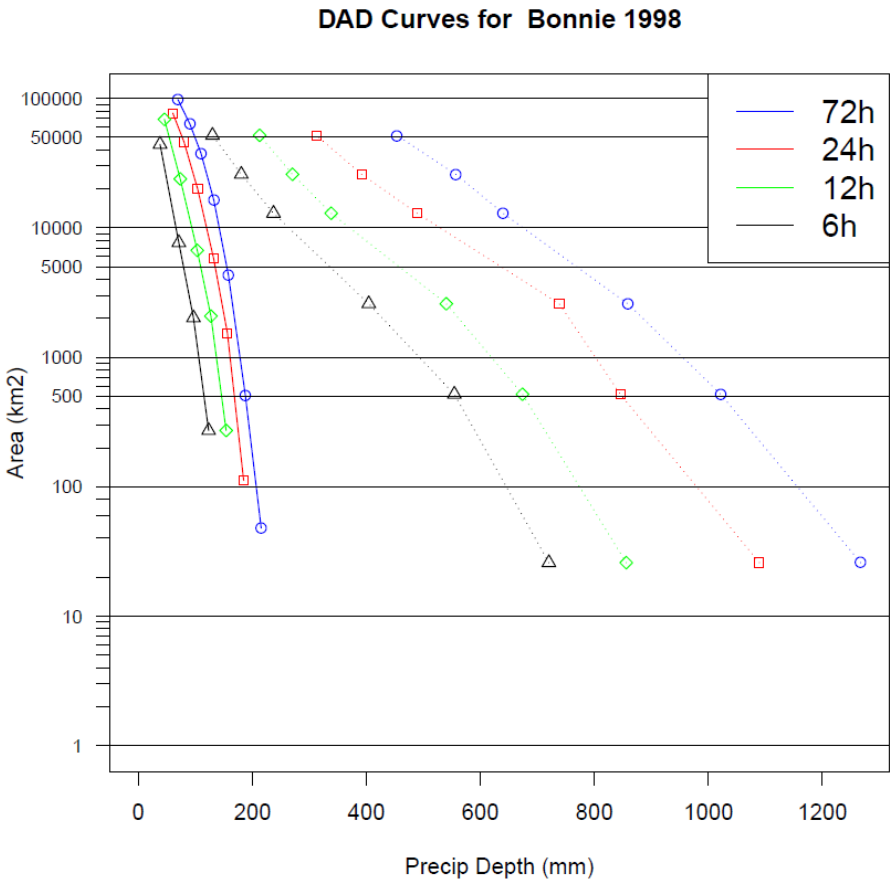


**Figure A.4** **Comparison of maximized depth-area-duration curves for Hurricane Bonnie (solid) and probable maximum precipitation values extracted from HMR 51 (dotted)**

### A.1.2 Hurricane Ernesto: August 30 – September 2, 2006

Hurricane Ernesto started as a tropical wave in the eastern Atlantic Ocean and moved westward on the southern side of a broad high pressure until it reached the Windward Islands, when the wave developed a surface circulation and became a tropical depression. The cyclone continued on a westward path south of Puerto Rico and Hispaniola, where it briefly reached hurricane status in the central Caribbean before weakening as it interacted with the topography of Haiti and Cuba. Ernesto then moved northward toward the Florida peninsula and then back offshore into the western Atlantic Ocean where it reintensified to a strong tropical storm prior to landfall near Wilmington, NC (Figure A.5). A mid-level trough impinged on the storm from the west and Ernesto moved north-northeastward across North Carolina and Virginia. [Brief synopsis derived from NHC preliminary reports; http://www.nhc.noaa.gov/]

Air temperatures across the Carolinas ranged from highs in the 90s, with 80s and upper 70s in the rain cooled air. Dewpoint temperatures during the morning hours ranged from the upper 60s to the upper 70s (Figure A.6). A cold front was positioned across the central Carolinas as Ernesto moved across the Florida peninsula. Southerly winds east of the front and northeasterly winds west of the front provided both Gulf of Mexico and Atlantic moisture sources. A strong pressure gradient between the approaching tropical storm and strong high pressure over eastern Canada led to enhanced easterly flow across the Carolinas and mid-Atlantic. Frontal enhancement of precipitation in the presence of ample moisture led to widespread rainfall across the Carolinas and Virginia (Figures A.5 and A.7). DADx estimates for Hurricane Ernesto (based on MPR), with comparison to HMR51 PMP, are shown in Figure A.8.

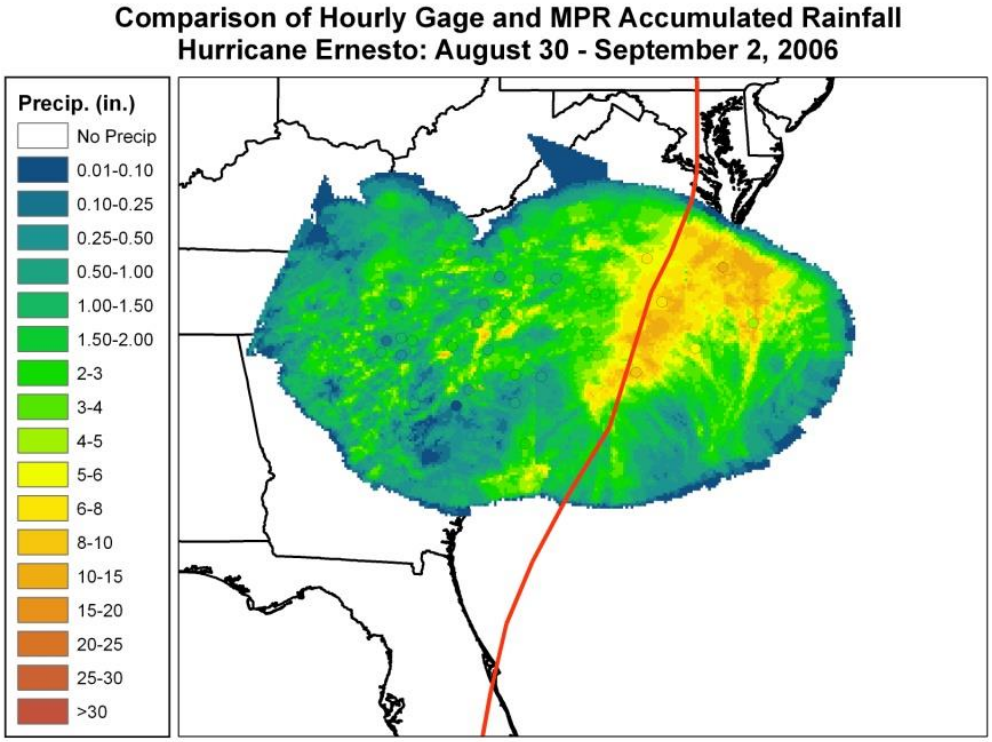


**Figure A.5 Storm total precipitation for Hurricane Ernesto with best storm track from NOAA shown in red**

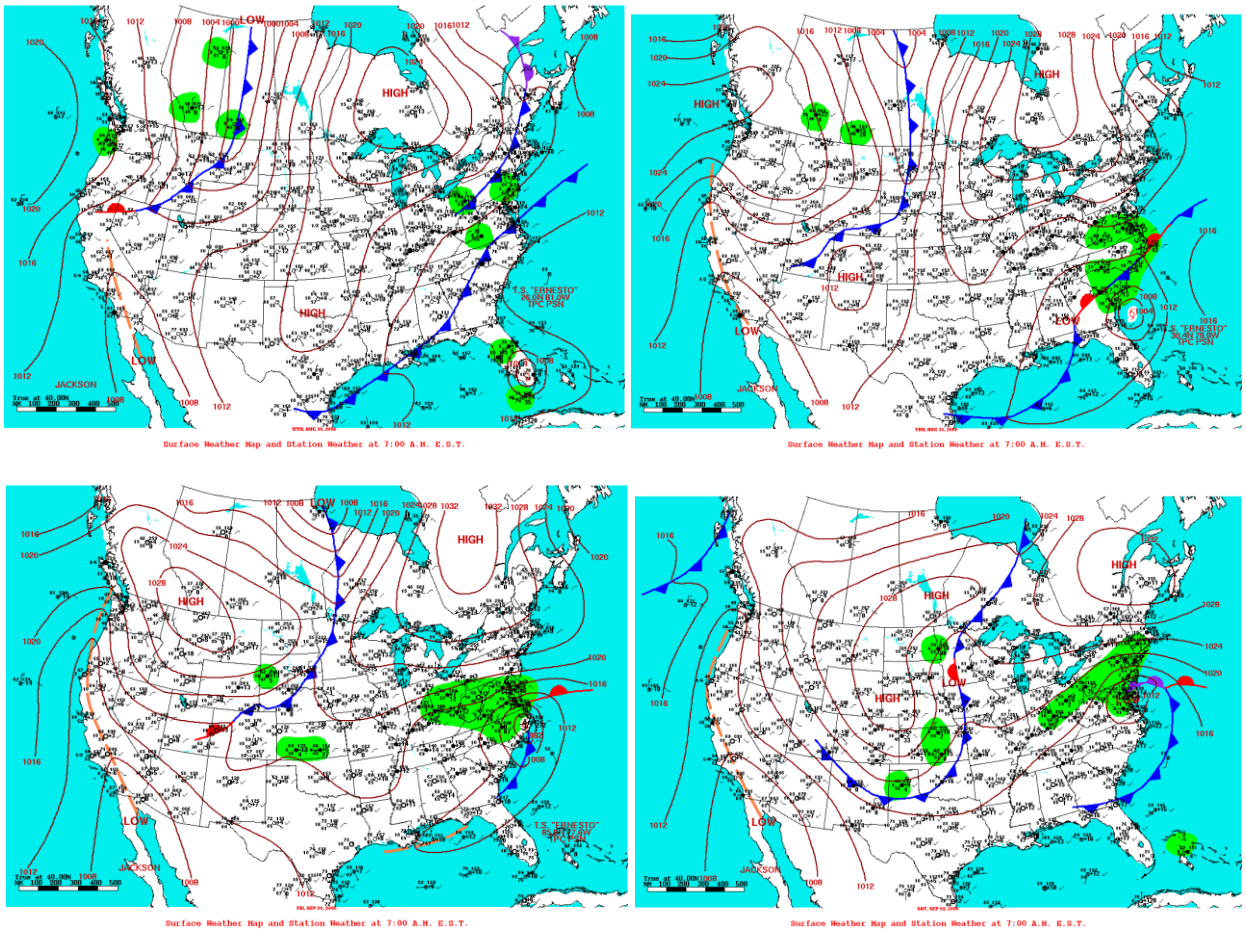


**Figure A.6** **Surface weather maps valid at 7 a.m. EST for the period August 30 – September 2, 2006. Source: NOAA Hydrometeorological Prediction Center, https://www.wpc.ncep.noaa.gov/dailywxmap/index.html**

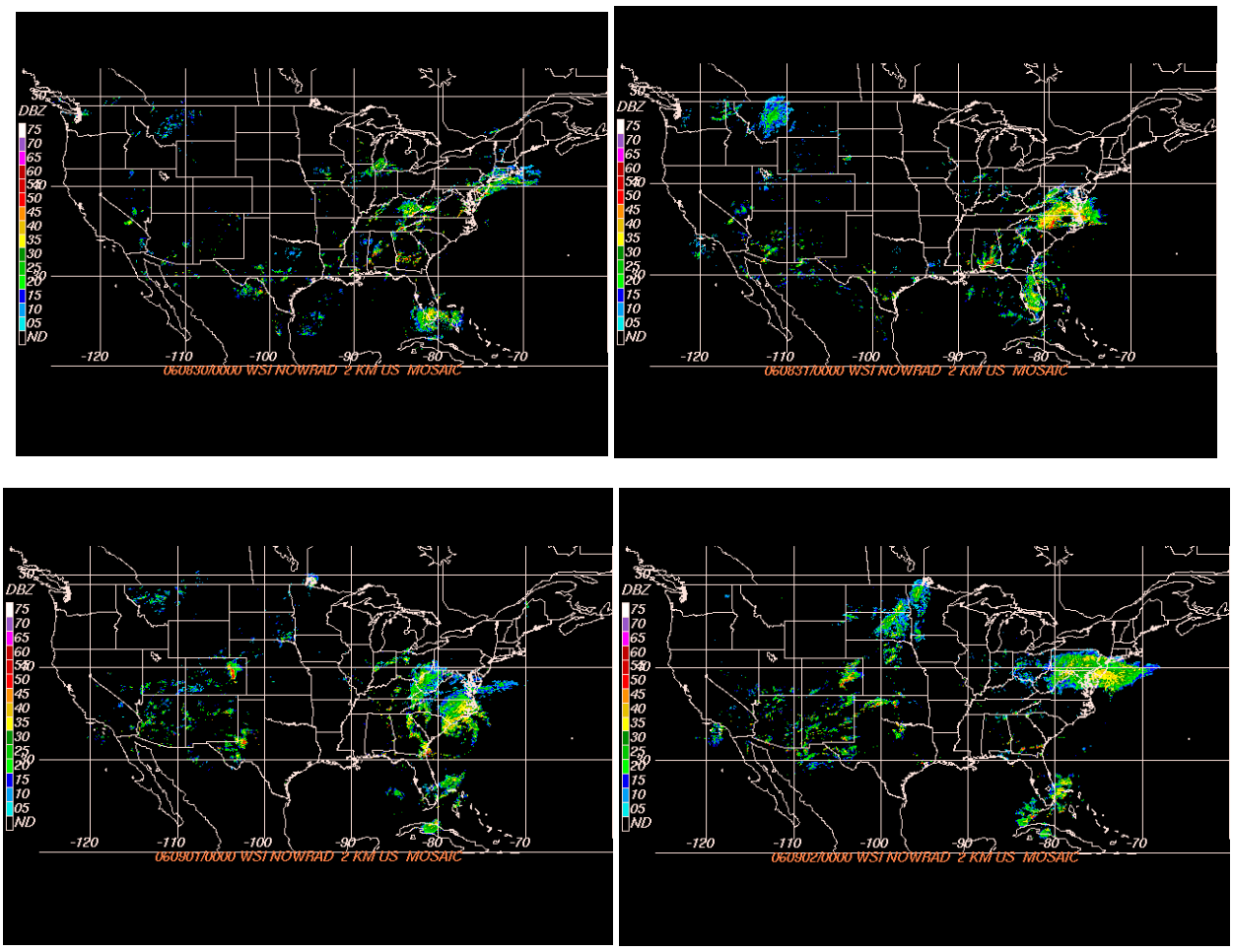


**Figure A.7** **National mosaic NEXRAD reflectivity images for the period August 30 – September 2, 2006. Imagery is valid at closest available time to 0000 UTC each day. Source: National Climatic Data Center, https://www.ncei.noaa.gov/products/radar/next-generation-weather-radar**

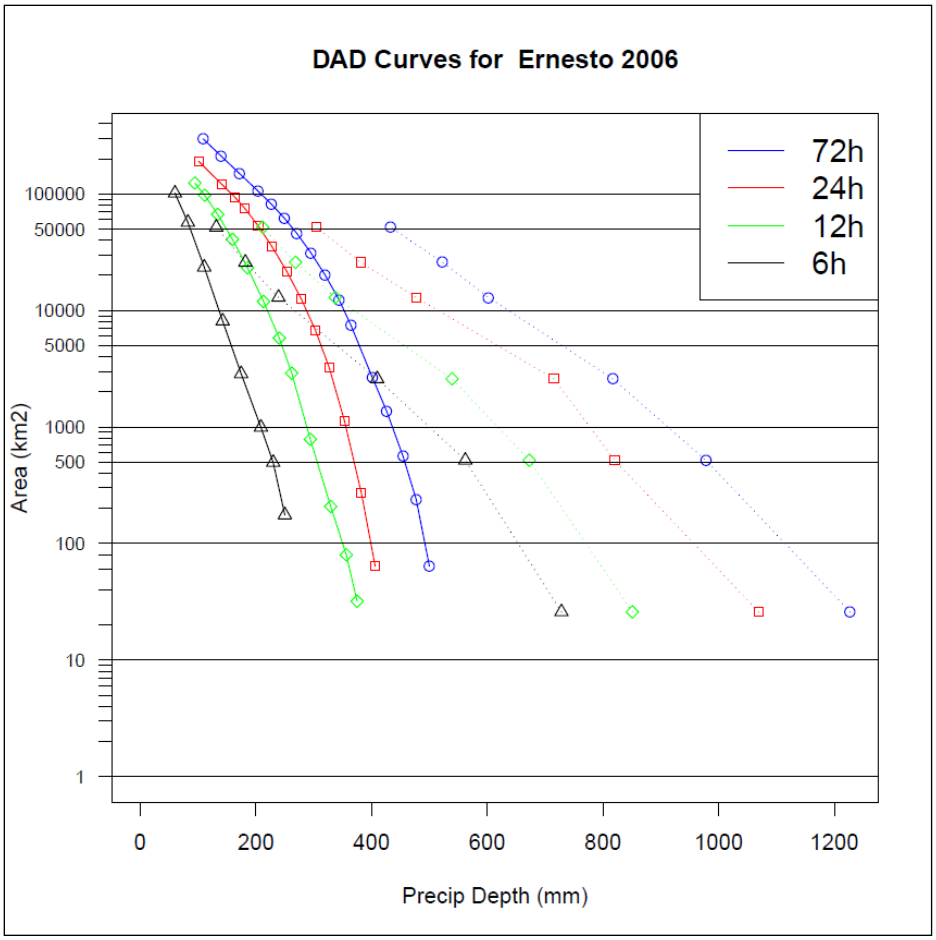


**Figure A.8 Comparison of maximized depth-area-duration curves for Hurricane Ernesto (solid) and probable maximum precipitation values extracted from HMR 51 (dotted)**

### A.1.3 Hurricane Floyd: September 14 – September 17, 1999

Hurricane Floyd started as a disorganized tropical wave in the eastern Atlantic Ocean and moved westward on the southern side of a broad high pressure. The tropical wave reached tropical depression status approximately 1000 miles east of the Lesser Antilles on 6 September and tropical storm status on 8 September. The cyclone slowly strengthened over the next few days and strengthened to Hurricane Floyd on 10 September around 200 miles east-northeast of the Leeward Islands. Floyd then moved on a northwest path to the north of the eastern Caribbean islands then turned westward and strengthened as the storm took aim at the Bahamas. A mid- to upper-level trough over the eastern U.S. eroded the subtropical ridge over the western Atlantic and Floyd turned north then northeast paralleling the coast of Florida. Hurricane Floyd made landfall near Cape Fear, NC on 16 September (Figure A.9). [Brief synopsis derived from NHC preliminary reports; http://www.nhc.noaa.gov/]

Air temperatures across the Carolinas ranged from highs in the 80s, with 60s and 70s in the rain cooled air. Dewpoint temperatures during the morning hours were generally in the 60s with several coastal locations in the low 70s (Figure A.10). A stationary front was positioned along the spine of the Appalachians with surface convergence enhanced by northwest winds west of

the front and northeast winds east of the frontal system. As Floyd approached the Carolinas, the frontal system shifted eastward to a position along the coastal plain. The airmass to the west over the Ohio Valley was also much cooler and drier with dewpoints in the 40s. Isentropic upglide and frontal enhancement through convergence of winds at the surface led to widespread rainfall across the eastern Carolinas and Virginia (Figures A.9 and A.11). More stable air and southwesterly shear from the mid-level trough limited the westward extent of rainfall. DADx estimates for Hurricane Floyd (based on MPR), with comparison to HMR51 PMP, are shown in Figure A.12.

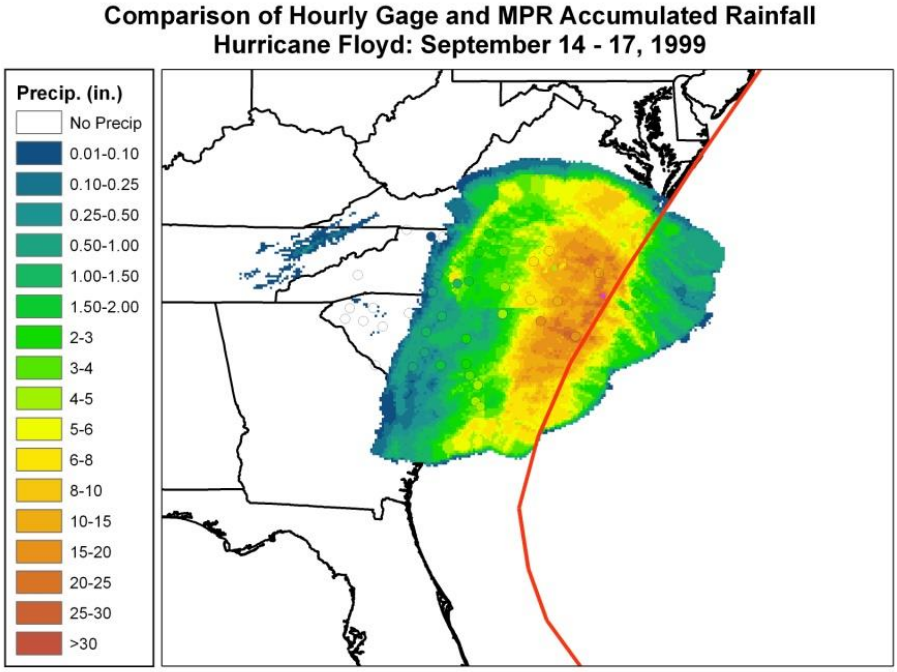


**Figure A.9 Storm total precipitation for Hurricane Floyd with best storm track from NOAA shown in red**

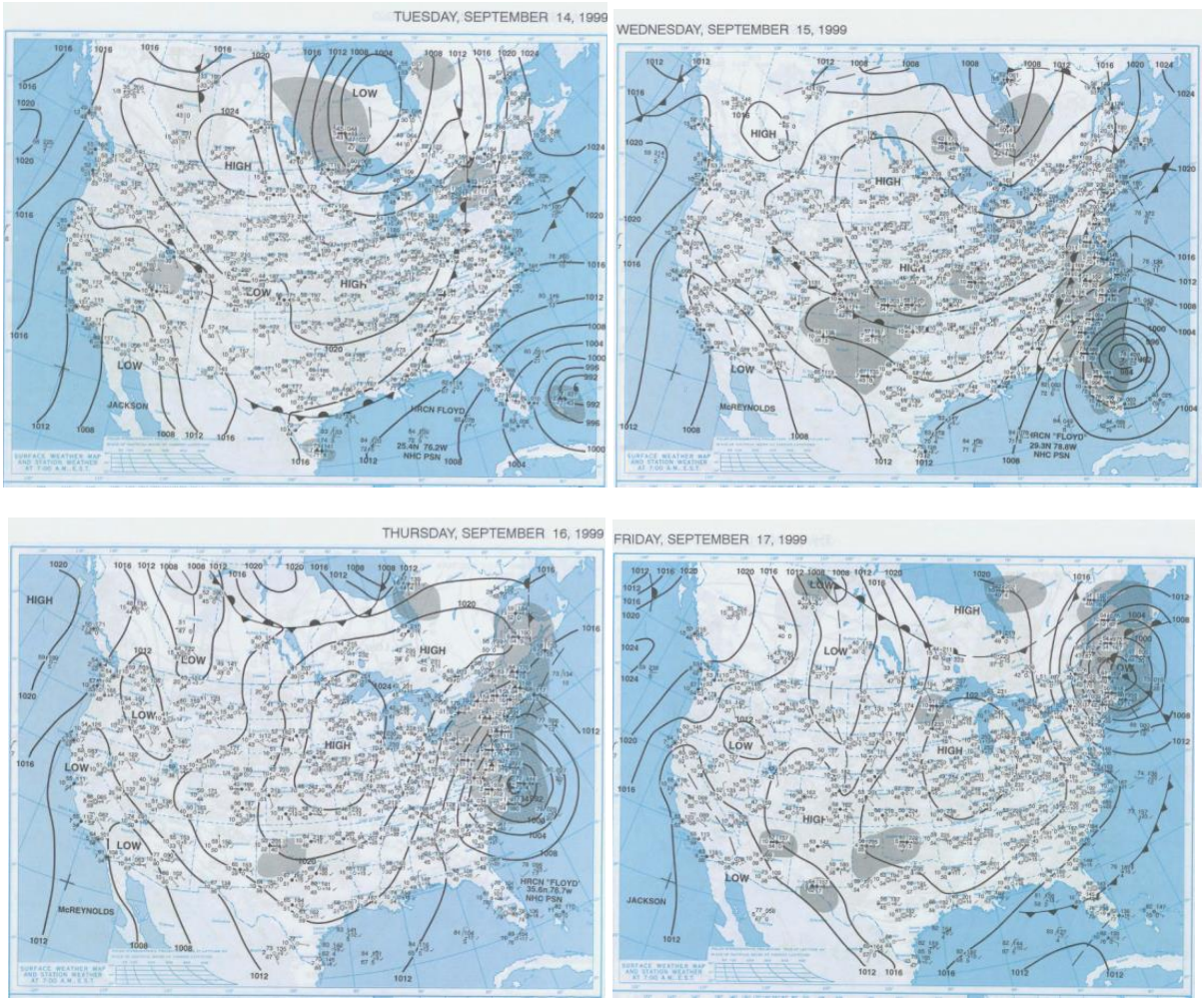


**Figure A.10 Surface weather maps valid at 7 a.m. EST for the period September 14 – 17, 1999. Source: NOAA Central Library, http://docs.lib.noaa.gov/rescue/dwm/data_rescue_daily_weather_maps.html**

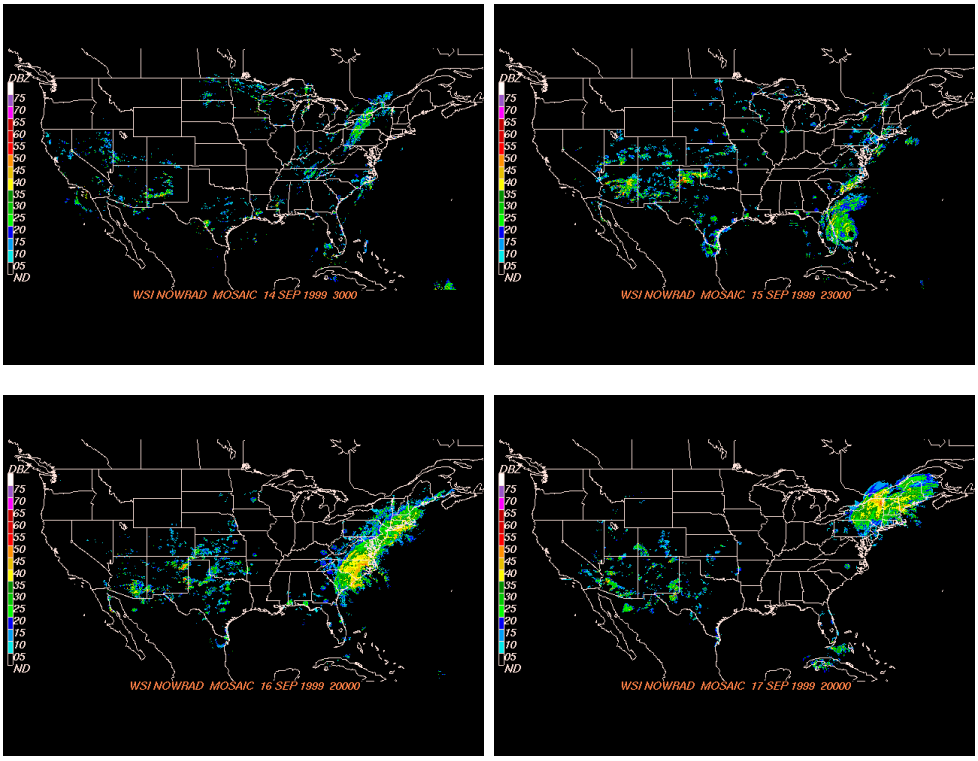


**Figure A.11 National mosaic NEXRAD reflectivity images for the period September 14 – 17, 1999. Imagery is valid at closest available time to 0000 UTC each day. Source: National Climatic Data Center, https://www.ncei.noaa.gov/products/radar/next-generation-weather-radar**

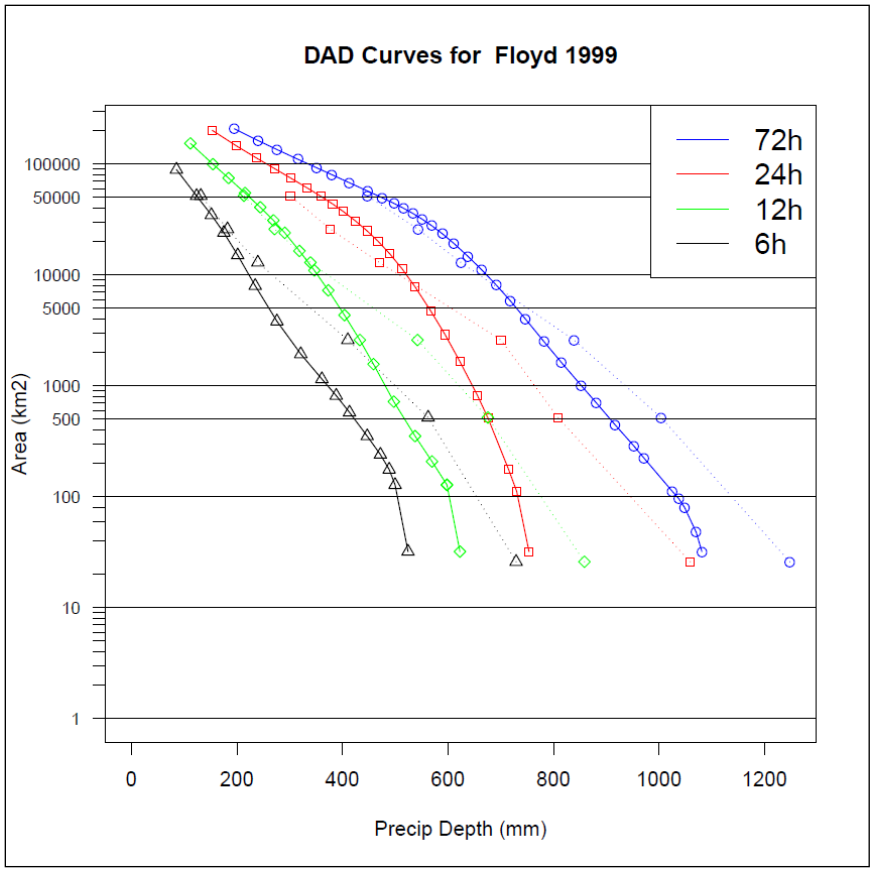


**Figure A.12 Comparison of maximized depth-area-duration curves for Hurricane Floyd (solid) and probable maximum precipitation values extracted from HMR 51 (dotted)**

### A.1.4 Hurricane Gaston: August 28 – September 1, 2004

Hurricane Gaston developed along a stalled cold front that moved off the Carolina coast on 22 August. A broad area of low pressure formed along the frontal boundary on 25 August and gradually became more organized with banded convection noted on 26 August. The low strengthened to a tropical depression on the 27th and tropical storm on the 28th. After meandering offshore for several days during development, a mid- to upper-level ridge developed northeast of Gaston on the 29th and with a mid-latitude trough approaching from the west, Gaston turned northwestward toward the SC coastline and made landfall near Awendaw, SC, on 29 August. The mid-latitude trough then turned Gaston north then northeastward across the eastern plains of northeast SC and southeast NC (Figure A.13). [Brief synopsis derived from NHC preliminary reports; http://www.nhc.noaa.gov/]

Air temperatures across the Carolinas ranged from highs in the mid-80s, with lower 80s in the rain cooled air. Dewpoint temperatures during the morning hours were generally in the upper 60s with several coastal locations in the low 70s (Figure A.14). Winds across the Carolinas were generally north or northeasterly in the wake of the frontal system that passed through on 22 August. Winds turned easterly north of the tropical cyclone as the circulation center strengthened. Due to the small circulation, the coverage of precipitation was limited to regions

near and along the track, though some scattered thunderstorms occurred inland as bands progressed westward toward the Appalachians (Figure A.13 and A.15). Any additional lift provided by the approaching cold front from the west by 31 August appears to be a limited contributor to rainfall amounts, except perhaps across extreme northeastern NC and southeast VA. DADx estimates for Hurricane Gaston (based on MPR), with comparison to HMR51 PMP, are shown in Figure A.16.

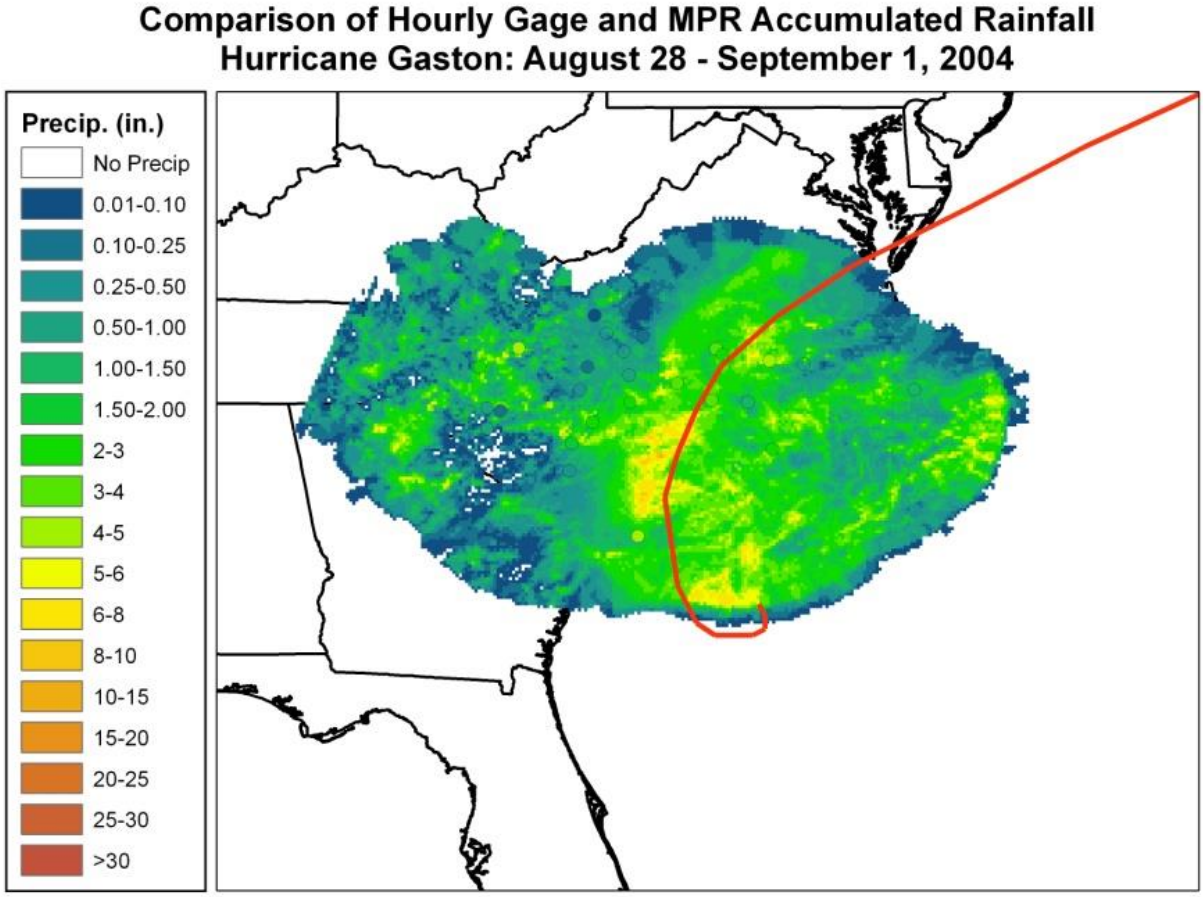


**Figure A.13 Storm total precipitation for Hurricane Gaston with best storm track from NOAA shown in red**

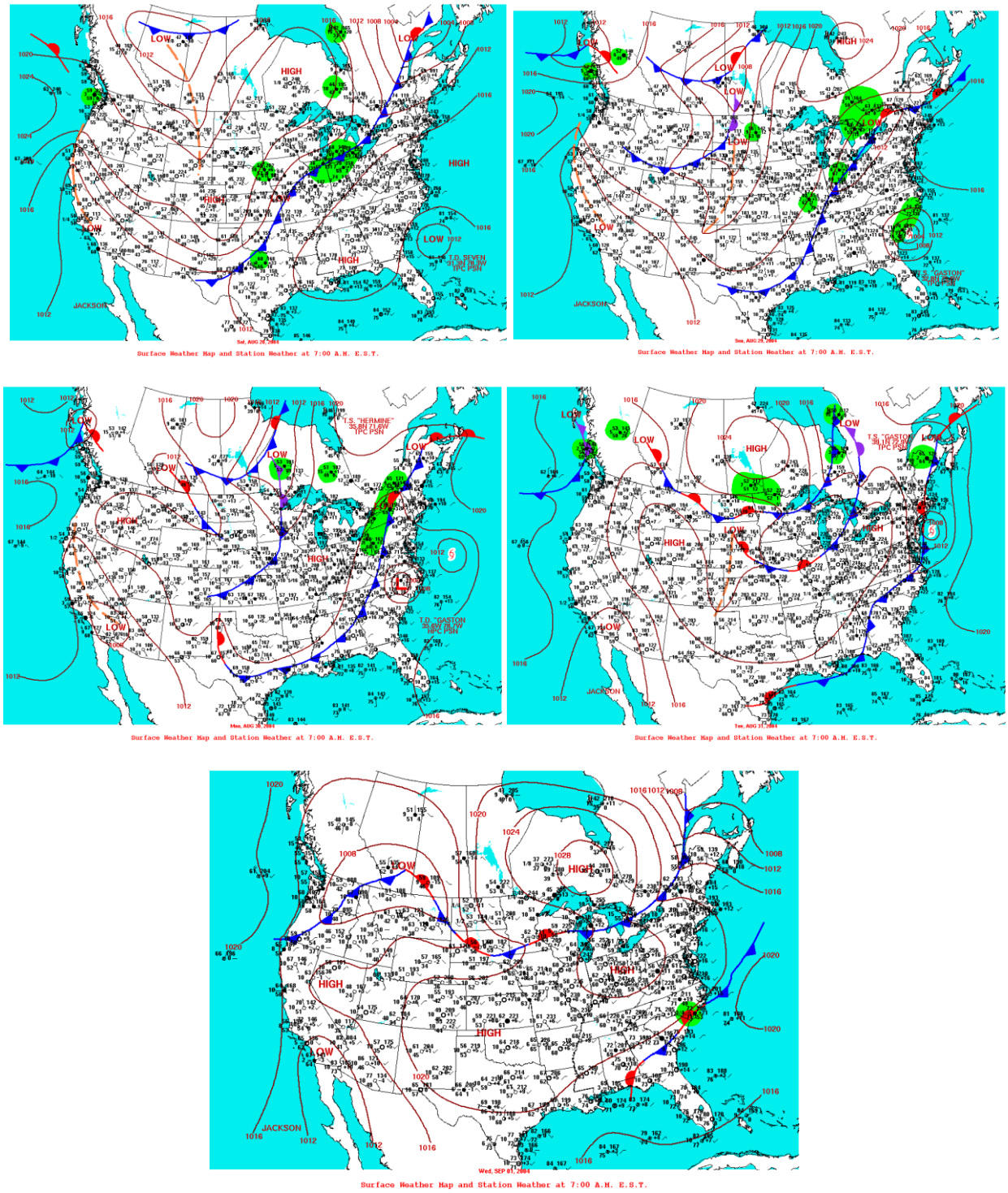


**Figure A.14 Surface weather maps valid at 7 a.m. EST for the period August 28 – September 1, 2004. Source: NOAA Hydrometeorological Prediction Center, https://www.wpc.ncep.noaa.gov/dailywxmap/index.html**

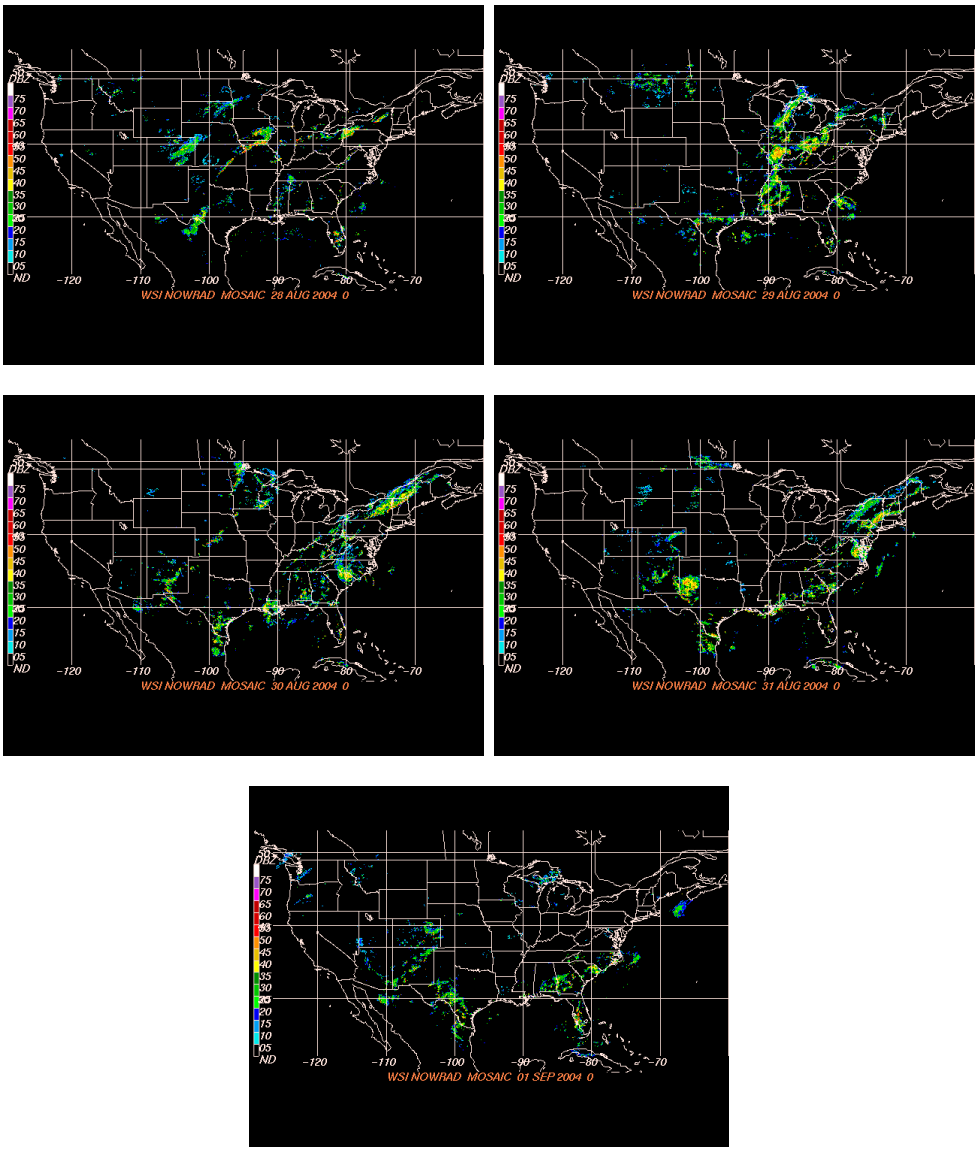


**Figure A.15** **National mosaic NEXRAD reflectivity images for the period August 28 – September 1, 2004. Imagery is valid at closest available time to 0000 UTC each day. Source: National Climatic Data Center, https://www.ncei.noaa.gov/products/radar/next-generation-weather-radar**

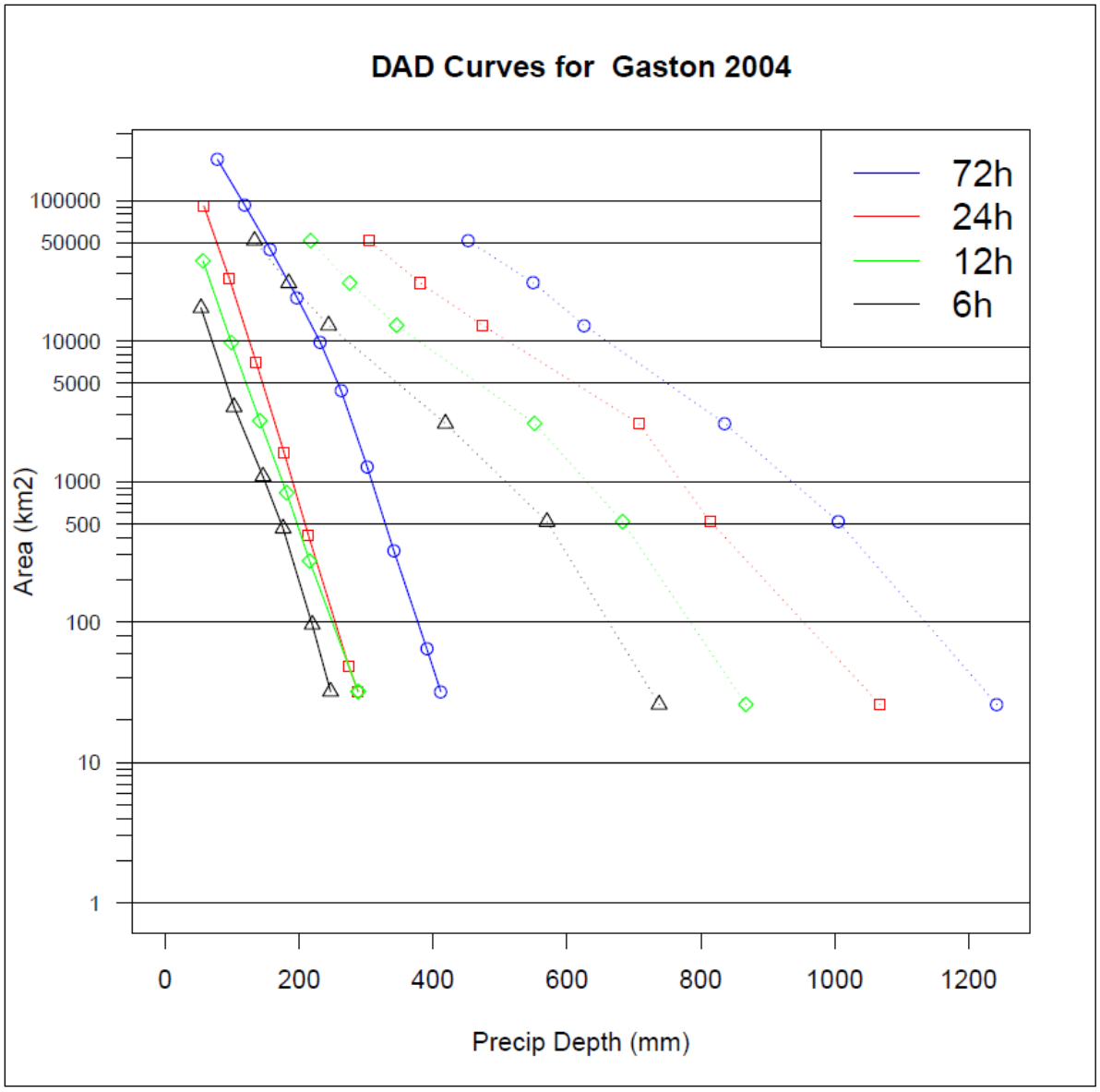


**Figure A.16** **Comparison of maximized depth-area-duration curves for Hurricane Gaston (solid) and probable maximum precipitation values extracted from HMR 51 (dotted)**

## A.2 Direct Storm Tracks

### A.2.1 Hurricane Fran: September 4 – September 8, 1996

Hurricane Fran formed quickly on 23 August after moving off the African coast as a strong tropical wave just a day before. Fran moved generally west-northwestward across the Atlantic Ocean with fluctuations in intensity and speed generally driven by interactions with Hurricane Edouard several hundred miles to the northwest. As Edouard moved away by 31 August, the subtropical ridge north of Fran reinforced and Fran moved steadily west-northwest just north of the Bahamas. A cyclonic circulation over the Tennessee Valley then began to influence the storm and turned Fran northwestward then north between the cyclone over TN and the subtropical ridge over the northwest Atlantic. Fran made landfall near Cape Fear, NC on 6 September (Figure A.17). [Brief synopsis derived from NHC preliminary reports; http://www.nhc.noaa.gov/]

Air temperatures across the Carolinas ranged from highs in the upper 70s to mid-80s, with mid-70s in the rain cooled air. Dewpoint temperatures during the morning hours were generally in the upper 60s and lower 70s (Figure A.18). Winds across the Carolinas were light and variable until Fran approached the Southeast US on 5 September when winds were northeasterly within the storm's broad circulation. Due to the enhanced southeasterly flow at mid- and upper levels – the same driving the storm in a northwesterly path – the precipitation was generally confined to a region near and along the track. Scattered thunderstorms along banding features from the hurricane produced lighter but still notable amounts near the Appalachians (Figures A.17 and A.19). There were no notable synoptic scale fronts in the vicinity of the Carolinas during the storm, though the upper level low over the Tennessee Valley may have been a contributing factor to enhanced instability, including predecessor rainfall in the form of thunderstorms across the Carolinas on 4 – 5 September. DADx estimates for Hurricane Fran (based on MPR), with comparison to HMR51 PMP, are shown in Figure A.20.

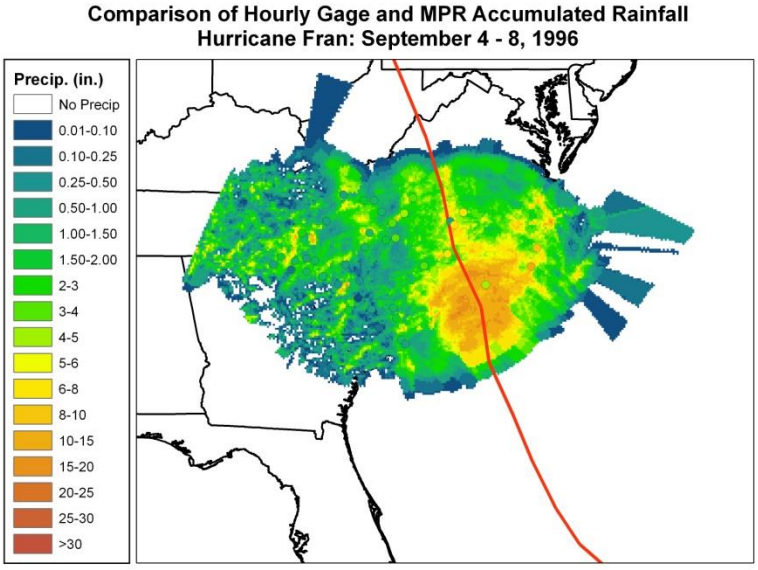


**Figure A.17 Storm total precipitation for Hurricane Fran with best storm track from NOAA shown in red**

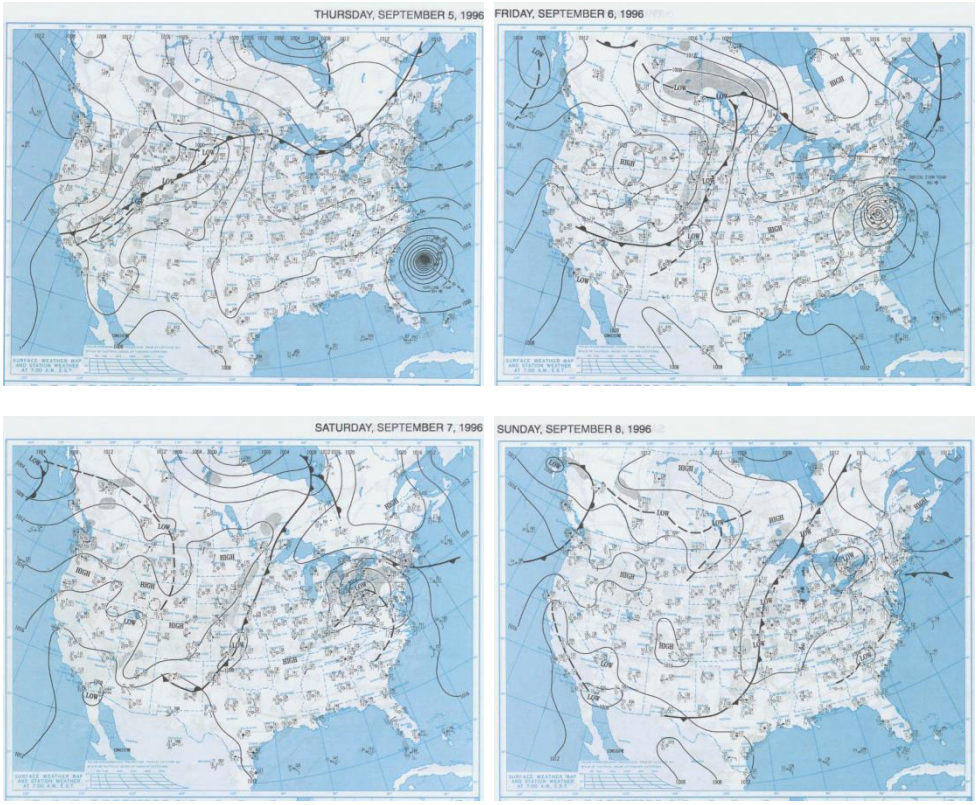


**Figure A.18 Surface weather maps valid at 7 a.m. EST for the period September 4 – 8, 1996. Source: NOAA Central Library, http://docs.lib.noaa.gov/rescue/dwm/data_rescue_daily_weather_maps.html**

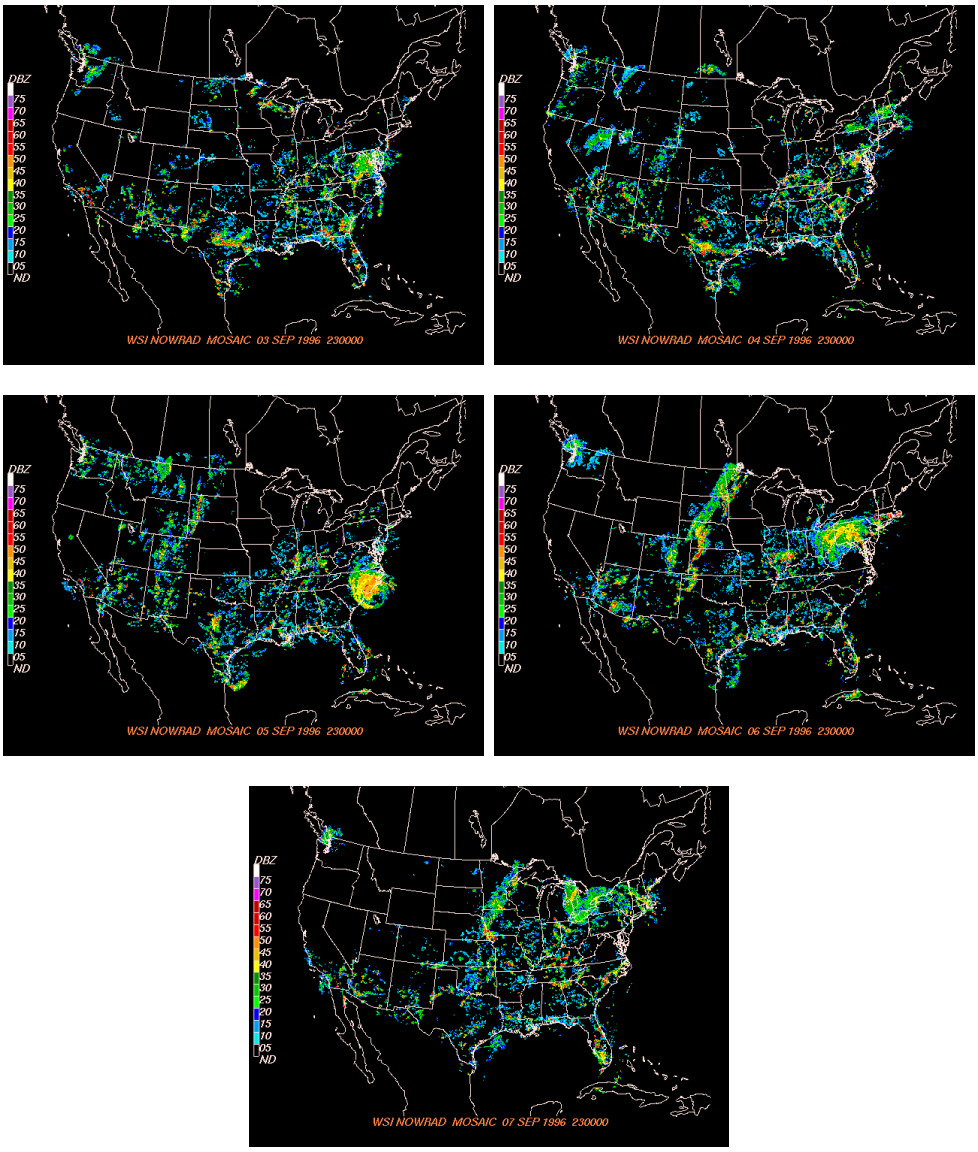


**Figure A.19** **National mosaic NEXRAD reflectivity images for the period September 4 – 8, 1996. Imagery is valid at closest available time to 0000 UTC each day. Source: National Climatic Data Center, https://www.ncei.noaa.gov/products/radar/next-generation-weather-radar**

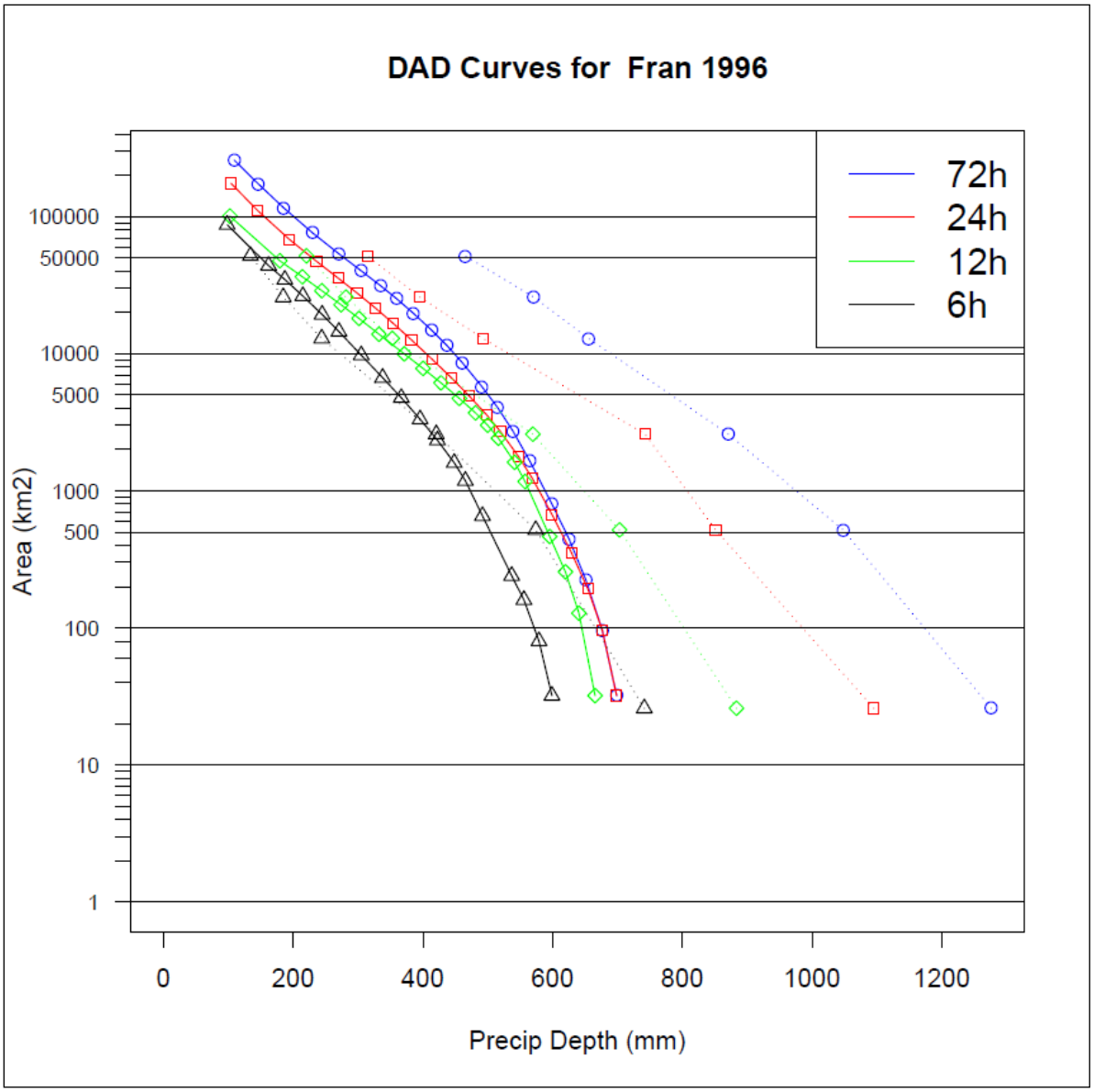


**Figure A.20 Comparison of maximized depth-area-duration curves for Hurricane Fran (solid) and probable maximum precipitation values extracted from HMR 51 (dotted)**

## A.3 Stalled Offshore Storm Tracks

### A.3.1 Hurricane Dennis: August 29 – September 8, 1999

Hurricane Dennis formed from a tropical wave that moved off of Africa on 17 August. The wave developed into a depression on 24 August and into a tropical storm the same day. On 26 August, despite westerly shear, Dennis reached hurricane status. Dennis moved northwest past the Bahamas and then north in response to a mid-latitude trough on 28 – 30 August. The storm passed 60 miles off the NC coast before moving east-northeast as the trough passed to the

north. Weak steering currents caused the cyclone to drift offshore through 2 September. Dennis weakened due to interaction with a cold front and mid-latitude trough. High pressure built north of Dennis and created a southward drift on 2 September. By 3 September, the ridge shifted east and the storm moved northwestward toward the coast, making landfall near Cape Lookout, NC on 4 September. The remnants were absorbed into a larger low pressure system on 9 September (Figure A.21). [Brief synopsis derived from NHC preliminary reports; http://www.nhc.noaa.gov/]

Air temperatures across the Carolinas varied during the duration of the storm's impact on the Carolinas. Temperatures ranged from highs in the upper 60s following the first frontal passage to the mid-80s to low 90s at other times. Rain-cooled temperatures were generally in the 70s. Dewpoint temperatures during the morning hours were in the 50s in the post-frontal airmass, but were otherwise in the upper 60s and lower 70s (Figures A.22 and A.23). Winds across the Carolinas were north or northwesterly except when wind direction was driven by the proximity of the storm center. Due to the erratic motion, banded precipitation frequented the coastal sections of NC as the circulation advected warm, moist air inland. In addition, the frontal system that moved through on 30 August may have enhanced rainfall, particularly in extreme northeastern NC (Figures A.21, A.24, and A.25). DADx estimates for Hurricane Dennis (based on MPR), with comparison to HMR51 PMP, are shown in Figure A.26.

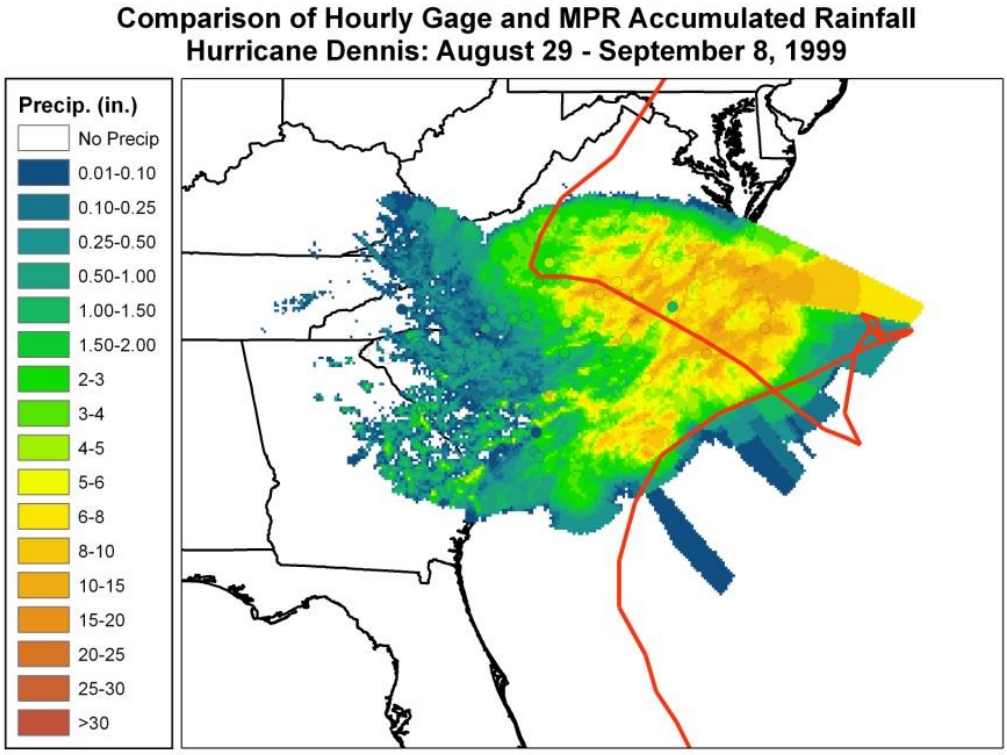


**Figure A.21 Storm total precipitation for Hurricane Dennis with best storm track from NOAA shown in red**

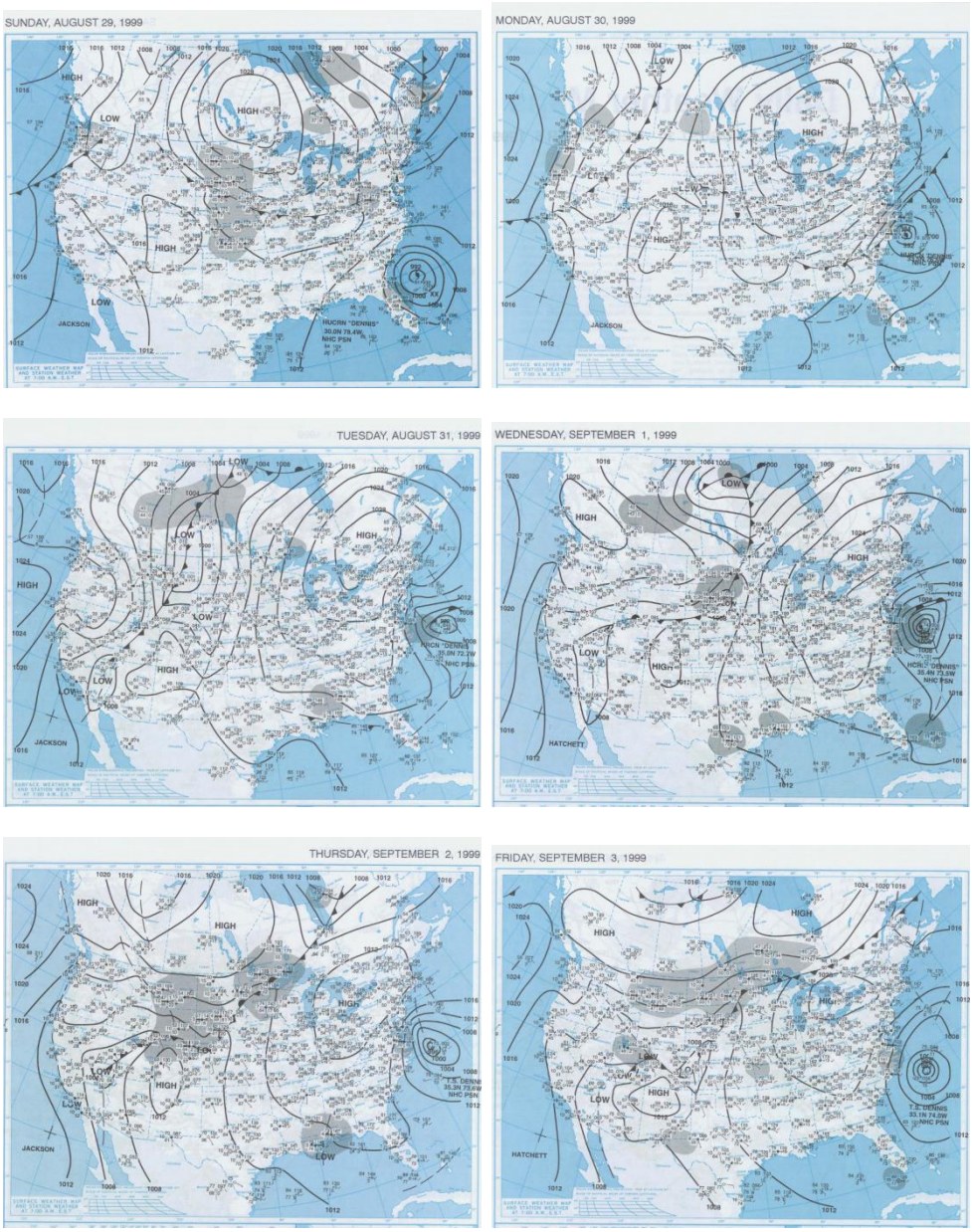


**Figure A.22 Surface weather maps valid at 7 a.m. EST for the period August 29 – September 3, 1999. Source: NOAA Central Library, https://www.wpc.ncep.noaa.gov/dailywxmap/index.html**

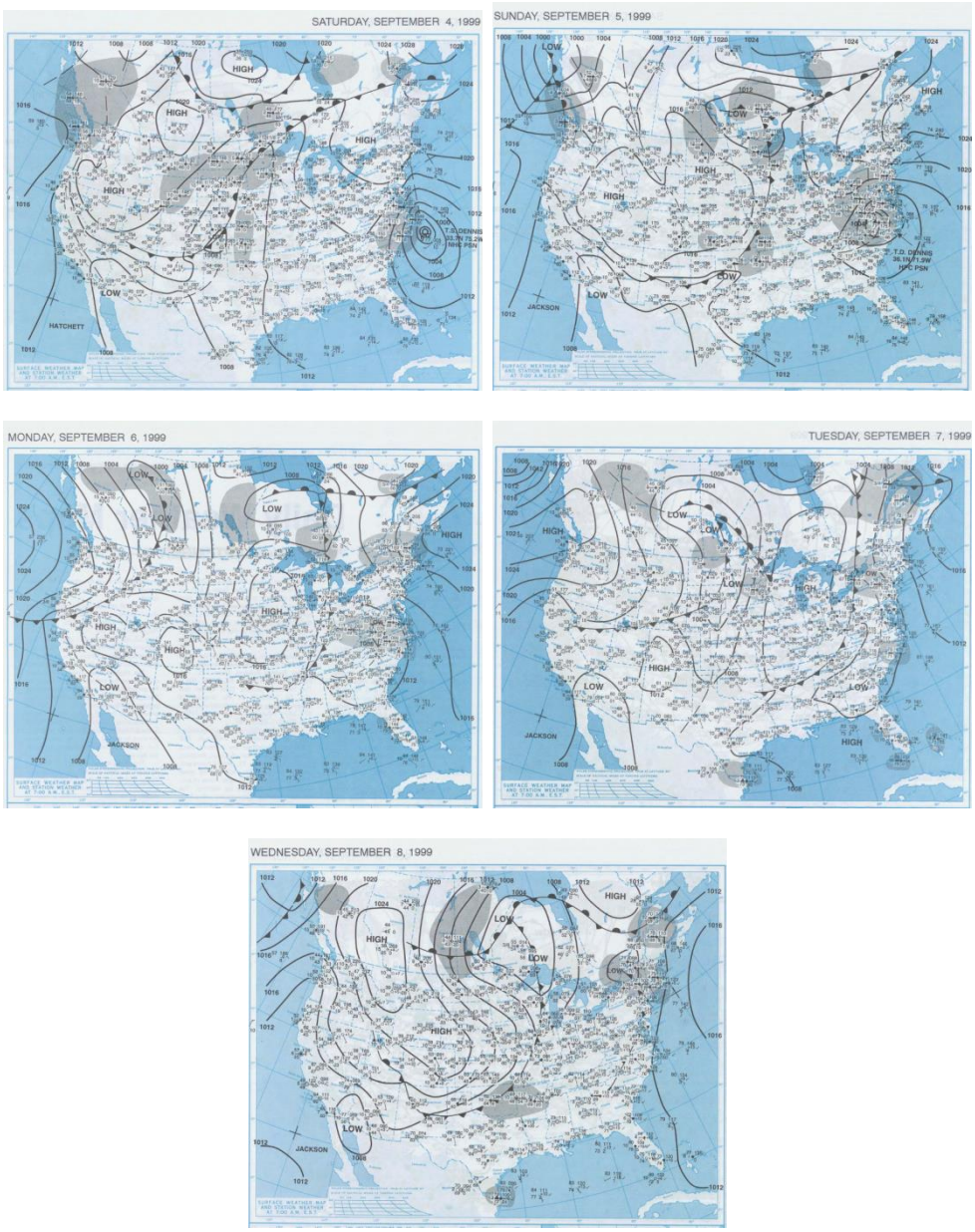


**Figure A.23 Surface weather maps valid at 7 a.m. EST for the period September 4 – 8, 1999. Source: NOAA Central Library, https://www.wpc.ncep.noaa.gov/dailywxmap/index.html**

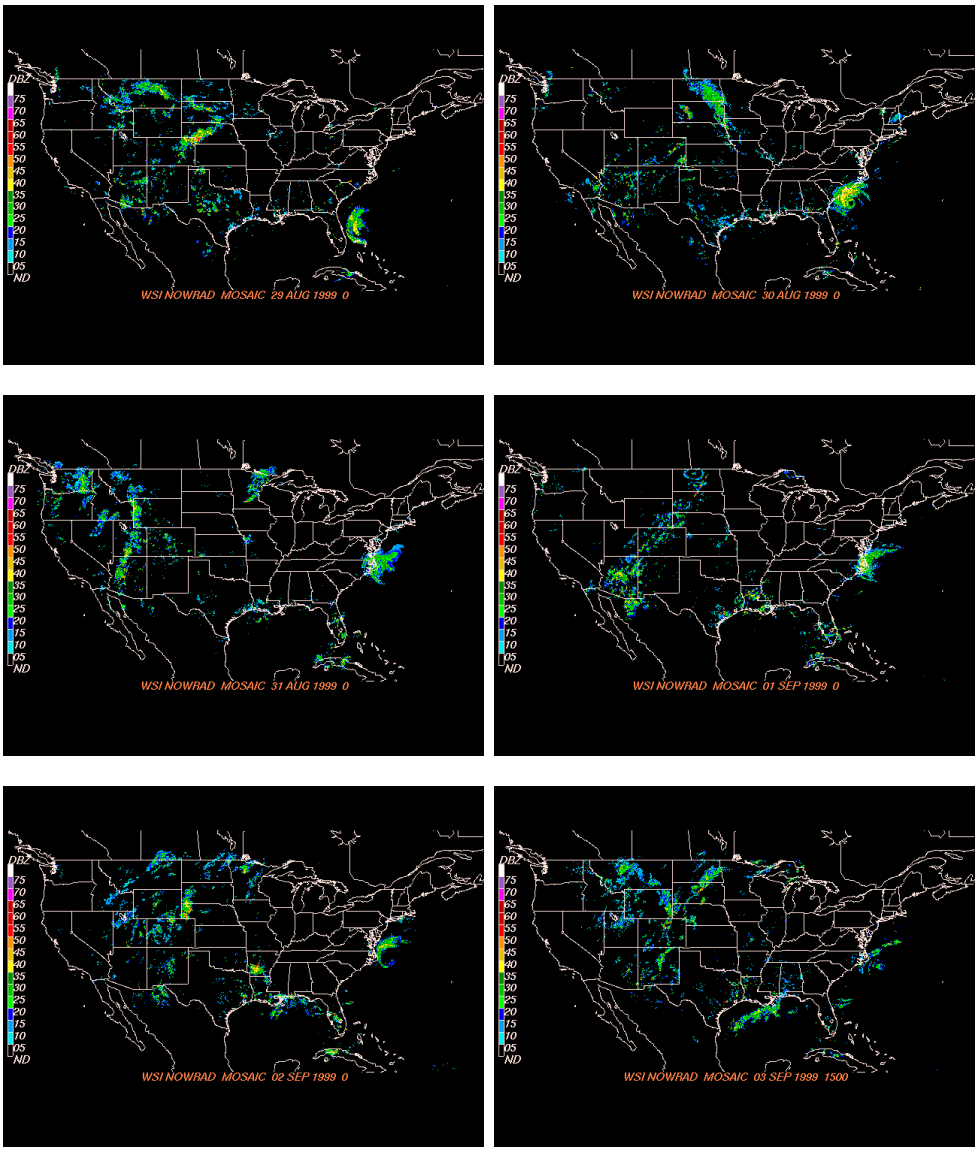


**Figure A.24** **National mosaic NEXRAD reflectivity images for the period August 29 – September 3, 1999. Imagery is valid at closest available time to 0000 UTC each day. Source: National Climatic Data Center, https://www.ncei.noaa.gov/products/radar/next-generation-weather-radar**

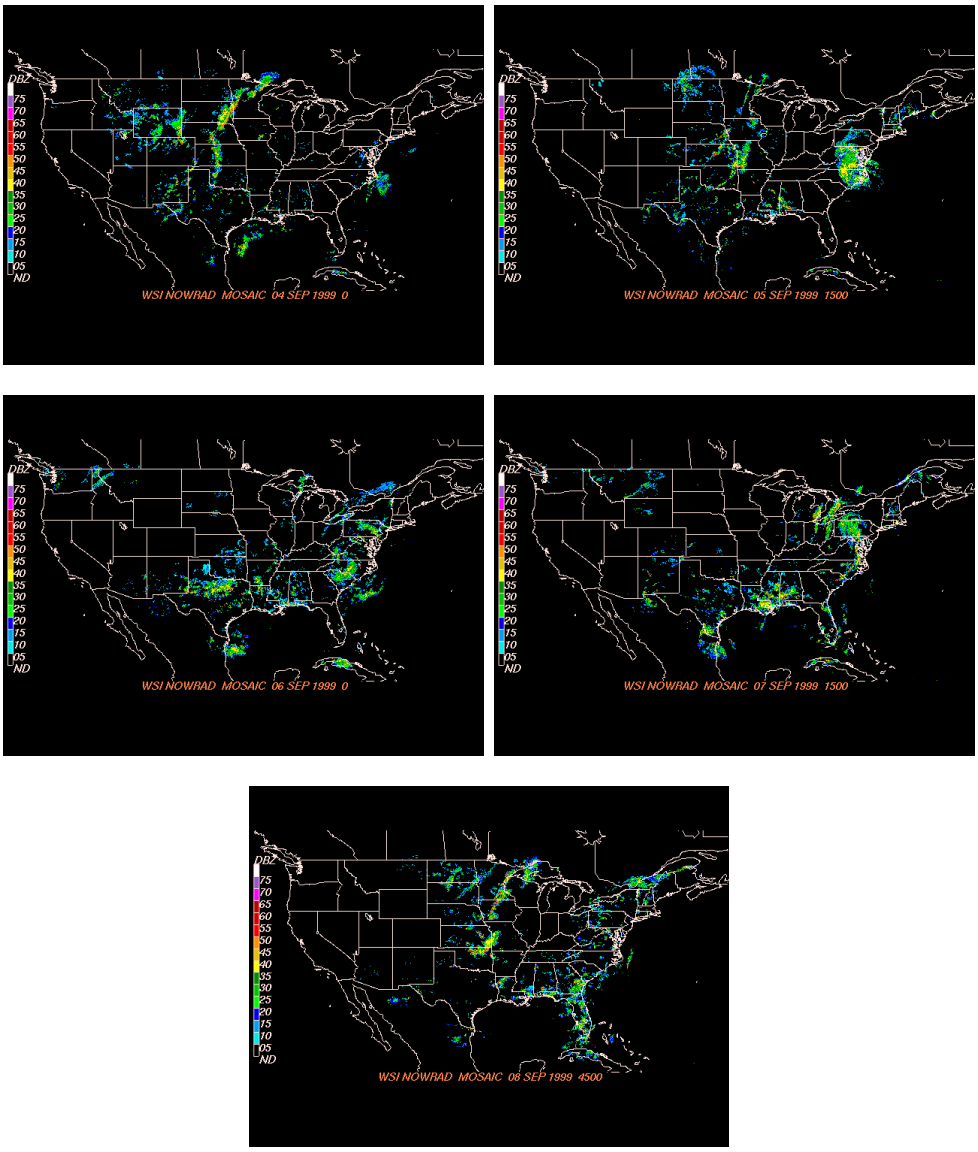


**Figure A.25** **National mosaic NEXRAD reflectivity images for the period September 4 – September 8, 1999. Imagery is valid at closest available time to 0000 UTC each day. Source: National Climatic Data Center, https://www.ncei.noaa.gov/products/radar/next-generation-weather-radar**

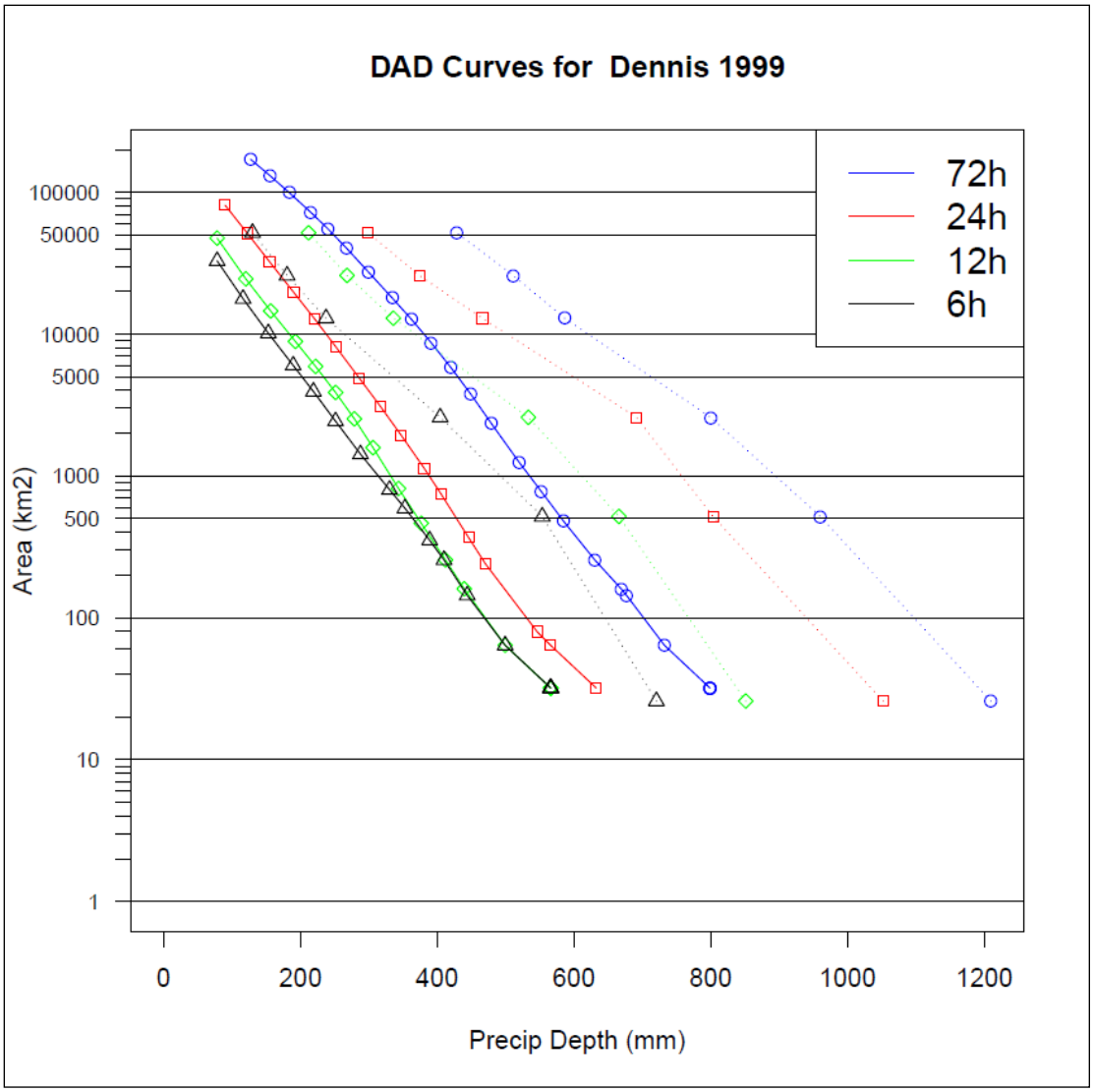


**Figure A.26 Comparison of maximized depth-area-duration curves for Hurricane Dennis (solid) and probable maximum precipitation values extracted from HMR 51 (dotted)**

### A.3.2 Hurricane Ophelia: September 12 – September 15, 2005

Hurricane Ophelia formed along a cold front that moved off the east coast of the US on 1 September. On 4 September an area of low pressure developed along the frontal boundary in the vicinity of the Bahamas. By 6 September, the low gained enough tropical characteristics to become a depression and strengthened to a tropical storm on 7 September. The storm moved erratically and fluctuated between storm and hurricane status off the coast of Florida for the next several days under weak steering conditions. Ophelia then moved northwestward toward NC on 13 September and then drifted east-northeast just off the North Carolina coast on 14-15. An upper-level trough and cold front approached from the west and accelerated the storm to the

northeast (Figure A.27). [Brief synopsis derived from NHC preliminary reports; http://www.nhc.noaa.gov/]

Air temperatures across the Carolinas ranged from highs in the mid-80s to near 90 with lower 80s in the rain-cooled air. Dewpoint temperatures during the morning hours were in the upper 60s and lower 70s (Figure A.28). Winds across the Carolinas were generally northerly except when wind direction was driven by the proximity of the storm center. Due to the slow and erratic motion, banded precipitation frequented the coastal sections of NC as the circulation advected warm, moist air inland. The frontal system which accelerated Ophelia to the northeast was not a significant contributor to enhanced rainfall over the Carolinas, but may have influenced totals along the New England coastline. (Figures A.27 and A.29). DADx estimates for Hurricane Ophelia (based on MPR), with comparison to HMR51 PMP, are shown in Figure A.30.

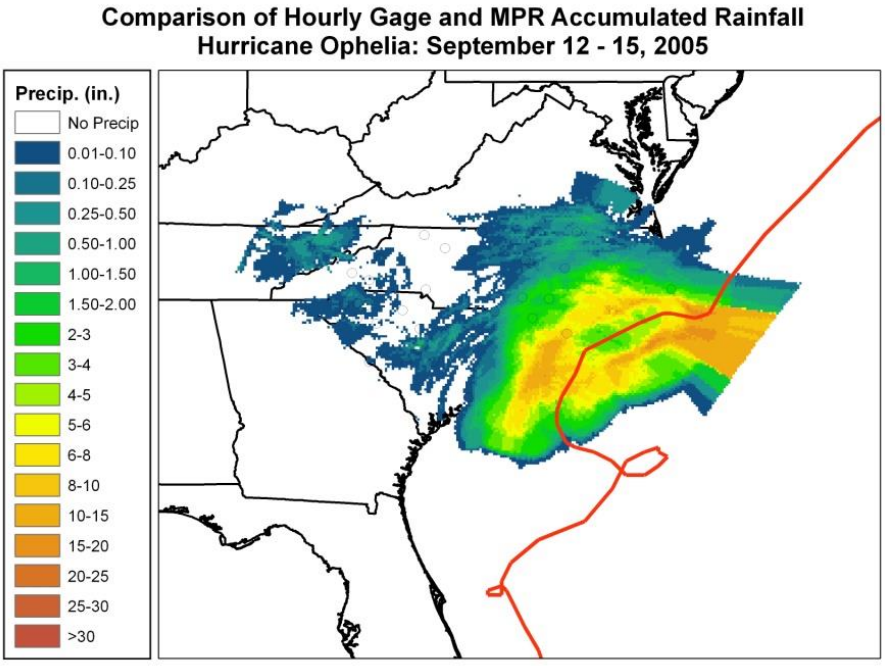


**Figure A.27 Storm total precipitation for Hurricane Ophelia with best storm track from NOAA shown in red**

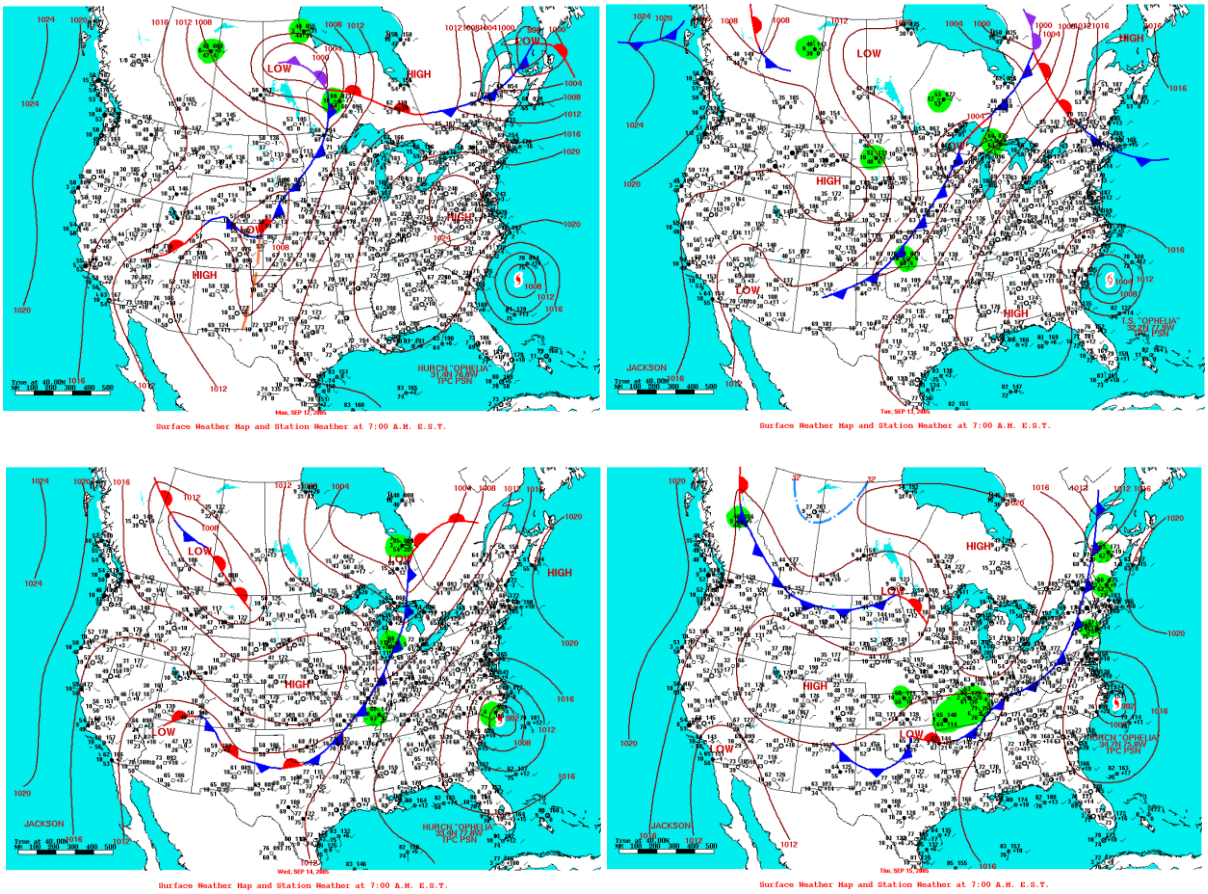


**Figure A.28** **Surface weather maps valid at 7 a.m. EST for the period September 12 – September 15, 2005. Source: NOAA Hydrometeorological Prediction Center, https://library.noaa.gov/Collections/Digital-Collections/US-Daily-Weather-Maps**

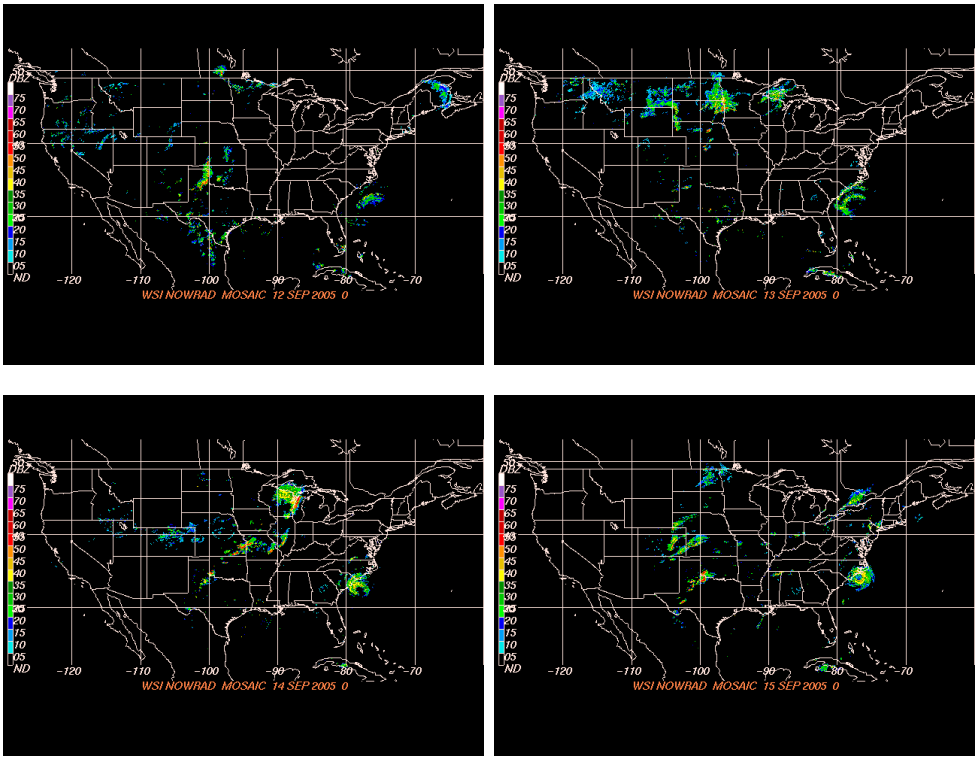


**Figure A.29** **National mosaic NEXRAD reflectivity images for the period September 12 – 15, 2005. Imagery is valid at closest available time to 0000 UTC each day. Source: National Climatic Data Center, https://www.ncei.noaa.gov/products/radar/next-generation-weather-radar**

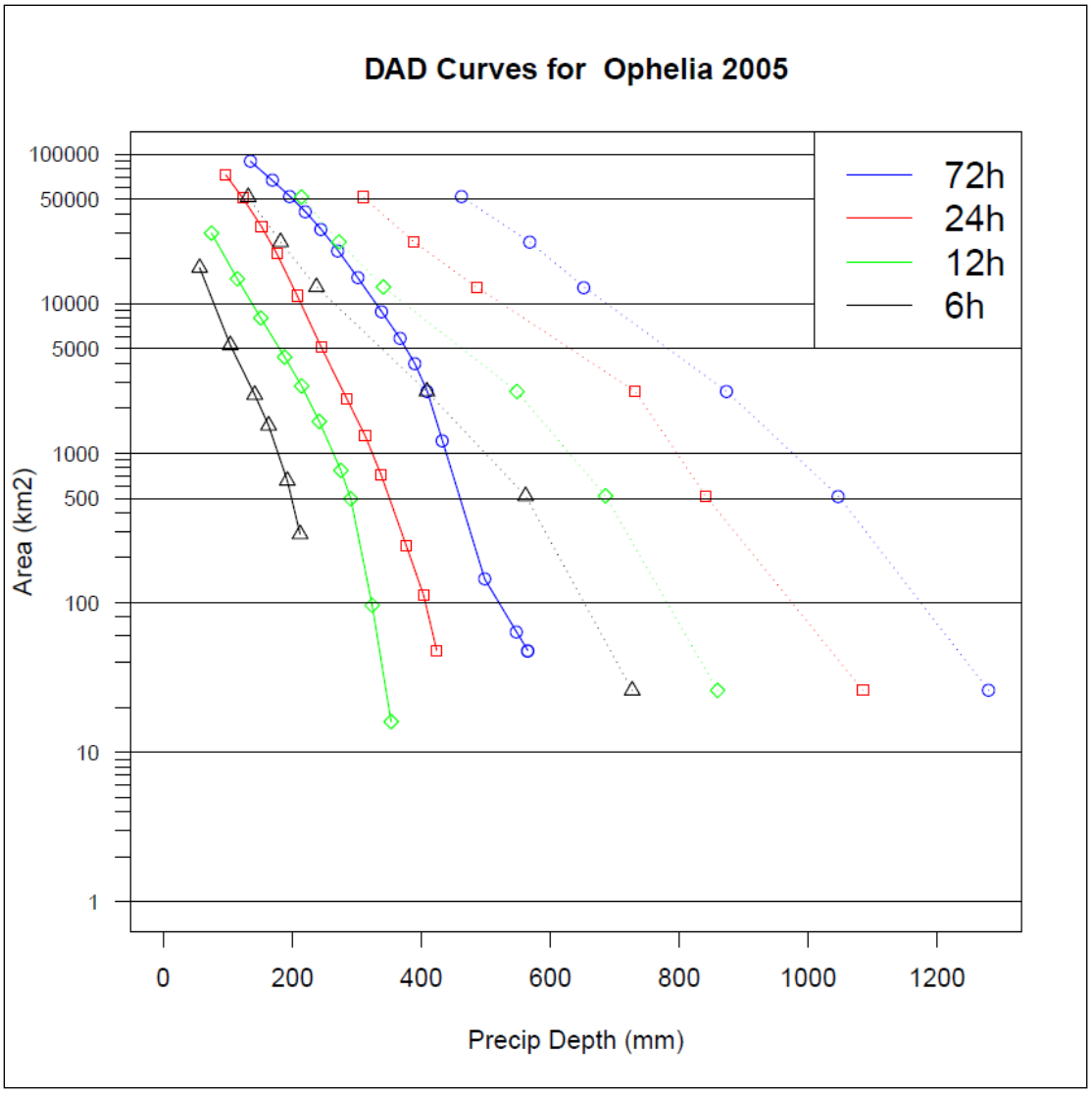


**Figure A.30** **Comparison of maximized depth-area-duration curves for Hurricane Ophelia (solid) and probable maximum precipitation values extracted from HMR 51 (dotted)**

## A.4 West of Appalachians Storm Tracks

### A.4.1 Hurricane Frances: September 6 – September 9, 2004

Hurricane Frances developed from a tropical wave that moved off the African coast on 21 August. The wave gained organization on 25 August to become a depression then a storm later that same day. Frances became a hurricane on 26 August and continued on a west-northwest path across the Atlantic. Steering currents weakened as the storm passed over the northwestern Bahamas before making landfall on the east Florida peninsula near Hutchinson Island on 5 September. The storm moved northwestward across Florida before re-emerging briefly in the Gulf of Mexico and making a second landfall on the Florida Panhandle on 6 September. The storm continued northwestward until a mid-latitude trough and associated cold front recurved the circulation to the northeast along the spine of the Appalachians (Figure A.31). [Brief synopsis derived from NHC preliminary reports; http://www.nhc.noaa.gov/]

Air temperatures across the Carolinas ranged from highs in the 80s with 70s in the rain-cooled air. Dewpoint temperatures during the morning hours were in the upper 60s and lower 70s (Figure A.32). Winds across the Carolinas were generally easterly, advecting moisture inland from the Atlantic. The winds turned southerly ahead of the front transporting moisture from the Gulf of Mexico into the Carolinas as well. Southwesterly flow aloft ahead of the approaching cold front created significant shear ahead of the front, leading to a tornado outbreak across the Carolinas. The frontal system became nearly stationary across the western NC mountains as the circulation center of Frances crossed the region, further enhancing the rainfall in orographic terrain (Figures A.31 and A.33). DADx estimates for Hurricane Frances (based on MPR), with comparison to HMR51 PMP, are shown in Figure A.34.

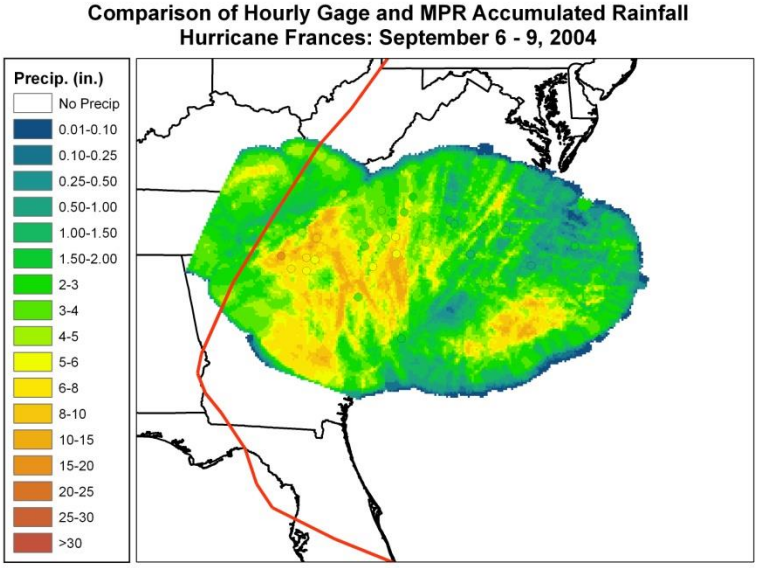


**Figure A.31 Storm total precipitation for Hurricane Frances with best storm track from NOAA shown in red**

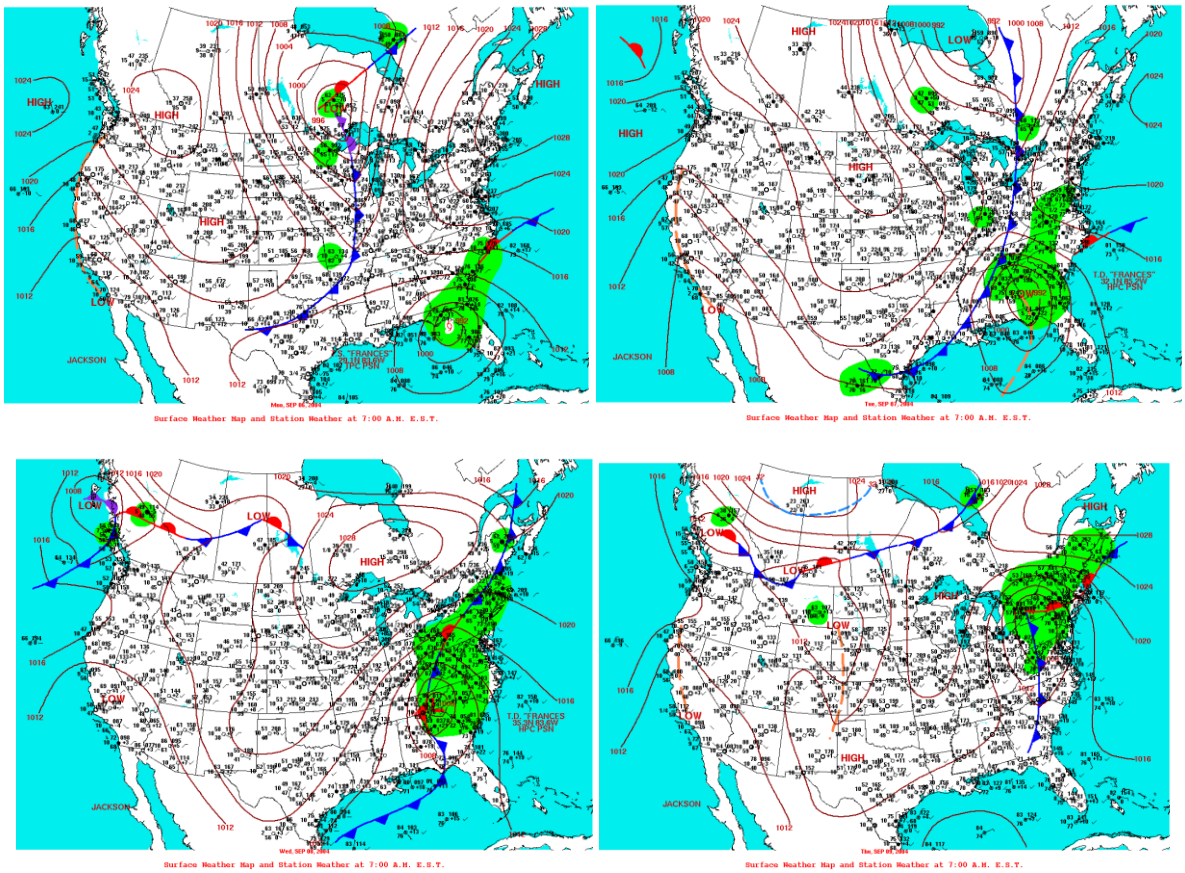


**Figure A.32** **Surface weather maps valid at 7 a.m. EST for the period September 6 – 9, 2004. Source: NOAA Hydrometeorological Prediction Center, https://library.noaa.gov/Collections/Digital-Collections/US-Daily-Weather-Maps**

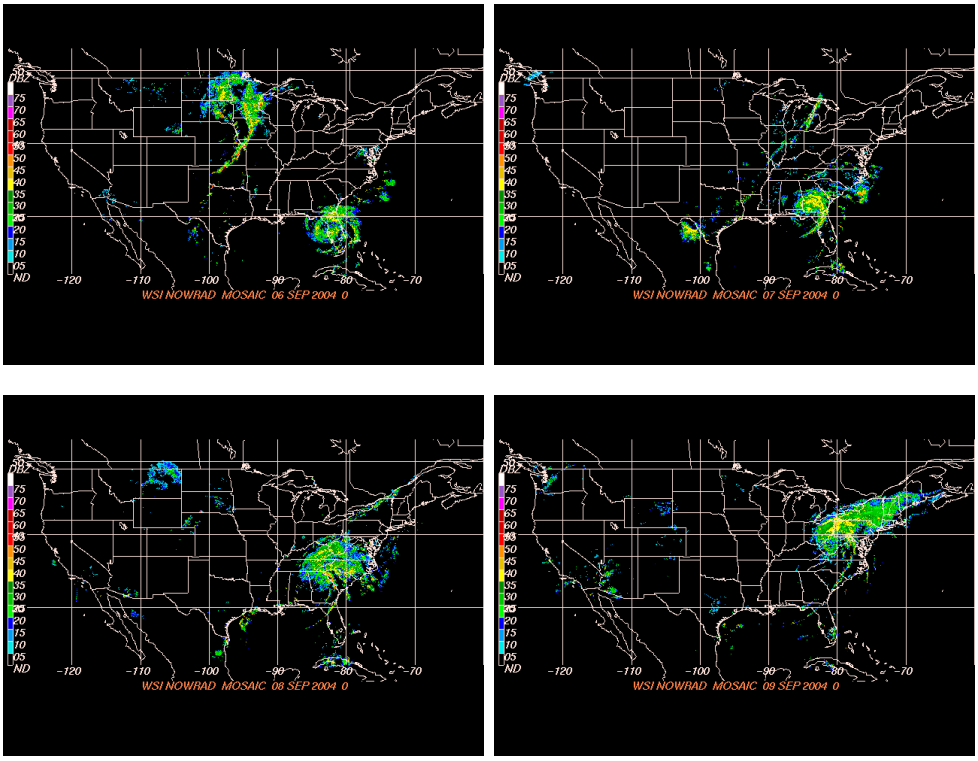


**Figure A.33** **National mosaic NEXRAD reflectivity images for the period September 6 – 9, 2004. Imagery is valid at closest available time to 0000 UTC each day. Source: National Climatic Data Center, https://www.ncei.noaa.gov/products/radar/next-generation-weather-radar**

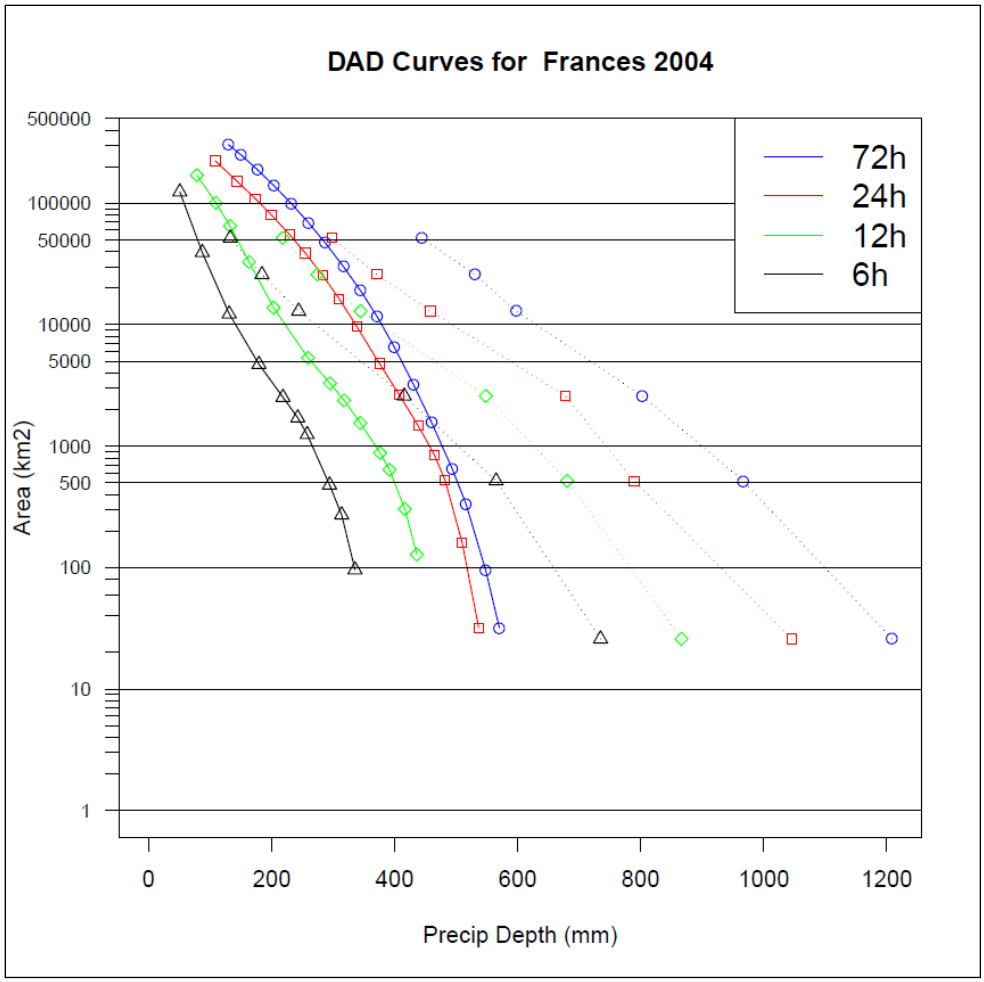


**Figure A.34 Comparison of maximized depth-area-duration curves for Hurricane Frances (solid) and probable maximum precipitation values extracted from HMR 51 (dotted)**

### A.4.2 Hurricane Ivan: September 15 – September 18, 2004

Hurricane Ivan developed from a tropical wave that moved off Africa on 31 August. The wave gained organization quickly and on 2 August, a tropical depression formed. The depression strengthened to a tropical storm on 3 September then to a hurricane by 5 September. The system moved west or west-northwestward across the southern Atlantic Ocean at low latitudes over the next week and passed just south of Jamaica on 11 September. A weakness in the subtropical ridge over the Gulf of Mexico allowed the storm to turn northwest across the northwestern Caribbean. An approaching trough then turned Ivan to the north then north-northeast with a landfall near Gulf Shores, AL on 16 September. Ivan continued a northeasterly track across the Appalachians and merged with a frontal system over the Virginia on 18 September (Figure A.35). Remnants of Ivan then moved south in the western Atlantic Ocean and eventually restrengthed to tropical storm status before moving into the Gulf of Mexico and making landfall in Texas. [Brief synopsis derived from NHC preliminary reports; http://www.nhc.noaa.gov/]

Air temperatures across the Carolinas ranged from highs in the 70s to low 80s with 70s in the rain-cooled air. Dewpoint temperatures during the morning hours were in the upper 60s and lower 70s (Figure A.36). Winds across the Carolinas were generally easterly or north-easterly, advecting moisture inland from the Atlantic. The winds turned southerly ahead of the front transporting moisture from the Gulf of Mexico into the Carolinas as well. Southwesterly flow aloft ahead of the approaching cold front created significant shear ahead of the front, leading to a tornado outbreak across the Carolinas. The frontal system became nearly stationary across the western NC mountains as the circulation center of Frances turned extratropical, further enhancing the rainfall in orographic terrain (Figures A.35 and A.37). DADx estimates for Hurricane Ivan (based on MPR), with comparison to HMR51 PMP, are shown in Figure A.38.

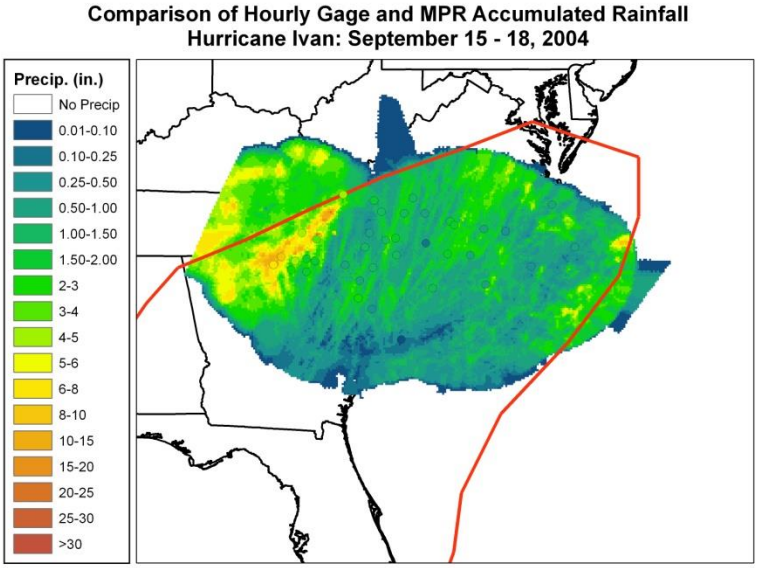


**Figure A.35 Storm total precipitation for Hurricane Ivan with best storm track from NOAA shown in red**

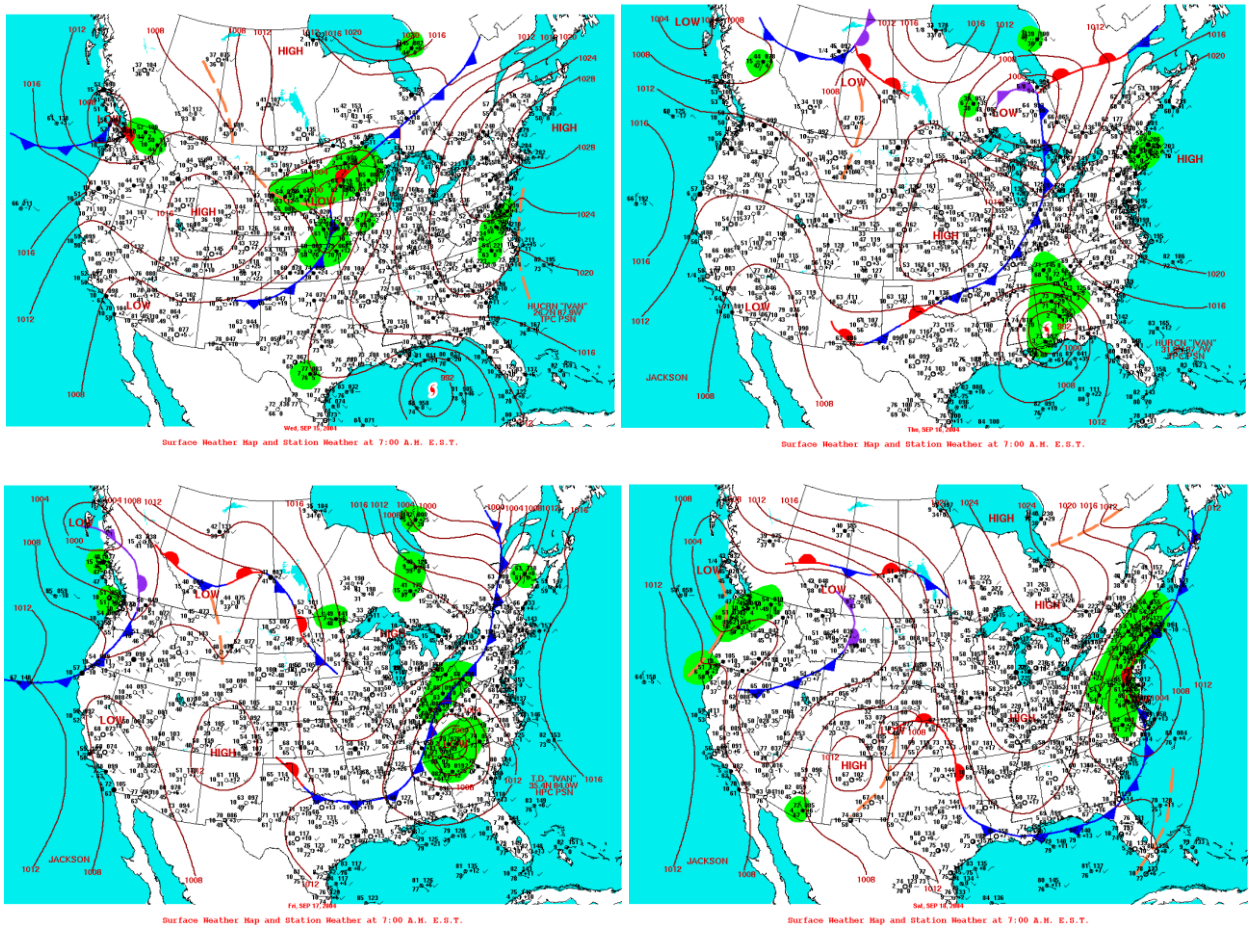


**Figure A.36** **Surface weather maps valid at 7 a.m. EST for the period September 15 – September 18, 2004. Source: NOAA Hydrometeorological Prediction Center, https://library.noaa.gov/Collections/Digital-Collections/US-Daily-Weather-Maps**

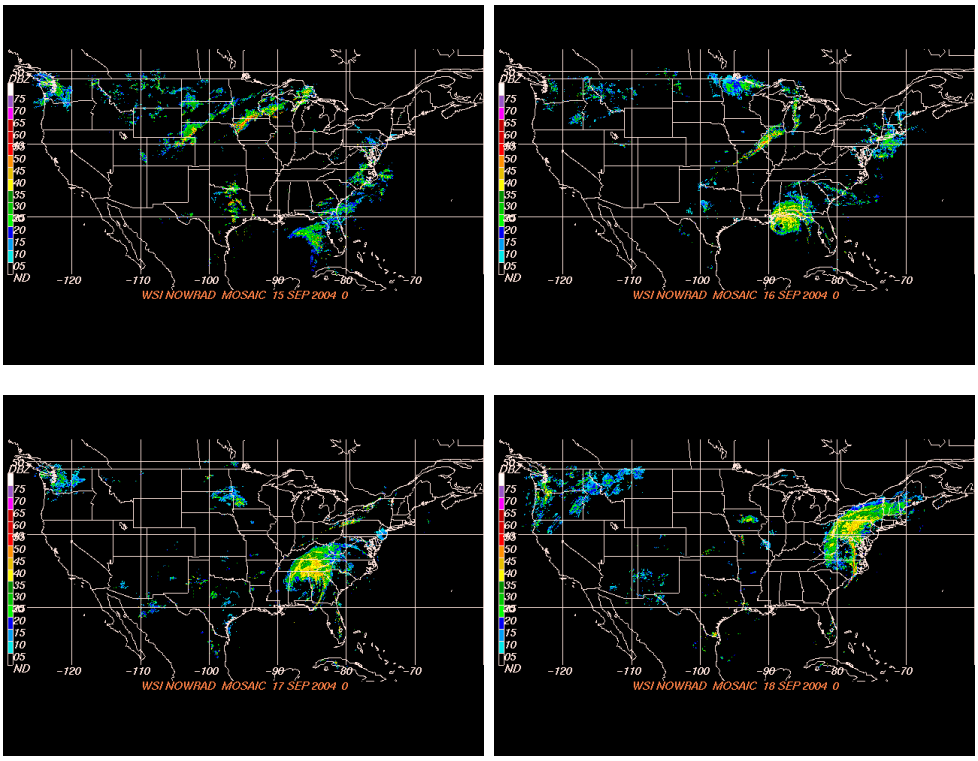


**Figure A.37** **National mosaic NEXRAD reflectivity images for the period September 15 – 18, 2004. Imagery is valid at closest available time to 0000 UTC each day. Source: National Climatic Data Center, https://www.ncei.noaa.gov/products/radar/next-generation-weather-radar**

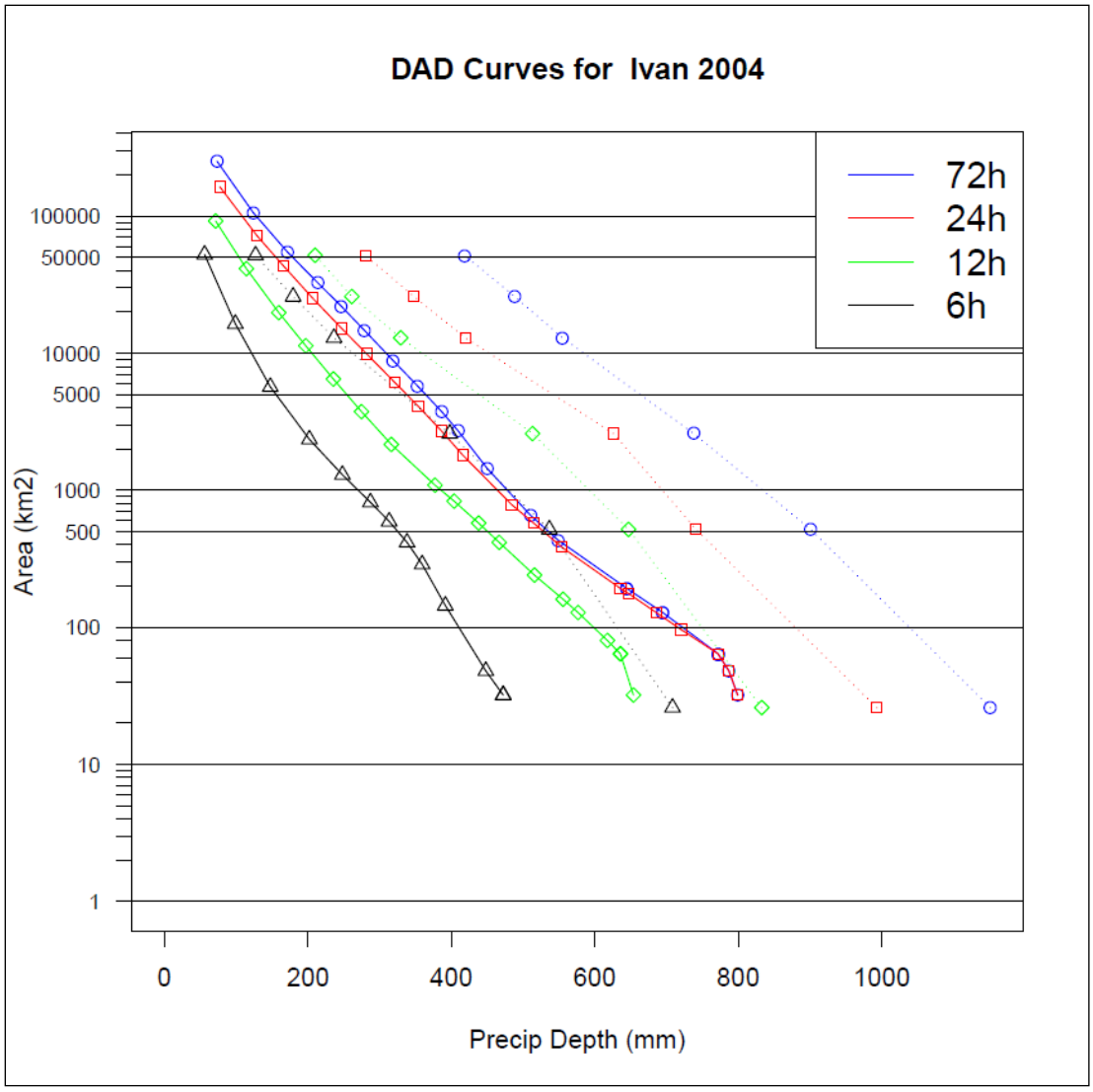


**Figure A.38** **Comparison of maximized depth-area-duration curves for Hurricane Ivan (solid) and probable maximum precipitation values extracted from HMR 51 (dotted)**

## A.5 East of Appalachians Storm Tracks

### A.5.1 Hurricane Earl: September 1 – September 4, 1998

Hurricane Earl developed from a tropical wave that moved off the African coast on 17 August and continued westward over the next two weeks. The wave was slow to organize, partially due to the outflow of Hurricane Bonnie to the north over the western North Atlantic. The wave finally gained strength and was upgraded to a depression in the Bay of Campeche on 31 August. Tropical Storm Earl formed later on 31 August about 500 miles south-southwest of New Orleans. On 2 September, Earl gained hurricane status and strengthened to a Category 2 storm before landfall near Panama City, FL on 3 September as a Category 1. The storm moved on a generally northeasterly path across the Gulf of Mexico and Southeast US in southwesterly flow aloft ahead of a weak frontal boundary over the Ohio Valley (Figure A.39). [Brief synopsis derived from NHC preliminary reports; http://www.nhc.noaa.gov/]

Air temperatures across the Carolinas ranged from highs in the upper 80s to low 90s with 70s in the rain-cooled air. Dewpoint temperatures during the morning hours were in the upper 60s and lower 70s (Figure A.40). Winds across the Carolinas were generally light and variable but turned southeasterly as the storm approached from the southwest. In addition to the weak frontal boundary over the Ohio Valley, a dissipating frontal system existed across the Carolinas on 1 – 2 September. Interaction with these frontal systems may have enhanced the precipitation across portions of South Carolina (Figures A.39 and A.41). DADx estimates for Hurricane Earl (based on MPR), with comparison to HMR51 PMP, are shown in Figure A.42.

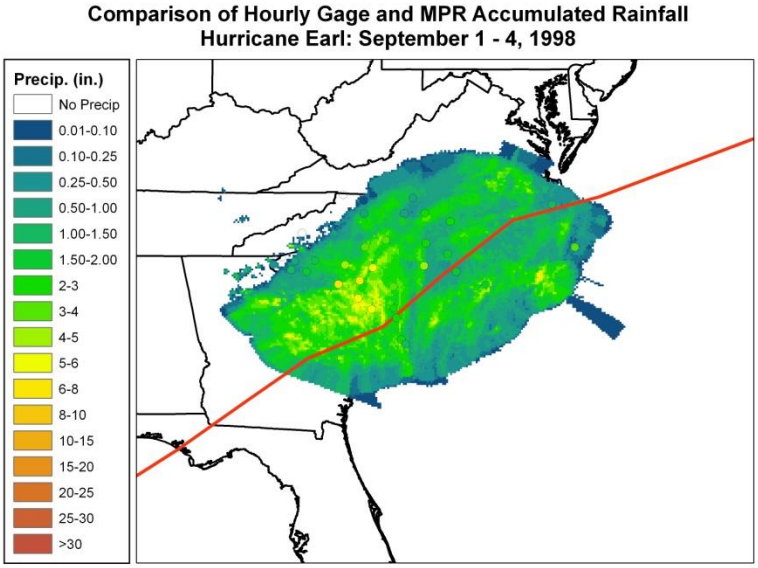


**Figure A.39 Storm total precipitation for Hurricane Earl with best storm track from NOAA shown in red**

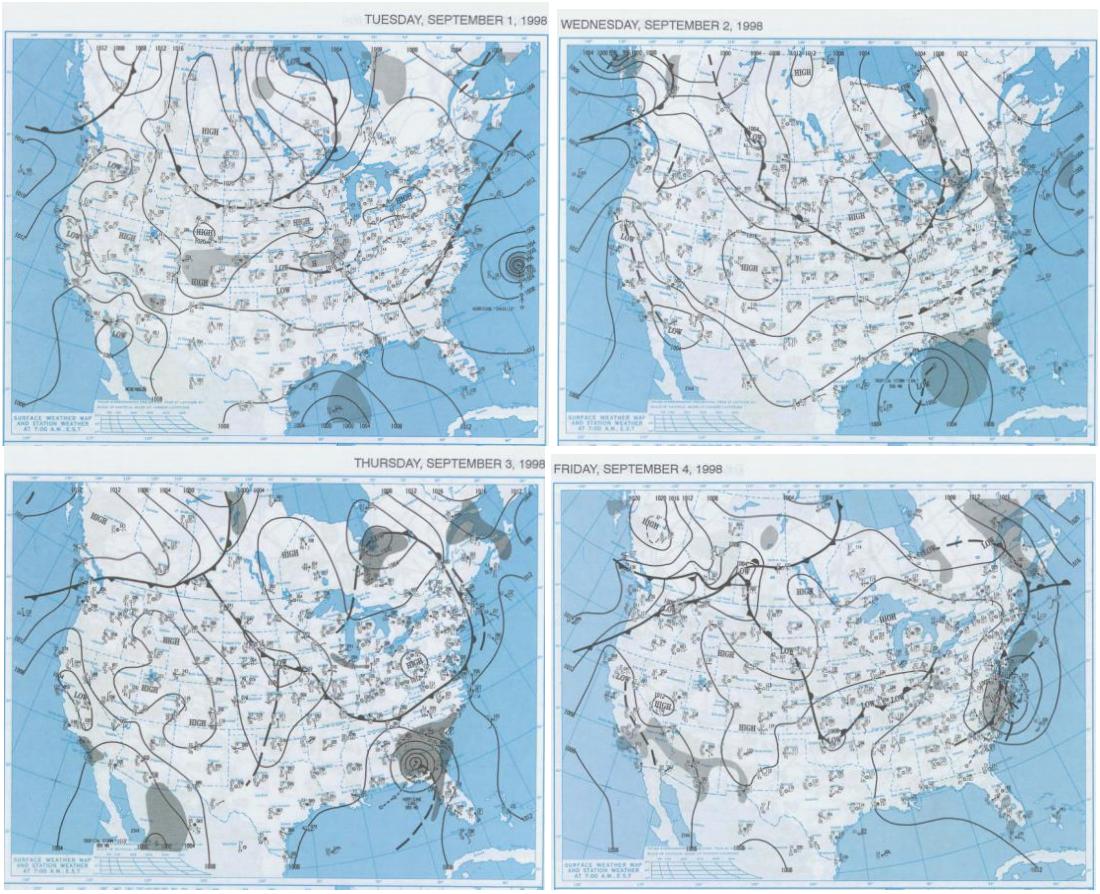


**Figure A.40 Surface weather maps valid at 7 a.m. EST for the period September 1 – 4, 1998. Source: NOAA Central Library, https://www.wpc.ncep.noaa.gov/dailywxmap/index.html**

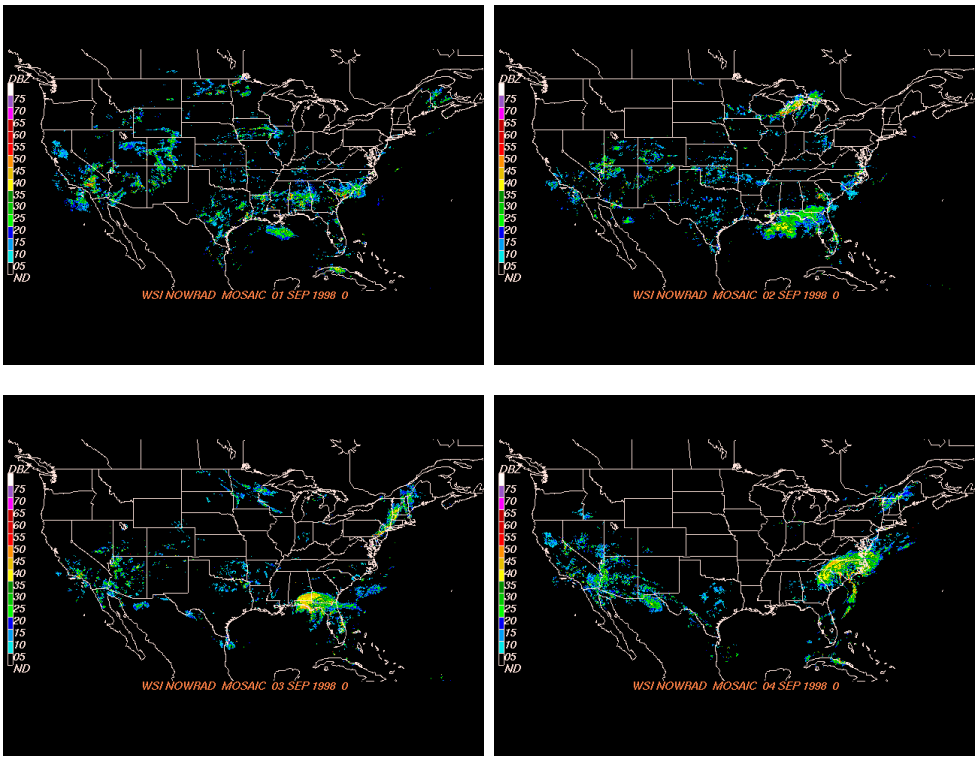


**Figure A.41** **National mosaic NEXRAD reflectivity images for the period September 1 – September 4, 1998. Imagery is valid at closest available time to 0000 UTC each day. Source: National Climatic Data Center, https://www.ncei.noaa.gov/products/radar/next-generation-weather-radar**

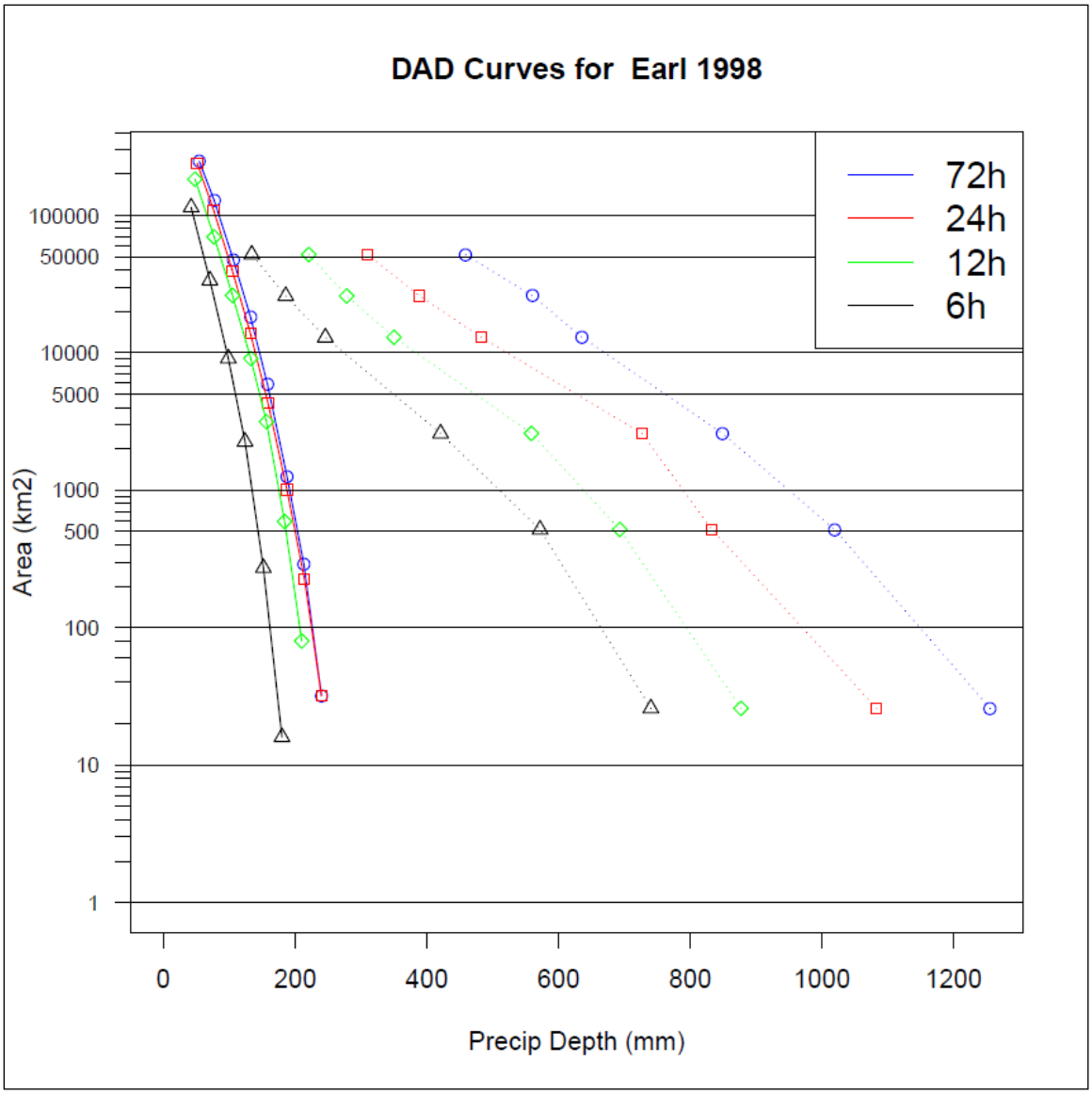


**Figure A.42** **Comparison of maximized depth-area-duration curves for Hurricane Earl (solid) and probable maximum precipitation values extracted from HMR 51 (dotted)**

## MAXIMUM PRECIPITATION PERIODS FOR 10 STORMS WITH MPR DATA

| | Bonnie98 | Precip (mm) | Dennis99 | Precip (mm) | Earl98 | Precip (mm) |
|---|---|---|---|---|---|---|
| Start | 8/26/1998 | | 8/29/1999 | | 9/1/1998 | |
| End | 8/29/1998 | | 9/8/1999 | | 9/4/1998 | |
| 1h | 14, 24 | 77.6,60.2 | 203, 217 | 181,168.40 | 23, 67 | 131.9,79.2 |
| 6h | 10,19 | 121.8,110.4 | 214 | 443.5 | 21, 65 | 170.4,155.3 |
| 12h | 19 | 134.9 | 211 | 443.8 | 61 | 187 |
| 24h | 7 | 151.8 | 201 | 480.2 | 57 | 199.1 |
| 72h | 1 | 166.9 | 152 | 621.2 | 18 | 199.1 |

***72h tied 18-20***

| Ernesto06 | Precip (mm) | Floyd99 | Precip (mm) | Fran96 | Precip (mm) | Frances04 | Precip (mm) |
|---|---|---|---|---|---|---|---|
| 8/30/2006 | | 9/14/1999 | | 9/4/1996 | | 9/6/2004 | |
| 9/2/2006 | | 9/17/1999 | | 9/8/1996 | | 9/9/2004 | |
| 35, 56 | 123.1,76.5 | 12,58 | 182.9,159.8 | 23, 44 | 277.8,135.5 | 35,45 | 110.8,110.1 |
| 29, 51 | 236.7,206.5 | 53 | 398.8 | 44 | 453.3 | 42 | 259.7 |
| 50 | 300.1 | 48 | 476.1 | 38 | 514.3 | 41 | 332.1 |
| 40 | 333.2 | 38 | 576.6 | 37 | 521.8 | 37 | 401.22 |
| 1 | 412 | 1 | 828.3 | 1 | 528.2 | 8 | 423.8 |

| Gaston04 | Precip (mm) | Ivan04 | Precip (mm) | Ophelia05 | Precip (mm) |
|---|---|---|---|---|---|
| 8/28/2004 | | 9/15/2004 | | 9/12/2005 | |
| 9/1/2004 | | 9/18/2004 | | 9/15/2005 | |
| 99, 105 | 125.4,75.3 | 51,57 | 101.9,91.2 | 89,79 | 104.5,98.0 |
| 102 | 153.1 | 54 | 330.5 | 77 | 313.8 |
| 97 | 167.2 | 51 | 464.3 | 73 | 416.7 |
| 30,97 | 212.5,169.7 | 47 | 549.4 | 61 | 448.1 |
| 35 | 249.3 | 19 | 564.1 | 21 | 461.9 |

***Also 24h: 35, 168.8***
***Also 12h: 35,148.5***
***Also 6h: 40, 124.8***
***Also 1h: 45, 64.0***

*NOTE:* *First values are actual maximum; values after comma are maximum within 72h period*
*Additional notes in bold italics*

**Figure A.43 Summary of the maximum precipitation periods for each of the top 10 storms used in the DAD analyses**

# APPENDIX B SCRIPTS AND DESCRIPTIONS

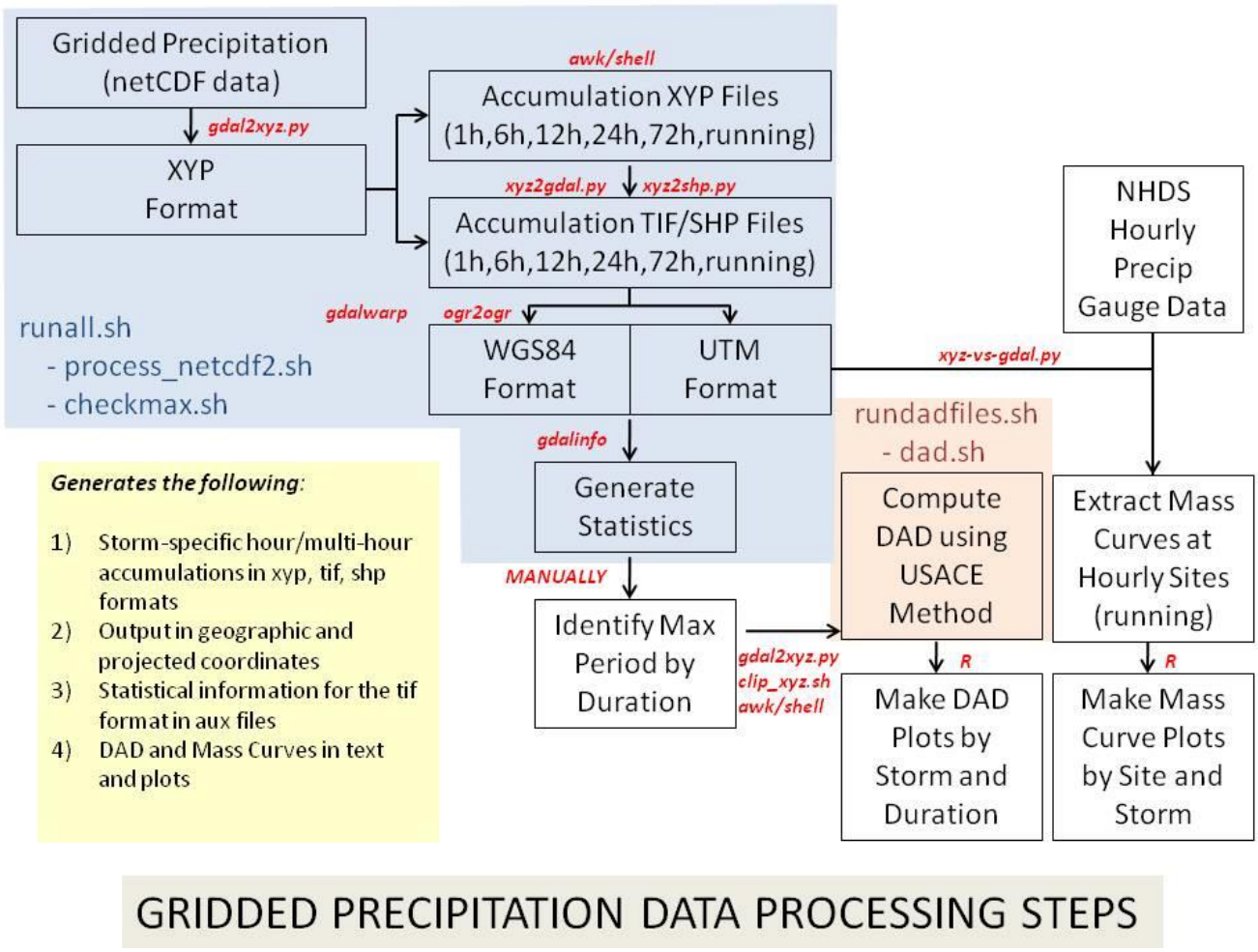


**Figure B-1 Detailed flow chart of the precipitation processing steps. Scripts/program used to process are shown in red**

## B.1 Processing of Monthly netCDF Files of SST and PW

1) Values for every $n^{th}$ month are extracted from the netCDF file [gdal2xyz.py] for the period of record and then concatenated by column using bash scripting [pr -tm].
2) Values of latitude-longitude for each grid cell are extracted from the netCDF file [gdal2xyz.py] and exported to a latlon file.
3) R is then used to calculate the mean and standard deviation by row (i.e., grid cell) to generate approximate 1-in-100 year values using the formula

mean+2*sd = 100-year value.

4) The 100-year values are concatenated with the latlon file [pr -tm], then used to generate a grid of 100-year values [xyz2gdal.py].
5) Values from the 100-year grid are extracted at the origination points from HYSPLIT [xyz-vs-gdal.py].

## B.2 Processing of Daily netCDF Files of SST and PW

Values and latitude-longitude for each grid cell are extracted from the netCDF file [gdal2xyz.py] for the given day.

The values are then used to generate a grid of representative values [xyz2gdal.py].

Values from the representative grid are extracted at the origination points from HYSPLIT [xyz-vs-gdal.py].

## B.3 Processing of netCDF Files of MPR

1) Put .nc files in appropriate directory.
2) Put scripts4anal.zip in directory and unzip.
3) The netCDF files are then converted to grids and ASCII text files for each hour and accumulated at various durations [runall.sh].
4) Compute the DAD for each of the grids at each duration [rundad.sh].
5) Compute the mass curves for each of the grids for each site [masscurves_mpr.sh].

## B.4 Creating Plots of DAD and DADx

1) Copy the DAD text files that match the start hour of maximum mean precipitation from the rundad.sh script (found in each storm directory under the tif_hhh/utm folder to the DAD folder.
2) Plot the DAD curves for each storm and each duration [dad_bystorm.R, dad_byduration].
3) Maximize the DAD curves for each storm [dad_bystorm_maximized.R]. Only a portion of this script will be run then do instructions “Compare New DADs to HMR Grids or Storms” before continuing. See scripts for details.

## B.5 Compare New DADs to HMR Grids/Storms

1) If comparing to past storms, enter the values from the DADx tables in the HMR into individual text files and read them into R [readin_hmr51_twostorms.R].
2) If comparing to HMR51 grids, generate the average location for all area sizes at each duration for each of the individual storms which is found in the DAD text files. [performed in first half of dad_bystorm_maximized.R script]
3) The output files from each of this script and each of the appropriate area duration HMR grids must be converted to WGS84 coordinates [cs2cs, gdalwarp].
4) Then, the values from the respective HMR grids can be extracted for each duration and area size [xyz-vs-gdal.py].
5) Concatenate each of the duration files in order of area from largest to smallest [cat].

6) Continue with number 3 under “Creating Plots of DAD”.

*Note: Linear interpolation is used to calculate differences between the HMRs and DADx files since the area sizes differ [linear_interp.R]*

## B.6 Make Boxplots of HYSPLIT-generated IPMFs

1) Use the online HYSPLIT tool to generate 24 hour, back-trajectories based on point maximum precipitation location. The output will provide a text file with the latitude-longitude pairs for the potential moisture sources.
2) Using the text file, extract the values from the maximum and representative grids [xyz-vs-gdal.py].
3) Convert the SST values to PW values [maximization_sheet.xls]. Concatenate these values with storm number and export to a new text file.
4) Read in the new text files into R and generate all possible combinations for each storm [maxratios.R, maxratios_ncep.R]
5) Similarly, to compare these values to HMR storms- generally follow steps 1 to 4, then plot [other3_plots.R].

## B.7 Get Point Data and Run Mass Curve Analysis

1) Collect hourly precipitation point data from NHDS for all sites in NC and SC.
2) Concatenate all site information after removing lines with extraneous text [grep, cat].
3) Read in data for each storm and accumulate by hour [read_hourly.R].
4) Plot the mass curves for each site and storm, along with differences/ratios between sites [mass_curves.R].

## B.8 Calculate Difference between MPR and Gauges

For points with storm total accumulations greater than zero, MPR values from storm total grids are extracted at those locations and differences are output [xyz-vs-gdal.py].

## B.9 Perform Trend Analysis on SST and Td

1) Process the netCDF monthly files for each month during the period of record [process_sst_nc.sh, process_td_nc.sh].
2) Compute the trends for SST, including conversion of specific humidity to Td. [sst_trend.R, td_computations.R]
3) Extract latitude-longitude pairs from netCDF file and append to slope files output from R [gdal2xyz.py, pr –tm]
4) Convert files to grids for display [xyz2gdal.py].

## B.10 Maximum/Minimum Precipitation at Each Duration

Though not shown in the current document, plots of the maximum and mean values of each storm at each duration and then plots for each duration for all storms may be generated [plot_maxmean.R].

# APPENDIX C ELECTRONIC FILES DIRECTORY AND SCRIPTS

## C.1 Directory Tree of Electronic Files

The following is a directory tree for the Task 2-Storm Analysis portion of the NRC project with brief descriptions.

The main scripts for processing are located in the MPR folder. The runall.sh and rundadfiles.sh scripts should be run in that order and edited appropriately for the storms which will be processed if other than the 10 used here. Each other script in the directory should have a description within the file and can be opened in a text editor (preferably WordPad or vi). netCDF files of MPR should be placed in the appropriate subdirectories (e.g., Bonnie1998) before running scripts. You must also have a file that contains the lat-lon values for each point in the MPR grid (e.g., hrap_points2.txt).

In addition, you must have the following software installed to run (or similar):

| | |
|---|---|
| OSGeo4W | which includes GRASS, msys, QGIS, and GDAL libraries<br>http://osgeo4w.osgeo.org |
| Python | (earlier than version 3.0)<br>http://www.python.org |
| R | Statistical Computing Software<br>http://www.r-project.org |

Using msys allows the user to process in a Windows environment using a linux-type terminal window, though the most expeditious method is to use a Linux/Unix operating system. In Windows, you will need to add Python to your PATH in environmental variables.

Folder: task2_stormanal

| | |
|---|---|
| \|-hurricanetracks | NOAA tropical cyclone tracks |
| \|-Hysplit | Back-trajectory information |
| \|---hy_gifs | Images of 10 storm back-trajectory |
| \|---hysplit_old3_masscurve | 3 storms with mass curves w/hysplit |
| \|---hysplit_old3_wxmap | 3 storms with wx map w/hysplit |
| \|---ncepncar_pw | PW grid computations |
| \|-----august | August PW grid computations |
| \|-----september | September PW grid computations |
| \|---newest_files | Most recent output |
| \|---origfiles | Original processing files |
| \|---three_storms_compare | 3 storms comparison |
| \|-----tyro | Tyro, VA files |
| \|-----yankeetown | Yankeetown, FL files |
| \|-----zerbe | Zerbe, PA files |
| \|-Irene2011 | SAME AS BONNIE BUT IRENE–used .shp |
| \|---backup | holds backup files- required! |
| \|---shp_1h | |
| \|---src_text | |
| \|---tif_12h | |
| \|-----utm | |
| \|---tif_1h | |
| \|-----utm | |

|---tif_24h
|-----utm
|---tif_6h
|-----utm
|---tif_72h
|-----utm
|---tif_running
|-MPR MPR main directory
|---arc_data shapefiles, etc used
|---ArcGraphics Images(totals/tracks,gage compare)
|---Bonnie1998 Bonnie main directory
|-----radar NCDC radar imagery
|-----sfcmap Surface weather maps
|-----shp_1h Hourly point shapefiles of MPR
|-----src_text files made/used in scripts
|-----tif_12h 12h accum grids wgs
|-------utm 12h accum grids utm
|-----tif_1h 1h accum grids wgs
|-------utm 1h accum grids utm
|-----tif_24h 24h accum grids wgs
|-------utm 24h accum grids utm
|-----tif_6h 6h accum grids wgs
|-------utm 6h accum grids utm
|-----tif_72h 72h accum grids wgs
|-------utm 72h accum grids utm
|-----tif_running running total accum grids
|---DAD DAD main directory
|-----contours contour shapefiles for Floyd & Fran
|-----extract1inch grid of 1 inch contour
|-----fran_investigate_croparea info used to test effect of buffer
|---Dennis1999 SAME AS BONNIE BUT FOR DENNIS
|-----radar
|-----sfcmap
|-----shp_1h
|-----src_text
|-----tif_12h
|-------utm
|-----tif_1h
|-------utm
|-----tif_24h
|-------utm
|-----tif_6h
|-------utm
|-----tif_72h
|-------utm
|-----tif_running
|---Earl1998 SAME AS BONNIE BUT FOR EARL
|-----radar
|-----sfcmap
|-----shp_1h
|-----src_text

|-----tif_12h
|-------utm
|-----tif_1h
|-------utm
|-----tif_24h
|-------utm
|-----tif_6h
|-------utm
|-----tif_72h
|-------utm
|-----tif_running
|---Ernesto2006 SAME AS BONNIE BUT FOR ERNESTO
|-----radar
|-----sfcmap
|-----shp_1h
|-----src_text
|-----tif_12h
|-------utm
|-----tif_1h
|-------utm
|-----tif_24h
|-------utm
|-----tif_6h
|-------utm
|-----tif_72h
|-------utm
|-----tif_running
|---Floyd1999 SAME AS BONNIE BUT FOR FLOYD
|-----radar
|-----sfcmap
|-----shp_1h
|-----src_text
|-----tif_12h
|-------utm
|-----tif_1h
|-------utm
|-----tif_24h
|-------utm
|-----tif_6h
|-------utm
|-----tif_72h
|-------utm
|-----tif_running
|---Fran1996 SAME AS BONNIE BUT FOR FRAN
|-----radar
|-----sfcmap
|-----shp_1h
|-----src_text
|-----tif_12h
|-------utm
|-----tif_1h

|-------utm
|-----tif_24h
|-------utm
|-----tif_6h
|-------utm
|-----tif_72h
|-------utm
|-----tif_running
|---Frances2004 SAME AS BONNIE BUT FOR FRANCES
|-----radar
|-----sfcmap
|-----shp_1h
|-----src_text
|-----tif_12h
|-------utm
|-----tif_1h
|-------utm
|-----tif_24h
|-------utm
|-----tif_6h
|-------utm
|-----tif_72h
|-------utm
|-----tif_running
|---Gaston2004 SAME AS BONNIE BUT FOR GASTON
|-----radar
|-----sfcmap
|-----shp_1h
|-----src_text
|-----tif_12h
|-------utm
|-----tif_1h
|-------utm
|-----tif_24h
|-------utm
|-----tif_6h
|-------utm
|-----tif_72h
|-------utm
|-----tif_running
|---Ivan2004 SAME AS BONNIE BUT FOR IVAN
|-----radar
|-----sfcmap
|-----shp_1h
|-----src_text
|-----tif_12h
|-------utm
|-----tif_1h
|-------utm
|-----tif_24h
|-------utm

|-----tif_6h
|-------utm
|-----tif_72h
|-------utm
|-----tif_running
|---mpr_accums Accum MPR txt files for mass curves
|---Ophelia2005 SAME AS BONNIE BUT FOR OPHELIA
|-----radar
|-----sfcmap
|-----shp_1h
|-----src_text
|-----tif_12h
|-------utm
|---------old_dad
|-----tif_1h
|-------utm
|-----tif_24h
|-------utm
|---------old_dad
|-----tif_6h
|-------utm
|---------old_dad
|-----tif_72h
|-------utm
|-----tif_running
|---other_programs Other misc programs/scripts
|---OtherStorms Main dir for other storm data
|-----Alberto1994 Weather maps/radar if avail
|-----Allison1995 “”
|-----Beryl1994 “”
|-----Danny1997 “”
|-----David1979 “”
|-----Dennis1981 “”
|-----Diana1984 “”
|-----Fay2008 “”
|-----Gloria1985 “”
|-----Hermine1998 “”
|-----Hugo1989 “”
|-----Jerry1995 “”
|-----MarcoKlaus1990 “”
|-----Opal1995 “”
|-----Rapidan1995 “”
|-----TD10A1994 “”
|---r_plots Hrly stats by storm(not in report)
|-NHDS Main dir for dly/hrly point precip
|---Daily Daily metadata and scripts
|---Hourly Main hourly point directory
|-----accum_files Text files with point hourly accum
|-----diff_with_grid Text/shape files w/ pt diffs w/MPR
|-----mpr_accums Accum MPR txt files for mass curves
|-----orig_data Original point text files of precip

| | |
|---|---|
| \|-----pdfs | Plots of differences by storm/gauge |
| \|-----programs | Other useful scripts |
| \|-sst_climo | Monthly mean SST files and scripts |
| \|-supporting_docs | Docs, report, related presentations |
| \|-td_climo | Monthly mean Td files and scripts |

## C.2 Scripts Summary

The main processing scripts are listed below.

| | |
|---|---|
| addaux2utmfiles.sh | Adds auxiliary files to .tif files in UTM coords for ease in plotting using GIS (added to runall.sh) |
| addaux2utmfiles_singles.sh | Same as above, but for one file or folder at a time |
| checkmax.sh | Generates the max and mean value of the MPR field for selection of maximum overlapping durations |
| clip_xyz.sh | Clips and xyz file to a polygon boundary |
| dad.sh | Performs DAD computations using USACE methodology (Doug Clemetson) |
| dad3.sh/dad4.sh | Checks the effects of polygon clipping and rainfall displaced from the tropical cyclone rainfall area. |
| masscurves_mpr.sh | Generates the mass curves using the hourly MPR data for each storm |
| process_netcdf2.sh | main processing file- called from runall.sh |
| runall.sh | runs the processes for all the files, except DAD- e.g., process_netcdf2.sh, checkmax.sh (for WGS and UTM files) |
| rundadfiles.sh | performs dad.sh for each of the files |
| rundadfiles_single.sh | performs dad.sh for a specified folder/file |
| rundadfiles_single_floyd.sh | performs dad4.sh for Floyd to test sensitivity of effect of no polygon clipping |
| rundadfiles_single_fran.sh | performs dad3.sh for Fran to test sensitivity of effect of clipping to exclude extraneous precip in W NC |

# APPENDIX D
# COMMUNICATION/COLLABORATION

As part of this research project, Reclamation contacted several entities for assistance in collecting and analyzing datasets. These contacts and type of assistance that they provided are listed below.

Peter Corrigan
Service Hydrologist
NWS Roanoke WFO
Blacksburg, VA
HMRs 57/59

Doug Kluck
Climate Services Director
NWS Central Region
Kansas City, MO
HMRs 57/59

Doug Fenn
Former NWS employee
c/o Doug Kluck
Email Correspondence
HMRs 57/59

Doug Clemetson
Chief, Hydrology Section
USACE
Omaha, NE
DAD Software

David Roth
Forecaster
NOAA HPC
Camp Springs, MD
HPC TC Data

Brian Nelson
Physical Scientist
NESDIS/NCDC
Asheville, NC
MPR

Judith Bradberry
Senior HAS Forecaster
SERFC
Peachtree City, GA
MPE/MPR

Dongsoo Kim
Physical Scientist
NESDIS/NCDC
Asheville, NC
MPR

Xungang Yin
Contractor
NESDIS/NCDC
Asheville, NC
Hourly/Daily Data

Trisha Palmer
Meteorologist
NWS Atlanta WFO
Peachtree City, GA
AMS Conference

NRC FORM 335
(12-2010)
NRCMD 3.7

U.S. NUCLEAR REGULATORY COMMISSION

# BIBLIOGRAPHIC DATA SHEET

*(See instructions on the reverse)*

1. REPORT NUMBER
(Assigned by NRC, Add Vol., Supp., Rev., and Addendum Numbers, if any.)

NUREG/CR-7132

2. TITLE AND SUBTITLE

Application of Radar-Rainfall Estimates to Probable Maximum Precipitation in the Carolinas

3. DATE REPORT PUBLISHED

| MONTH | YEAR |
|---|---|
| June | 2022 |

4. FIN OR GRANT NUMBER


5. AUTHOR(S)

R. Jason Caldwell, John F. England, Jr., Victoria L. Sankovich


6. TYPE OF REPORT

Technical

7. PERIOD COVERED (Inclusive Dates)


8. PERFORMING ORGANIZATION - NAME AND ADDRESS (If NRC, provide Division, Office or Region, U. S. Nuclear Regulatory Commission, and mailing address; if contractor, provide name and mailing address.)

U.S. Department of the Interior - Bureau of Reclamation - Technical Service Center Water and Environmental Resources Division
Flood Hydrology and Emergency Management Group
Denver, Colorado 80225


9. SPONSORING ORGANIZATION - NAME AND ADDRESS (If NRC, type "Same as above", if contractor, provide NRC Division, Office or Region, U. S. Nuclear Regulatory Commission, and mailing address.)

DRA
RES
U.S. Nuclear Regulatory Commission
Washington, D.C. 20555-0001

10. SUPPLEMENTARY NOTES

E. Yegorova

11. ABSTRACT (200 words or less)


Probable Maximum Precipitation (PMP) is a widely-used concept in the design and assessment of critical infrastructure such as dams and nuclear facilities. In the Southeastern United States, PMP estimates are from Hydrometeorological Report 51 (HMR 51). The database of extreme storms used in HMR51 was last updated in the late 1970s. This study focuses on warm-season tropical cyclones in the Carolinas region of the Southeast United States, as these systems are the critical maximum rainfall mechanisms that result in extreme floods. We investigate ten tropical cyclones that impacted the Carolinas during the period 1996-2007. The major focus is to identify if these recent storms challenge the PMP values from HMR 51, in order to assess the adequacy of existing PMP estimates and the need for potentially updating the PMP estimates in a North Carolina-South Carolina pilot region. The results suggest that Hurricanes Floyd (1999) and Fran (1996) approach or exceeded HMR 51 PMP at larger area sizes. Hurricane Floyd exceeded the PMP at durations of 24 and 72 hours, while Fran exceeded PMP at a 6-hour duration. The results of the current study should be considered preliminary but suggest an increase in HMR51 PMP estimates for large area sizes may be warranted along the Carolina coasts, based on in place maximization of Floyd and Fran over the Carolinas.



12. KEY WORDS/DESCRIPTORS (List words or phrases that will assist researchers in locating the report.)

PMP, TC, tropical cyclone, hurricane, Carolina, precipitation, LIP, radar, rainfall, DAD


13. AVAILABILITY STATEMENT

unlimited

14. SECURITY CLASSIFICATION

*(This Page)*
unclassified

*(This Report)*
unclassified

15. NUMBER OF PAGES

16. PRICE

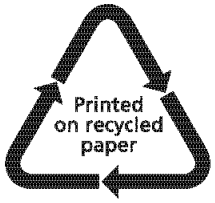


Federal Recycling Program


UNITED STATES
NUCLEAR REGULATORY COMMISSION
WASHINGTON, DC 20555-0001

OFFICIAL BUSINESS